

Submitted by  
**Jan Legerský**

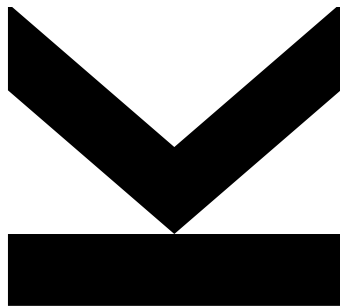
Submitted at  
**Research Institute for  
Symbolic Computation**

Supervisor and  
First Examiner  
**Josef Schicho**

Second Examiner  
**Tibor Jordán**

May 2019

# Flexible and Rigid Labelings of Graphs



Doctoral Thesis  
to obtain the academic degree of  
Doktor der technischen Wissenschaften  
in the Doctoral Program  
Technische Wissenschaften



# Eidesstattliche Erklärung

Ich erkläre an Eides statt, dass ich die vorliegende Dissertation selbstständig und ohne fremde Hilfe verfasst, andere als die angegebenen Quellen und Hilfsmittel nicht benutzt bzw. die wörtlich oder sinngemäß entnommenen Stellen als solche kenntlich gemacht habe. Die vorliegende Dissertation ist mit dem elektronisch übermittelten Textdokument identisch.

Linz, Mai 2019

Jan Legerský



# Kurzfassung

Rigiditätstheorie untersucht ebene und räumliche Realisierungen von Graphen, die gegebenen Bedingungen durch Kantenlängen genügen. Eine Realisierung ist mit einer Kantenbeschriftung kompatibel, wenn die euklidische Distanz zwischen zwei adjazenten Knoten gleich der Beschriftung dieser Kante ist. Wir sagen, dass zwei Realisierungen kongruent sind, wenn sie sich nur durch starre Transformationen unterscheiden. Beschriftungen mit unendlich vielen nicht-kongruenten kompatiblen Realisierungen heißen flexibel, wohingegen jene mit einer positiven endlichen Anzahl an Realisierungen starr genannt werden.

Ein Graph heißt generisch starr, wenn die durch eine generische Realisierung induzierte Beschriftung starr ist. Ein solcher Graph kann aber trotzdem eine nicht-generische flexible Beschriftung haben. Der Fokus dieser Arbeit ist es diese nicht-generischen flexiblen Beschriftungen zu untersuchen. Wir zeigen, dass eine flexible Beschriftung genau dann existiert, wenn es eine so genannte NAC-Färbung gibt. Diese NAC-Färbung ist eine Färbung der Kanten in rot und blau, sodass jeder Zyklus des Graphen entweder einfarbig ist oder darin von jeder Farbe mindestens zwei Kanten existieren.

In Realisierungen, die mit einer von einer NAC-Färbung kommenden Beschriftung kompatibel sind, können sich nicht-adjazente Knoten überlappen. Der Fokus liegt jedoch auf ordentlichen flexiblen Beschriftungen, das heißt auf solchen, die unendlich viele knoten-injektive Realisierungen haben. Wir liefern eine kombinatorische notwendige Bedingung für die Existenz einer ordentlichen flexiblen Beschriftung, welche auf den NAC-Färbungen des Graphen basiert. Durch verschiedene Konstruktionen von ordentlichen flexiblen Beschriftungen zeigen wir, dass diese Bedingung auch hinreichend für alle Graphen bis acht Knoten, aber nicht im allgemeinen, ist.

Das Konzept der NAC-Färbungen wird durch spezielle aktive Färbungen wieder verwendet. Damit werden Werkzeuge für die Untersuchung von möglichen Familien ordentlich flexibler Beschriftungen generisch starrer Graphen erstellt. Diese aktiven NAC-Färbungen liefern algebraische Einschränkungen für die Kantenlängen. Weiters beschreiben wir eine Methode um mögliche aktive NAC-Färbungen zu finden indem wir Färbungen auf Teilgraphen in Form eines 4-Zyklus einschränken. Diese Werkzeuge verwenden wir schließlich um die ordentlichen flexiblen Beschriftungen bestimmter generisch starrer Graphen mit sieben Knoten zu klassifizieren.

Neben flexiblen Beschriftungen untersuchen wir auch starre Beschriftungen. Die Realisierungen, die mit einer starren Beschriftung kompatibel sind, sind im Allgemeinen komplexe Lösungen eines algebraischen Systems. Für manche generisch starre Graphen

---

haben wir Beschriftungen mit vielen reellen Lösungen gefunden indem wir rund um Einheitslängen geprüft haben. Wir beschreiben weiters eine Methode, die auf Koppelkurven basiert und starre Beschriftungen mit einer hohen Anzahl an reellen Realisierungen für bestimmte minimal starre Graphen im dreidimensionalen Raum liefert.

# Abstract

Rigidity Theory studies realizations of a graph in the plane or space satisfying constraints given by edge lengths. A realization is compatible with a given edge labeling of the graph if the Euclidean distance of any two adjacent vertices is equal to the label of this edge. We say that two realizations are congruent if they differ only by a rigid transformation. Labelings with infinitely many non-congruent compatible realizations are called flexible, whereas if the number of non-congruent compatible realizations is positive and finite, they are called rigid.

A graph is called generically rigid if the labeling induced by a generic realization is rigid. Nevertheless, it still may admit a non-generic flexible labeling. This is the main focus of the thesis — to study non-generic flexible labelings. We show that a flexible labeling exists if and only if there is a so called NAC-coloring. A NAC-coloring is a coloring of the edges in red and blue such that for every cycle, either all edges of the cycle have the same color, or there are at least two blue and two red edges.

Since nonadjacent vertices might coincide in realizations compatible with a flexible labeling coming from a NAC-coloring, we restrict ourselves to flexible labelings that are proper, i.e., they have infinitely many vertex-injective realizations. We provide a necessary combinatorial condition on the existence of a proper flexible labeling, which is based on all NAC-colorings of the graph. By various constructions of proper flexible labelings, we prove that this condition is also sufficient for all graphs up to eight vertices, but not in general.

Some tools for studying possible families of proper flexible labelings of a generically rigid graph are presented. The concept of NAC-colorings is used again, since some NAC-colorings are active for a specific motion of the graph. Active NAC-colorings provide algebraic constraints for the edge lengths. Moreover, we describe a method determining possible active NAC-colorings based on restrictions to 4-cycle subgraphs. We apply the tools to classify all proper flexible labelings of a certain generically rigid graph with seven vertices.

Besides flexible labelings, we study also rigid labelings. The realizations compatible with a rigid labeling are solutions of an algebraic system, which are in general complex. For some generically rigid graphs, we have found labelings with many real solutions using sampling around unit distance lengths. We also describe a method based on coupler curves which gives rigid labelings with a high number of real realizations for some minimally rigid graphs in 3-space.





# Acknowledgments

The greatest thanks go to my supervisor Josef. I appreciate his kindness and willingness to discuss mathematical problems anytime and explain to me everything he knows. It was always motivating for me to see his enthusiasm in Mathematics, from proving a theorem for a paper to solving an exercise just for its own beauty. His brilliant ideas were essential for my doctoral thesis. I have enjoyed a lot the days we spent together doing research as well as hiking or climbing.

I would like to thank Georg for his help with everything I needed during my doctoral studies, all the discussions we had from programming to scouting and of course for the hours we spent writing and polishing our papers. I am grateful for his patience with proofreading the thesis.

I thank Matteo for everything he taught me about Algebraic Geometry and all philosophical discussions. I have learnt many things also from all other colleagues in the symbolic computation group and they deserve my thanks: Jose, Mehdi, Christoph, Niels, Elaine, Oliver, Audie, Zijia and Barbara. I am happy for all lunches with Alex, Jakob, Ralf, Sebastian, Ali, Carsten, Antonio, Jordi and others at Gasthaus Hametner. Furthermore, I thank RISC secretaries and all other colleagues.

It was a great experience to be a member ARCADES network — I thank Ioannis for giving us this opportunity by leading the project, Christos for doing the bureaucracy and all other supervisors for organizing the events. I learnt many things during the doctoral schools and other workshops from the speakers and the ARCADES students Clement, Fatmanur, Vangelis, Kostas, Alvaro, Sotiris, Yairon, Theofanis, Andrea, Francesco, Ahmed and Michael. We enjoyed a lot of fun together. I am grateful for my ARCADES secondment I could spend in Athens by working on an interesting question with my coauthors Vangelis, Ioannis and Elias. EU deserves to be acknowledged by saying that this project has received funding from the European Union's Horizon 2020 research and innovation programme under the Marie Skłodowska-Curie grant agreement No 675789. I thank Joanneum Research and RISC Software for the experience of internships outside academia.

I would like to express my gratitude to all my teachers at the high school and university, especially Alena Kroupová who brought my interest to Mathematics and taught me the basics by requiring me to solve countless exercises, and the members of TIGr in Prague who enlarged my mathematical horizons during my bachelor and master degree.

Nothing would be possible without my parents who always support me and my scout friends who encouraged me to accept challenges. My special thanks go to Jana for her love, support and patience.



# Contents

<b>1. Introduction</b>	<b>1</b>
1.1. Rigidity Theory . . . . .	5
1.2. Implementation . . . . .	9
<b>2. Existence of a Flexible Labeling</b>	<b>11</b>
2.1. Combinatorial Characterization . . . . .	11
2.2. Graphs with NAC-colorings . . . . .	20
2.3. A Conjecture on Laman graphs . . . . .	24
2.4. Flexible Labelings in Dimension Three . . . . .	28
<b>3. Movable Graphs</b>	<b>31</b>
3.1. Constant Distance Closure . . . . .	31
3.2. Constructions . . . . .	36
<b>4. On the Classification of Motions</b>	<b>47</b>
4.1. Leading coefficients system . . . . .	48
4.2. Active NAC-colorings of quadrilaterals . . . . .	51
4.3. Determining active NAC-colorings . . . . .	54
4.4. Classification of motions of $Q_1$ . . . . .	66
<b>5. Number of Real Realizations compatible with a Rigid Labeling</b>	<b>83</b>
5.1. Algebraic formulation . . . . .	84
5.2. Laman Graphs . . . . .	86
5.3. Geiringer Graphs . . . . .	88
<b>6. Conclusion</b>	<b>97</b>
<b>A. Appendix</b>	<b>99</b>
A.1. Graph Theory . . . . .	99
A.2. Algebraic Geometry . . . . .	100
A.3. Valuations . . . . .	101
<b>Bibliography</b>	<b>103</b>



# 1. Introduction

One of the core questions of Rigidity Theory is the number of realizations of a graph in the plane or space such that the distances between adjacent vertices are equal to given edge labels. Since any rotation or translation of a realization yields another realization compatible with the same edge lengths, only non-congruent realizations are counted. A labeling is said to be *flexible* if the number of compatible non-congruent realizations is infinite, otherwise *rigid*. Figure 1.1 shows the 3-prism (Desargues) graph illustrating that a graph might have both a flexible and a rigid labeling. Notice that the flexible labeling of the 3-prism is very specific — the triangles are congruent and the vertical bars have the same length. A graph is called *generically rigid* if the labeling obtained by measuring the distances of adjacent vertices in a generic realization is rigid. The main focus of this thesis is on flexible, necessarily non-generic, labelings of generically rigid graphs in the plane. Besides that, we study also rigid instances with many real realizations both in the plane and space.

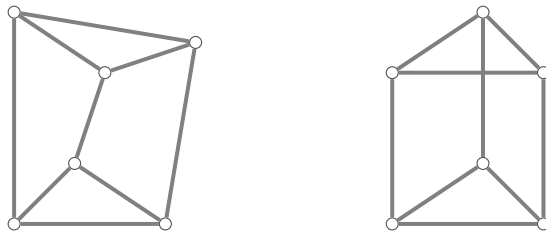


Figure 1.1.: The 3-prism graph with a rigid (left) and flexible (right) labeling. The upper triangle can move along a circle in the flexible case.

A graph with a flexible labeling in the plane can be viewed as a planar linkage — the vertices represent rotational joints connecting links corresponding to the edges. A linkage moves paradoxically if the underlying graph is generically rigid. We briefly summarize the history of studying such over-constrained mechanisms: at the end of the 19-th century, Dixon [16] gave two constructions making the complete bipartite graph  $K_{3,3}$  flexible (see also [63, 53]). The first construction gives a flexible labeling by placing the vertices of each part on one of the two orthogonal lines. In the second one, the vertices lie in the corners of two concentric rectangles with perpendicular/parallel sides, see Figure 1.2. Also other examples like Burmester’s focal point mechanism [8] or constructions by Wunderlich [62, 64] are known. For bipartite graphs, infinitesimal motions have been studied [6, 61] as well as the existence of a flexible labeling [44]. Walter and Husty [60] proved in 2007 using resultants that the constructions for  $K_{3,3}$  given by Dixon are the

only possible ones. In general, flexible labelings of individual graphs, resp. the class of bipartite graphs, were studied.

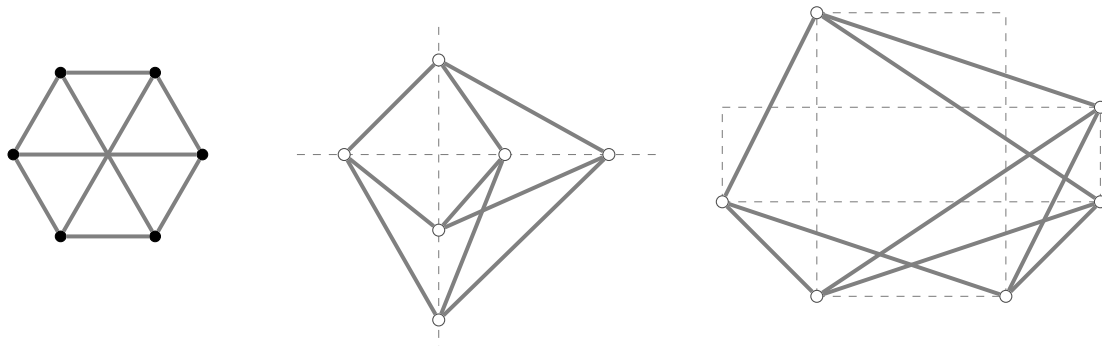


Figure 1.2.: The complete bipartite graph  $K_{3,3}$  (left) and Dixon's constructions of flexible labelings of  $K_{3,3}$  (middle and right).

We aim to develop more general techniques. Our first result is the combinatorial characterization of the graphs that admit a flexible labeling. We prove that a graph has a flexible labeling if and only if it has a *NAC-coloring*. A NAC-coloring is a coloring of edges in red and blue such that for every cycle, either all edges have the same color or there are at least two edges of each color. A flexible labeling is constructed from a NAC-coloring by placing the vertices into a grid so that the edges do not create any diagonals. The other direction uses valuations of the function field of the curve of realizations compatible with a flexible labeling.

We give a necessary condition on the existence of a NAC-coloring exploiting 3-cycles in the graph. We also show that certain vertex or edge cuts imply a NAC-coloring. We conjecture that the necessary condition is also sufficient for *minimally rigid* graphs in the plane — a generically rigid graph is minimally rigid if the graph with any edge removed is not generically rigid. The conjecture is proved for a large subclass.

The realizations compatible with a flexible labeling coming from NAC-coloring are not always vertex-injective, namely, some nonadjacent vertices might coincide. A flexible labeling is called *proper* if there are infinitely many non-congruent vertex-injective realizations. Clearly, the over-constrained mechanisms mentioned above have a proper flexible labeling. We provide a necessary condition on the existence of a proper flexible labeling — a graph  $G$  can have a proper flexible labeling only if the graph obtained from  $G$  by adding some extra edges based on the NAC-colorings of  $G$  is not complete. We list all generically rigid graphs up to 8 vertices that satisfy the necessary condition. By various constructions, we prove that these graphs actually have a proper flexible labeling. Nevertheless, an example showing that the condition is not sufficient for an arbitrary number of vertices is given.

---

Next, we present tools for determining possible families of proper flexible labelings for a given graph  $G$ . A set of NAC-colorings of  $G$  can be assigned to a curve of realizations compatible with a flexible labeling. We propose a method determining such *active* NAC-colorings using 4-cycle subgraphs of  $G$ . Next, an active NAC-coloring satisfying a certain assumption imposes algebraic constraints on the labeling. We illustrate the methods by giving an alternative proof for the result of Walter and Husty [60] classifying the proper flexible labelings of  $K_{3,3}$ . We also apply the technique to obtain the classification of the proper flexible labelings of a 7-vertex generically rigid graph, which had not been known before.

Regarding the rigid labelings, the precise number of non-congruent compatible realizations for a given minimally rigid graph in the plane or space have been investigated in recent years. For instance, Borcea and Streinu proved that the 3-prism has up to 24 realizations in the plane [7]. A common approach is to consider the complex solutions of the algebraic system describing the realizations. The number of complex solutions is bounded for instance by the mixed volume of the system. Then, one tries to find edge lengths maximizing the number of real solutions. This has been done for the minimally rigid graphs in the plane up to 7 vertices [7, 17]. In the space, the number of real realizations was settled for the minimally rigid graphs with 6 vertices [19]. Recently, a combinatorial algorithm counting the number of complex solutions in the plane was proposed [9]. The algorithm was used to compute the numbers for all minimally rigid graphs in the plane up to 12 vertices [25]. The same paper gives also the numbers for all minimally rigid graphs in the space up to 10 vertices via Gröbner basis computation.

Our contribution is the following — we specify edge lengths with many real solutions for minimally rigid graphs in the plane up to 10 vertices that have the maximum number of complex solutions among all minimally rigid graphs with the same number of vertices. The edge lengths are obtained by random sampling close to unit lengths. In the spatial case, we propose a sampling method inspired by coupler curves and the approach of [7]. We focus on the minimally rigid graph with 7, resp. 8, vertices that has the maximum number of solutions. Using our implementation of the method, we obtained edge lengths such that the solutions for the 7-vertex graph are all real. For the graph on 8 vertices, we obtain edge lengths with many real realizations. Using known techniques for gluing graphs together [7, 25], we improve the asymptotic lower bounds on the number of real realizations.

## Structure of the thesis

In the next section of this chapter, we give a brief introduction into Rigidity Theory, define precisely the basic objects used in the thesis and recall some known results. The chapter ends by introducing a software implementation supporting this thesis.

The main result of Chapter 2 is the combinatorial characterization of graphs that admit a flexible labeling in the plane using NAC-colorings. We present some necessary, resp. sufficient, conditions on the existence of a NAC-coloring. For the class of minimally rigid graphs in the plane, we conjecture a necessary and sufficient condition. To support the conjecture, we prove it for a large subclass.

In Chapter 3 we restrict to flexible labelings with infinitely many vertex-injective compatible realizations, since flexible labelings constructed from NAC-colorings are not always vertex-injective. We give a combinatorial necessary condition on the existence of a proper flexible labeling of a graph. The condition is based on all NAC-colorings of the graph. Describing some constructions of proper flexible labelings, we show that the condition is also sufficient up to 8 vertices, but not in general.

In Chapter 4, we propose some methods that can be used to study possible families of proper flexible labelings. They again exploit the concept of NAC-colorings. We illustrate the tools on the known example of Dixon's motions of  $K_{3,3}$  and we apply them to give the full classification of proper flexible labelings of a 7-vertex generically rigid graph.

We turn our attention to rigid labelings both in the plane and space in Chapter 5. The goal is to find edge lengths such that the number of real solutions of the algebraic system describing compatible realizations is as high as possible. While we do this by sampling around unit lengths in the planar case, we propose a sampling strategy inspired by coupler curves in the space. The obtained numbers of real realizations are then used to improve the lower bounds on the maximum number of real realizations among all generically rigid graphs with a given number of vertices.

The appendix covers the notions of Graph Theory, Algebraic Geometry and valuations used in this thesis.

Chapter 2 is based on the published paper [27] by the author of this thesis together with Georg Grasegger and Josef Schicho. The material of Chapter 3 have been submitted to a journal by the same authors. Chapter 4 was partially presented in [28] and is under preparation for submission also by the same authors. The content of Chapter 5 is a joint work with Elias Tsigaridas, Vangelis Bartzos and Ioannis Emiris. The part about spatial realizations was published as a conference paper [2]. An extension paper containing also the planar case, spherical realizations and distance geometry formulations has been submitted by the same authors [1]. The latter two topics of the extension paper are not part of this thesis.

Throughout this thesis we distinguish pictures of graphs in the following way — if a figure depicts only combinatorial properties of a graph, then the vertex circles are filled, compare Figure 1.2. On the other hand, if we want to illustrate also edge lengths, then the vertex circles are empty and the layout corresponds to one of the compatible realizations. This convention holds also if there are vertex labels inside the circles.



## 1.1. Rigidity Theory

Rigidity Theory concepts are described in the language of Graph Theory. All graphs we consider in this thesis are simple and undirected. Given a graph  $G$ , we denote the set of vertices and edges of  $G$  by  $V_G$  and  $E_G$  respectively, and we use  $uv$  for an edge  $\{u, v\} \in E_G$  to simplify the notation. Appendix A.1 gives a brief summary of the graph-theoretical concepts used in the thesis.

The object we study is a graph with a labeling of edges by positive real numbers. The realizations of the graph in the plane or space are required to be such that the distances between adjacent vertices correspond to the labeling. We are interested in whether the number of such realizations counted modulo rotations and translations is finite or infinite, depending on the labeling.

**Definition 1.1.** *Let  $d \in \{2, 3\}$  and  $G$  be a connected graph with at least  $d$  vertices. Let  $\lambda: E_G \rightarrow \mathbb{R}_+$  be an edge labeling of  $G$ . A map  $\rho = (\rho_x, \rho_y): V_G \rightarrow \mathbb{R}^d$  is a realization of  $G$  compatible with  $\lambda$  if and only if  $\|\rho(u) - \rho(v)\| = \lambda(uv)$  for all edges  $uv \in E_G$ . We say that two realizations  $\rho_1$  and  $\rho_2$  are congruent if and only if there exists a direct Euclidean isometry  $\sigma$  of  $\mathbb{R}^d$  such that  $\rho_1 = \sigma \circ \rho_2$ .*

*The labeling  $\lambda$  is called*

- flexible, if the number of realizations of  $G$  compatible with  $\lambda$  modulo the congruence is infinite, or
- rigid, if the number of realizations of  $G$  compatible with  $\lambda$  modulo the congruence is finite and nonzero.

There is also the notion of *infinitesimal* rigidity and flexibility, but it plays no role in this thesis. We refer to [30, 52, 58] for various concepts in Rigidity Theory. Applications of rigid graphs are for instance in robotics [65], scene analysis [4] or molecular conformations [18, 42].

In order to simplify the notation, we write sometimes  $\lambda_{uv}$  for  $\lambda(uv)$ , or  $\lambda_{ij}$  for  $\lambda(v_i v_j)$ . The constraints on realizations in  $\mathbb{R}^2$  given by edge lengths  $\lambda$  can be modeled by the following system of polynomial equations for coordinates  $(x_u, y_u)$  for  $u \in V_G$ . The position of an edge  $\bar{u}\bar{v}$  is fixed to remove rigid motions and we take squares of Euclidean distances:

$$\begin{aligned} x_{\bar{u}} &= 0, & y_{\bar{u}} &= 0, \\ x_{\bar{v}} &= \lambda_{\bar{u}\bar{v}}, & y_{\bar{v}} &= 0, \\ (x_u - x_v)^2 + (y_u - y_v)^2 &= \lambda_{uv}^2 & \text{for all } uv \in E_G \setminus \{\bar{u}\bar{v}\}. \end{aligned} \tag{1.1}$$

A similar system can be constructed for realizations in  $\mathbb{R}^3$  by fixing also a third vertex to be in the  $xy$ -plane. The labeling  $\lambda$  is flexible if and only if there are infinitely many

solutions of the system. On the other hand,  $\lambda$  is rigid if there are only finitely many solutions.

It is known that if we restrict to generic labelings, then being flexible or rigid is a graph property.

**Definition 1.2.** *A graph is called generically rigid if the labeling induced by a generic realization in  $\mathbb{R}^d$  is rigid.*

By generic we mean that it avoids a certain proper algebraic subset. See [55] for an overview of various notions of genericity used in Rigidity Theory. An interesting class of generically rigid graphs are the minimal ones with respect to removing edges.

**Definition 1.3.** *A generically rigid graph is called minimally rigid if removing any edge yields a graph which is not generically rigid.*

Notice that the algebraic system (1.1) is well-constrained for a minimally rigid graph with a rigid labeling, namely, the number of variables equals the number of equations and the zero set is 0-dimensional.

Maxwell [45] pointed out that if a graph  $G$  is minimally rigid in  $\mathbb{R}^d$ , then

- (i)  $|E_G| = d|V_G| - \binom{d+1}{2}$ , and
- (ii)  $|E_H| \leq d|V_H| - \binom{d+1}{2}$  for each subgraph  $H$  of  $G$ .

The second property says that there is no over-constrained subsystem in (1.1). Pollaczek-Geiringer [47, 48] worked in the topic of minimally rigid graphs in  $\mathbb{R}^2$  and  $\mathbb{R}^3$ , but her results were forgotten til recently. In 1970 Laman rediscovered that in the planar case, Maxwell's condition is also sufficient:

**Theorem 1.4.** *A graph  $G$  is minimally rigid in  $\mathbb{R}^2$  if and only if  $|E_G| = 2|V_G| - 3$ , and  $|E_H| \leq 2|V_H| - 3$  for each subgraph  $H$  of  $G$ .*

Therefore, the minimally rigid graphs in the plane are called *Laman* graphs. In honour of Hilda Pollaczek-Geiringer, we use the name *Geiringer* graphs for the minimally rigid graphs in  $\mathbb{R}^3$ , as proposed in [25]. It is a difficult open problem to characterize Geiringer graphs — the well known example of the “double-banana” shows that Maxwell's condition is not sufficient.

Laman graphs are precisely the graphs that can be constructed by a sequence of Henneberg moves, see the definition below, starting from a single edge [32]. We distinguish also some subtypes of the two moves for the purpose of Section 2.3, see also Figure 1.3.

**Definition 1.5.** *Let  $G$  and  $G'$  be Laman graphs such that  $V_G = \{v\} \cup V_{G'}$ , where  $v \notin V_{G'}$ . The graph  $G$  is constructed from  $G'$  by a*

Henneberg I move from vertices  $u, u_1, u_2 \in V_{G'}$  if  $E_G = E_{G'} \cup \{u_1v, u_2v\}$ . The subtype is Ia if  $u_1u_2 \in E_{G'}$ , Ib otherwise.

Henneberg II move from vertices  $u, u_1, u_2 \in V_{G'}$  if  $u_1u_2 \in E_{G'}$  and  $E_G = E_{G'} \setminus \{u_1u_2\} \cup \{uv, u_1v, u_2v\}$ . The subtype is

IIa if  $uu_1 \notin E_G$  and  $uu_2 \notin E_G$ , or

IIb if either  $uu_1 \in E_G$  or  $uu_2 \in E_G$ , or

IIc if  $uu_1 \in E_G$  and  $uu_2 \in E_G$ .

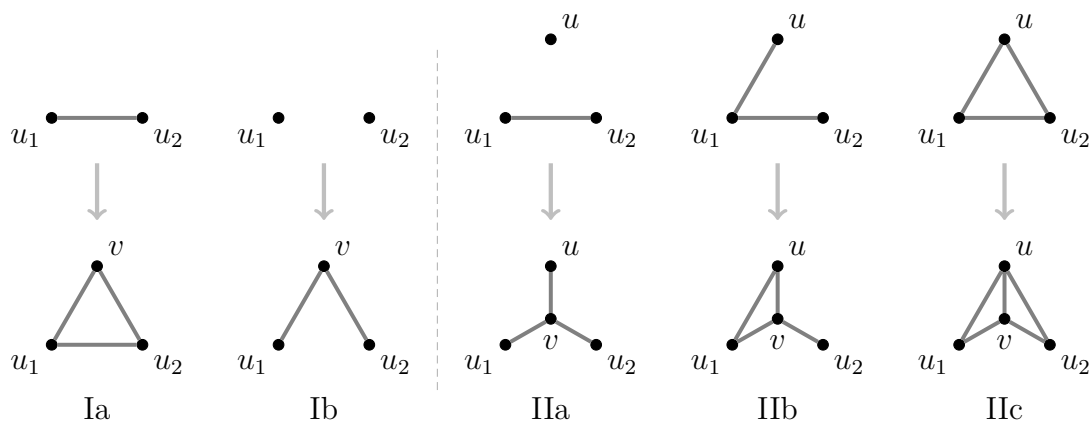


Figure 1.3.: Henneberg moves in  $\mathbb{R}^2$ .

There is also a set of Henneberg steps that allows to construct all Geiringer graphs from a triangle [56], but contrary to the planar case, it is not guaranteed that all constructed graphs are generically rigid.

Another characterization of Laman graphs uses so called 3T2 decompositions [13], but it is not needed in this work. Deciding whether a given graph is Laman can be done in  $O(|V_G|\sqrt{|V_G| \log |V_G|})$  steps [22]. The algorithms based on pebble games [36] can also find maximal Laman subgraphs, see [38].

We introduce now some notions related to flexible labelings that we use in Chapters 2, 3 and 4. In these chapters, we work only with realizations in  $\mathbb{R}^2$  (except for Section 2.4), hence, we assume this implicitly. We emphasize that the realizations in the definition of flexible labelings are not required to be injective. Namely, it can happen that two nonadjacent vertices are mapped to the same point in  $\mathbb{R}^2$ . Notice that adjacent vertices cannot coincide as the edge lengths are required to be positive. This is the setup of Chapter 2, flexible labelings constructed by the method presented there are not always non-injective. We remark that the existence of infinitesimally rigid realizations that are non-generic in the sense that two points coincide, resp. three points are collinear, is studied in [21], resp. [35]. On the other hand, Chapters 3 and 4 are focused

## 1. Introduction

---

on the graphs that have a labeling with infinitely many injective compatible realizations in  $\mathbb{R}^2$ :

**Definition 1.6.** *A flexible labeling  $\lambda$  of a graph  $G$  is called proper, if there exists infinitely many non-congruent injective realizations of  $G$  compatible with  $\lambda$ . We say that a graph is movable if it has a proper flexible labeling.*

We remark that non-movable graphs are called *absolutely 2-rigid* in [43]. Looking for proper flexible labelings could be modelled by extending the system (1.1) by the inequalities  $(x_u - x_v)^2 + (y_u - y_v)^2 \neq 0$  for all  $u, v \in V_G$  such that  $u \neq v$  and  $uv \notin E_G$ , but the zero set of such a system would not be an algebraic set. Therefore, we tackle the injectivity requirement differently in Chapter 3.

We want to study the system (1.1) from the point of view of Algebraic Geometry (see Appendix A.2 for a short summary of definitions). We consider irreducible components of the zero set of the system to be able to use function fields:

**Definition 1.7.** *Let  $\lambda$  be a flexible labeling of a graph  $G$ ,  $\bar{u}\bar{v}$  be an edge of  $G$ . Let  $\mathcal{R}(G, \lambda) \subseteq (\mathbb{R}^2)^{V_G}$  be the set of all realizations of  $G$  compatible with  $\lambda$ . We say that  $\mathcal{C}$  is an algebraic motion of  $(G, \lambda)$  w.r.t. the fixed edge  $\bar{u}\bar{v}$ , if it is an irreducible algebraic curve in  $\mathcal{R}(G, \lambda)$ , such that  $\rho(\bar{u}) = (0, 0)$  and  $\rho(\bar{v}) = (\lambda(\bar{u}\bar{v}), 0)$  for all realizations  $\rho \in \mathcal{C}$ . Since in many situations the role of  $\bar{u}\bar{v}$  does not matter, we also simply say that  $\mathcal{C}$  is an algebraic motion of  $(G, \lambda)$ . We denote the complex function field of  $\mathcal{C}$  by  $F(\mathcal{C})$ .*

An essential tool for studying flexible labelings in this work are certain functions of the function field  $F(\mathcal{C})$ . Together with the valuations of the function field  $F(\mathcal{C})$ , they provide a rich combinatorial information about the flexible labeling  $\lambda$ . A brief introduction into valuations can be found in Appendix A.3.

The following lemma clarifies that we do not have to specify the fixed edge of an algebraic motion.

**Lemma 1.8.** *Let  $\lambda$  be a flexible labeling of  $G$ . Let  $\mathcal{C}_{\bar{u}, \bar{v}}$  be an algebraic motion of  $(G, \lambda)$  w.r.t. an edge  $\bar{u}\bar{v}$ . If  $u'v' \in E_G$  and  $\varphi_{u', v'} : \mathcal{R}(G, \lambda) \rightarrow \mathcal{R}(G, \lambda)$  is given by*

$$(x_w, y_w)_{w \in V_G} \mapsto \left( \frac{(x_w - x_{u'}) (x_{v'} - x_{u'}) + (y_w - y_{u'}) (y_{v'} - y_{u'})}{\lambda(u'v')}, \frac{(y_w - y_{u'}) (x_{v'} - x_{u'}) - (x_w - x_{u'}) (y_{v'} - y_{u'})}{\lambda(u'v')} \right)_{w \in V_G},$$

*then  $\mathcal{C}_{u', v'} = \varphi_{u', v'}(\mathcal{C}_{\bar{u}, \bar{v}})$  is an algebraic motion of  $(G, \lambda)$  w.r.t. an edge  $u'v'$  and  $\varphi_{u', v'} : \mathcal{C}_{\bar{u}, \bar{v}} \rightarrow \mathcal{C}_{u', v'}$  is birational.*

*Proof.* By direct computation, one can check that  $u'v'$  is indeed fixed in  $\mathcal{C}_{u', v'}$  and that all realizations in  $\mathcal{C}_{u', v'}$  are compatible with  $\lambda$ . The rational inverse of  $\varphi_{u', v'}$  is  $\varphi_{\bar{u}, \bar{v}}$ .  $\square$

We conclude the section by describing Dixon's constructions, see Figure 1.2.

**Definition 1.9.** *Let  $\{ij: i \in \{1, 3, 5\}, j \in \{2, 4, 6\}\}$  be the edges of  $K_{3,3}$ . A proper flexible labeling of  $K_{3,3}$  with an algebraic motion  $\mathcal{C}$  is called*

Dixon I type *if for every realization  $\rho \in \mathcal{C}$ , the points  $\rho(1)$ ,  $\rho(3)$  and  $\rho(5)$ , resp.  $\rho(2)$ ,  $\rho(4)$  and  $\rho(6)$  are collinear and these two lines are orthogonal, or*

Dixon II type *if for every realization  $\rho \in \mathcal{C}$ , the points  $\rho(1)$ ,  $\rho(3)$  and  $\rho(5)$ , resp.  $\rho(2)$ ,  $\rho(4)$  and  $\rho(6)$ , lie in vertices of a rectangle  $R_1$ , resp.  $R_2$ , such that the intersection of diagonals of  $R_1$  and  $R_2$  is the same and the sides of  $R_1$  are parallel or perpendicular to the sides of  $R_2$  (see Figure 4.6).*

Easily, the Dixon I construction gives a proper flexible labeling for any bipartite graph and Dixon II can be extended to a motion of  $K_{4,4}$ . For curiosity, it is sketched in [49] that a planar linkage representing Dixon I motion of  $K_{4,4}$  can be build with the links in different layers so that the whole motion curve can be traversed without self-collisions, but this is not possible for Dixon II.

We postpone introducing the notation for the numbers of realizations compatible with a rigid labeling to Chapter 5, since it is the only chapter when it is used.

## 1.2. Implementation

Many concepts used in this thesis to study rigidity and flexibility in  $\mathbb{R}^2$  are implemented in our package `FlexRiLoG` [26], which is written in `SageMath` [57] using object-oriented design. At the end of each chapter of the thesis, there is a section listing relevant functionality. It is not meant to be a documentation, rather an overview how the theory is related to the implementation. For this reason, we do not include the full list of methods and we omit optional input arguments. The complete list can be found in the web-based documentation in [26]. Here is a brief summary of the classes:

`FlexRiGraph` is inherited from `SageMath` class `Graph` and provides methods for computing various combinatorial properties. For example there is a method for finding a NAC-coloring, which is then stored in the class `NACcoloring`.

`ParametricGraphMotion` is inherited from `GraphMotion`, which is a general class for handling algebraic motions, and can be used if an explicit parametrization of a motion is known. It can for instance create SVG animations of a motion.

`GraphGenerator` is a factory providing some predefined graphs, e.g. the 3-prism graph or the list of Laman graphs up to 8 vertices.

`MotionClassifier` implements the methods of Chapter 4 for classification of motions.

## 1. Introduction

---

We provide a supporting material [40] containing the computations needed for this thesis in the form of Jupyter notebooks using **FlexRiLoG**.

The methods of Chapter 5 dealing with realizations in  $\mathbb{R}^3$  are implemented in another package [3].

## 2. Existence of a Flexible Labeling

The main result of this chapter is a combinatorial characterization of the existence of a flexible labeling in the plane. In order to do this, we introduce a so called NAC-coloring. It is a coloring of edges by two colors such that for every cycle either all edges have the same color or there are at least two blue and two red edges. The way how a valuation of the function field of an algebraic motion yields a NAC-coloring is essential not only in this chapter, but also in studying flexible labelings in the rest of the thesis.

The notion of NAC-coloring is defined in Section 2.1. We prove one implication of the main theorem by describing how a NAC-coloring can be obtained from a certain valuation of the function field of an algebraic motion. The other implication is proved by explicit construction of a flexible labeling from a NAC-coloring.

The combinatorial characterization enables us to study properties of graphs with NAC-colorings further in Section 2.2. We give a necessary condition on the existence of a NAC-coloring and a few sufficient ones. A tight upper bound on the maximal number of edges allowing a flexible labeling is also provided.

In Section 2.3, we conjecture that the necessary condition of the existence of a NAC-coloring is actually sufficient for Laman graphs. To support our conjecture, we prove it for a large class of Laman graphs.

Section 2.4 shows that the question of existence of a flexible labeling for realizations in 3-space without further restrictions is easy.

The whole chapter was published as the paper [27] by the author of this thesis, except for Lemmas 2.11 and 2.12 which appear in [29].

### 2.1. Combinatorial Characterization

We begin the section with the definition of NAC-coloring and an equivalent formulation. Then, we introduce two functions in the function field of an algebraic motion for each edge of a graph. They were used in [9] to count the number of complex realizations of a Laman graph. The way how the images of these functions under a certain valuation of the function field yield a so called active NAC-coloring forms a keystone of studying flexibility in this thesis.

Obtaining an active NAC-coloring from a valuation allows to prove one direction of the combinatorial characterization of the existence of a flexible labeling. The other implication is done by explicit construction of an algebraic motion and flexible labeling from a NAC-coloring. We also generalize this construction in order to gain a larger set of flexible labelings.

At the end of this section, we prove two technical lemmas describing behaviour of active NAC-colorings under the change of the fixed edge and swapping colors.

**Definition 2.1.** *Let  $G$  be a graph and  $\delta: E_G \rightarrow \{\text{blue}, \text{red}\}$  be a coloring of edges.*

- (i) *A path, resp. cycle, in  $G$  is called unicolor, if all its edges have the same color.*
- (ii) *A cycle in  $G$  is an almost red cycle, resp. almost blue cycle, if exactly one of its edges is blue, resp. red.*

*A coloring  $\delta$  is called a NAC-coloring, if it is surjective and there are no almost blue cycles or almost red cycles in  $G$ . In other words every cycle is either unicolor or contains at least 2 edges in each color. The set of all NAC-colorings of  $G$  is denoted by  $\text{NAC}_G$ .*

Now, the abbreviation NAC can be explained — it stands for “No Almost Cycle”. Lemma 2.2 below provides a characterization that can be verified easily. Two subgraphs of  $G$  induced by a coloring  $\delta$  are used, namely,  $G_{\text{red}}^\delta = (V_G, E_{\text{red}}^\delta)$  and  $G_{\text{blue}}^\delta = (V_G, E_{\text{blue}}^\delta)$ , where  $E_{\text{red}}^\delta = \{e \in E_G: \delta(e) = \text{red}\}$  and  $E_{\text{blue}}^\delta = \{e \in E_G: \delta(e) = \text{blue}\}$ .

**Lemma 2.2.** *Let  $G$  be a graph. If  $\delta: E_G \rightarrow \{\text{blue}, \text{red}\}$  is a coloring of edges, then there are no almost blue cycles or almost red cycles in  $G$  if and only if the connected components of  $G_{\text{red}}^\delta$  and  $G_{\text{blue}}^\delta$  are induced subgraphs of  $G$ .*

*Proof.*  $\implies$  : Let  $M$  be a connected component of  $G_{\text{red}}^\delta$ . Assume that  $M$  is not an induced subgraph of  $G$ , namely, there exists an edge  $uv \in E_G$  such that  $u, v \in V_M$  but  $uv \notin E_M$ . Hence,  $uv$  is blue and there exists an almost red cycle which is a contradiction. This works analogously for connected components of  $G_{\text{blue}}^\delta$ .

$\impliedby$  : Assume that there exists an almost red cycle with a blue edge  $uv$ . The vertices  $u$  and  $v$  belong to the same connected component of  $G_{\text{red}}^\delta$  but  $uv$  is blue, i.e.,  $uv \notin E_{\text{red}}^\delta$  which contradicts that all connected components of  $G_{\text{red}}^\delta$  are induced subgraphs of  $G$ . Similarly for an almost blue cycle.  $\square$

Using Lemma 2.2, there is a straightforward algorithm checking whether a given coloring  $\delta$  is a NAC-coloring: we construct  $G_{\text{red}}^\delta$  and  $G_{\text{blue}}^\delta$ . If  $G_{\text{red}}^\delta$  or  $G_{\text{blue}}^\delta$  has no edges, then  $\delta$  is not surjective, thus, it is not a NAC-coloring. Otherwise, we decompose  $G_{\text{red}}^\delta$  and  $G_{\text{blue}}^\delta$  into connected components and check whether these components are induced subgraphs of  $G$ .

Clearly, if we swap colors of a NAC-coloring of  $G$ , we obtain another NAC-coloring of  $G$ .

**Definition 2.3.** *Let  $G$  be a graph. If  $\delta, \bar{\delta} \in \text{NAC}_G$  are such that  $\delta(e) = \text{blue} \iff \bar{\delta}(e) = \text{red}$  for all  $e \in E_G$ , then they are called conjugated.*



We introduce functions in the function field which are related to NAC-colorings. This is an essential concept of the thesis for investigating flexibility.

**Definition 2.4.** *Let  $\lambda$  be a flexible labeling of a graph  $G$  and  $\mathcal{C}$  be an algebraic motion of  $(G, \lambda)$ . For every  $u, v \in V_G$  such that  $uv \in E_G$ , we define  $W_{u,v}, Z_{u,v} \in F(\mathcal{C})$  by*

$$\begin{aligned} W_{u,v} &= (x_v - x_u) + i(y_v - y_u), \\ Z_{u,v} &= (x_v - x_u) - i(y_v - y_u). \end{aligned}$$

We use  $W_{u,v}^{\bar{u}\bar{v}}$ , resp.  $Z_{u,v}^{\bar{u}\bar{v}}$ , if we want to specify that  $\mathcal{C}$  is w.r.t. a fixed edge  $\bar{u}\bar{v}$ .

We remark that  $W_{u,v} = -W_{v,u}$  and  $Z_{u,v} = -Z_{v,u}$ , i.e., they depend on the order of  $u, v$ . In case we are computing valuations where the sign does not matter we might also write  $W_e$  for an edge  $e$ . Using (1.1), we have

$$\begin{aligned} W_{\bar{u},\bar{v}} &= \lambda_{\bar{u}\bar{v}}, & Z_{\bar{u},\bar{v}} &= \lambda_{\bar{u}\bar{v}}, \\ W_{u,v} Z_{u,v} &= \lambda_{uv}^2 & \text{for all } uv \in E_G. \end{aligned} \quad (2.1)$$

For all edges  $e \in E_G$ , we have  $\nu(W_e) + \nu(Z_e) = 0$  for every valuation  $\nu$  which is trivial on  $\mathbb{C}$ . By the definition of  $W_{u,v}$  and  $Z_{u,v}$ , the following equations hold for every cycle  $(u_1, \dots, u_n)$  in  $G$ :

$$\sum_{i=1}^n W_{u_i, u_{i+1}} = 0, \quad \sum_{i=1}^n Z_{u_i, u_{i+1}} = 0, \quad (2.2)$$

if we set  $u_{n+1} = u_1$ .

Recall that the valuation of a product is the sum of valuations and the valuation of a sum is the minimum of valuations. A consequence is that if a sum of functions equals zero, then there are at least two summands with the minimal valuation. This is used implicitly in the following theorem which explains how the functions  $W_e$  and  $Z_e$  yield a NAC-coloring.

**Lemma 2.5.** *Let  $\lambda$  be a flexible labeling of a graph  $G$ . Let  $F(\mathcal{C})$  be the complex function field of an algebraic motion  $\mathcal{C}$  of  $(G, \lambda)$ . If  $\alpha \in \mathbb{Q}$  and  $\nu$  is a valuation of  $F(\mathcal{C})$ , which is trivial in  $\mathbb{C}$ , such that there exist edges  $e, e'$  in  $E_G$  with  $\nu(W_e) = \alpha$  and  $\nu(W_{e'}) > \alpha$ , then  $\delta : E_G \rightarrow \{\text{red}, \text{blue}\}$  given by*

$$\begin{aligned} \delta(uv) = \text{red} &\iff \nu(W_{u,v}) > \alpha, \\ \delta(uv) = \text{blue} &\iff \nu(W_{u,v}) \leq \alpha. \end{aligned} \quad (2.3)$$

is a NAC-coloring.

*Proof.* The surjectivity of  $\delta$  follows from  $\delta(e) = \text{blue}$  and  $\delta(e') = \text{red}$ . We consider now a cycle  $(u_1, u_2, \dots, u_n)$ . If we assume that all edges  $u_1u_2, \dots, u_{n-1}u_n$  are red, then

$$\nu(W_{u_1, u_n}) = \nu(W_{u_1, u_2} + W_{u_2, u_3} + \dots + W_{u_{n-1}, u_n}) \geq \min \nu(W_{u_i, u_{i+1}}) > \alpha.$$

## 2. Existence of a Flexible Labeling

---

Hence, there is no almost red cycle. On the other hand, if  $u_1u_2, \dots, u_{n-1}u_n$  are all blue, then

$$\begin{aligned} \nu(W_{u_1, u_n}) &= -\nu(Z_{u_1, u_n}) = -\nu(Z_{u_1, u_2} + \dots + Z_{u_{n-1}, u_n}) \\ &\leq -\min \nu(Z_{u_i, u_{i+1}}) = \max \nu(W_{u_i, u_{i+1}}) \leq \alpha, \end{aligned}$$

which implies that  $u_1u_n$  is also blue. □

This motivates the assignment of some NAC-colorings to an algebraic motion.

**Definition 2.6.** *Let  $\mathcal{C}$  be an algebraic motion of  $(G, \lambda)$ . A NAC-coloring  $\delta \in \text{NAC}_G$  is called active w.r.t.  $\mathcal{C}$  if there exists a valuation  $\nu$  of  $F(\mathcal{C})$  and  $\alpha \in \mathbb{Q}$  such that (2.3) holds. The set of all active NAC-colorings of  $G$  w.r.t.  $\mathcal{C}$  is denoted by  $\text{NAC}_G(\mathcal{C})$ .*

Now we can characterize the existence of a flexible labeling.

**Theorem 2.7.** *A connected graph  $G$  with at least one edge has a flexible labeling if and only if it has a NAC-coloring.*

*Proof.*  $\implies$ : A direct consequence of Chevalley's Extension Theorem (see Appendix A.3) is that if  $z$  is an element of a function field that is transcendental over  $\mathbb{C}$ , then there exists at least one valuation  $\nu$  such that  $\nu(z) > 0$  and  $\nu(\mathbb{C}) = \{0\}$ .

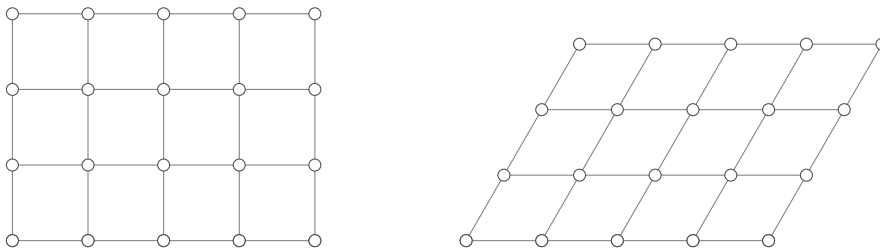
Let  $\lambda: E_G \rightarrow \mathbb{R}_+$  be a flexible labeling of  $G$  and  $\mathcal{C}$  be an algebraic motion of  $(G, \lambda)$  w.r.t. a fixed edge  $e = \bar{u}\bar{v}$ . There exists an edge  $e' \in E_G$  such that  $W_{e'}$  is transcendental over  $\mathbb{C}$ . Otherwise, there are only finitely many complex realizations of  $G$  and hence also only finitely many real ones, which would contradict that  $\lambda$  is flexible. Let  $\nu$  be a valuation of  $F(\mathcal{C})$  such that  $\nu(W_{e'}) > 0$  obtained by Chevalley's Extension Theorem. The valuation of  $W_{\bar{u}, \bar{v}}$  is zero, since  $W_{\bar{u}, \bar{v}} = \lambda_{\bar{u}\bar{v}} \in \mathbb{R}_+$ . Hence, Lemma 2.5 gives an active NAC-coloring of  $G$  w.r.t. the algebraic motion  $\mathcal{C}$ .

$\impliedby$ : Let  $\delta$  be a NAC-coloring. Let  $R_0, \dots, R_m$  be the sets of vertices of connected components of the graph  $G_{\text{red}}^\delta$  and  $B_0, \dots, B_n$  be the sets of vertices of connected components of the graph  $G_{\text{blue}}^\delta$ .

For  $\alpha \in [0, 2\pi)$ , we define a map  $\rho_\alpha: V_G \rightarrow \mathbb{R}^2$  by

$$\rho_\alpha(v) = i \cdot (1, 0) + j \cdot (\cos \alpha, \sin \alpha),$$

where  $i$  and  $j$  are such that  $v \in R_i \cap B_j$ . This means we place the vertices of the graph into a grid so that there are no diagonals.



The map  $\rho_\alpha$  gives a labeling  $\lambda_\alpha : E_G \rightarrow \mathbb{R}_+$ , where

$$\lambda_\alpha(uv) = \|\rho_\alpha(u) - \rho_\alpha(v)\|$$

for all edges  $uv \in E_G$ . We show that  $\lambda_\alpha$  is actually independent on the choice of  $\alpha$ . Let  $uv$  be an edge in  $E_G$  and  $i, j, k, l$  be such that  $u \in R_i \cap B_j$  and  $v \in R_k \cap B_l$ . If  $uv$  is red, then  $i = k$  and we have

$$\begin{aligned} \lambda_\alpha(uv) &= \|\rho_\alpha(u) - \rho_\alpha(v)\| = \|(i - k) \cdot (1, 0) + (j - l) \cdot (\cos \alpha, \sin \alpha)\| \\ &= |j - l| \cdot \|(\cos \alpha, \sin \alpha)\| = |j - l|. \end{aligned}$$

If  $uv$  is blue, then  $j = l$  and hence  $\lambda_\alpha(uv) = |k - i|$ .

Therefore,  $\rho_\alpha$  is a realization of  $G$  compatible with  $\lambda = \lambda_{\frac{\pi}{2}}$  for all  $\alpha \in [0, 2\pi)$ .

We also need to show that the codomain of  $\lambda$  is  $\mathbb{R}_+$ . In contrary, assume that  $\lambda(uv) = 0$  for some  $uv \in E_G$ . This implies that both  $u$  and  $v$  belong to the same  $R_i \cap B_j$ . This contradicts that  $\delta$  is a NAC-coloring since if  $uv$  is red, then there is an almost blue cycle and similarly if  $uv$  is blue, then there is an almost red cycle.

The labeling  $\lambda$  is flexible since there are infinitely many realizations  $\rho_\alpha$  which are non-congruent as  $\delta$  is surjective, i.e., there are edges in direction  $(0, 1)$  and also  $(\cos \alpha, \sin \alpha)$ .  $\square$

We illustrate the proof by examples for both implications. Firstly, we compute the active NAC-colorings of the non-degenerate algebraic motion of a deltoid.

**Example 2.8.** *Let  $Q$  be a 4-cycle with a labeling  $\lambda$  given by  $\lambda_{12} = \lambda_{14} = 1$  and  $\lambda_{23} = \lambda_{34} = 3$ . There is an algebraic motion  $\mathcal{C}$  of  $(Q, \lambda)$  that can be parametrized by*

$$\begin{aligned} \rho_t(1) &= (0, 0), & \rho_t(2) &= (1, 0), \\ \rho_t(3) &= \left( \frac{4(t^2 - 2)}{t^2 + 4}, \frac{12t}{t^2 + 4} \right), & \rho_t(4) &= \left( \frac{t^4 - 13t^2 + 4}{t^4 + 5t^2 + 4}, \frac{6t(t^2 - 2)}{t^4 + 5t^2 + 4} \right) \end{aligned}$$

for  $t \in \mathbb{R}$ . Now, we have

$$W_{1,2} = 1, \quad W_{2,3} = \frac{3(t + 2i)}{t - 2i}, \quad W_{3,4} = \frac{-3(t + i)}{t - i}, \quad W_{4,1} = \frac{-(t + i)(t + 2i)}{(t - i)(t - 2i)}.$$

Hence, the only nontrivial valuations correspond to the polynomials  $t \pm i$  and  $t \pm 2i$ . They give two pairs of conjugated NAC-colorings by taking a suitable threshold  $\alpha \in \{-1, 0\}$ , see Table 2.1 and Figure 2.1. We remark that  $|\text{NAC}_Q(\mathcal{C})| = 4$ , whereas  $|\text{NAC}_Q| = 6$ . The two non-active NAC-colorings correspond to the degenerate motion of  $(Q, \lambda)$ , where the vertices 2 and 4 coincide.

The following example illustrates the opposite implication of the proof of Theorem 2.7, i.e., how a flexible labeling is constructed from a NAC-coloring.

## 2. Existence of a Flexible Labeling

edge	$\lambda$	$\nu_{t+i}$	$\delta_1$	$\nu_{t-i}$	$\bar{\delta}_1$	$\nu_{t+2i}$	$\delta_2$	$\nu_{t-2i}$	$\bar{\delta}_2$
$\{1, 2\}$	1	0	blue	0	red	0	blue	0	red
$\{2, 3\}$	3	0	blue	0	red	1	red	-1	blue
$\{3, 4\}$	3	1	red	-1	blue	0	blue	0	red
$\{1, 4\}$	1	1	red	-1	blue	1	red	-1	blue

Table 2.1.: Valuations giving the active NAC-colorings of a deltoid.

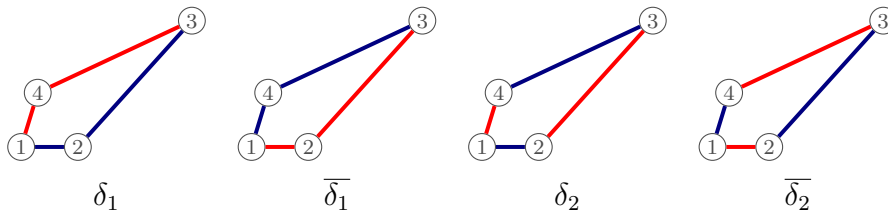
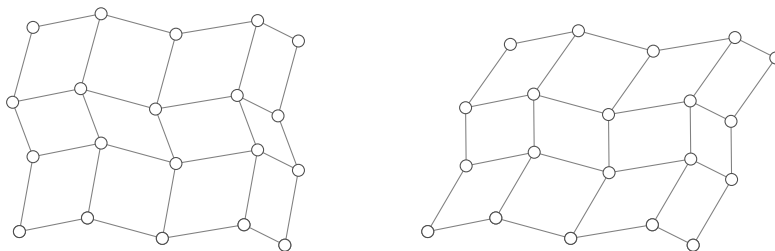


Figure 2.1.: Active NAC-colorings of a deltoid.

**Example 2.9.** In Figure 2.2, a graph with its NAC-colorings and realizations compatible with the constructed flexible labelings are shown. Note that for the first two colorings we have overlapping vertices in the realizations. For the last coloring this does not happen. However, there are some non-visible edges. A generalization of  $\rho_\alpha$  can prevent from this (see below).

In order to have more flexibility in the choice of lengths of a flexible labeling, we modify the “ $\Leftarrow$ ” part of the proof of Theorem 2.7 by using a “zigzag” grid instead of the normal one.



Let  $R_0, \dots, R_m$  and  $B_0, \dots, B_n$  be as before. Let  $a_0, \dots, a_n$  and  $b_0, \dots, b_m$  be pairwise distinct vectors in  $\mathbb{R}^2$  such that  $a_0 = b_0 = (0, 0)$ . For  $\alpha \in [0, 2\pi)$ , we define a map  $\rho'_\alpha: V_G \rightarrow \mathbb{R}^2$  by

$$\rho'_\alpha(v) = \begin{pmatrix} \cos \alpha & \sin \alpha \\ -\sin \alpha & \cos \alpha \end{pmatrix} \cdot a_j + b_i,$$

where  $i$  and  $j$  are such that  $v \in R_i \cap B_j$ . The map  $\rho'_\alpha$  gives a labeling  $\lambda'_\alpha: E_G \rightarrow \mathbb{R}_+$ , where

$$\lambda'_\alpha(uv) = \|\rho'_\alpha(u) - \rho'_\alpha(v)\| = \left\| \begin{pmatrix} \cos \alpha & \sin \alpha \\ -\sin \alpha & \cos \alpha \end{pmatrix} \cdot (a_j - a_l) + (b_i - b_k) \right\|$$

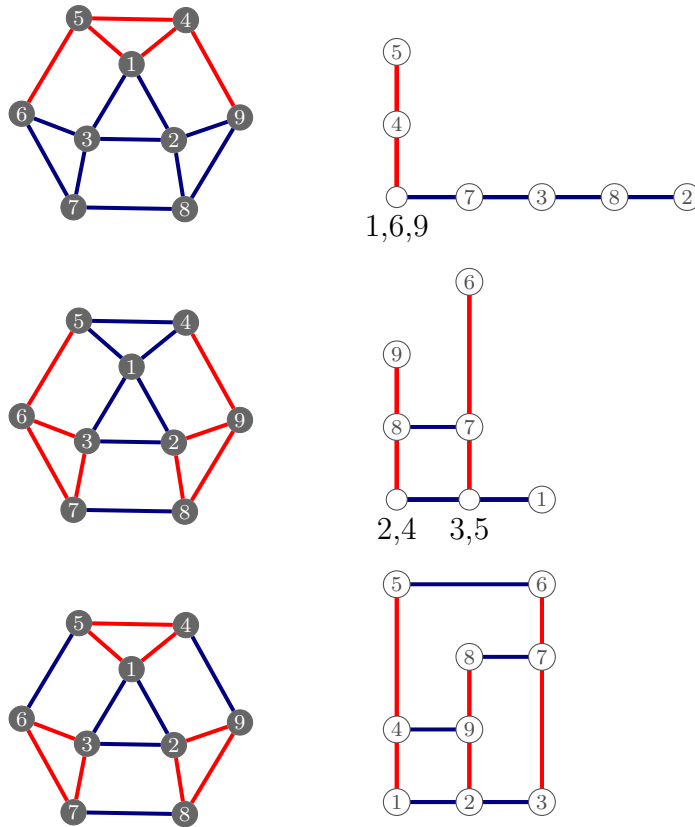


Figure 2.2.: For each NAC-coloring (left side), the proof of the implication  $\Leftarrow$  of Theorem 2.7 gives a flexible labeling together with a curve of realizations. In these realizations (right side), vertex positions may coincide or line segments may overlap.

for all edges  $uv \in E_G$  and  $i, j, k, l$  such that  $u \in R_i \cap B_j$  and  $v \in R_k \cap B_l$ . If  $uv$  is red, then  $i = k$  and we have

$$\lambda'_\alpha(uv) = \left\| \begin{pmatrix} \cos \alpha & \sin \alpha \\ -\sin \alpha & \cos \alpha \end{pmatrix} \cdot (a_j - a_l) \right\| = \|a_j - a_l\|.$$

If  $uv$  is blue, then  $j = l$  and hence

$$\lambda'_\alpha(uv) = \|(b_i - b_k)\|.$$

Therefore,  $\lambda'_\alpha$  is independent of  $\alpha$ , let  $\lambda' = \lambda'_{\frac{\pi}{2}}$ . Moreover, the codomain of  $\lambda'$  is indeed  $\mathbb{R}_+$ : if  $\lambda'(uv) = 0$  for some edge  $uv \in E_G$ , then both  $u$  and  $v$  belong to the same  $R_i \cap B_j$ , which leads to a contradiction in the same way as in the previous proof. To conclude, the labeling  $\lambda'$  is flexible since there are infinitely many realizations  $\rho'_\alpha$  which are non-congruent as  $\delta$  is surjective.

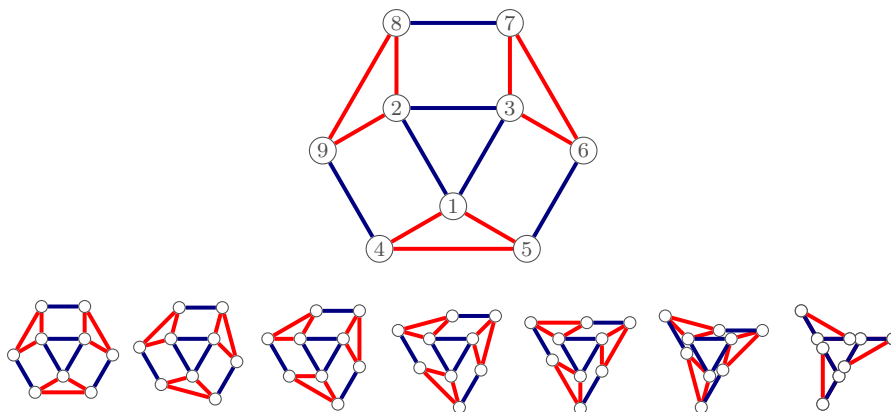
We apply this construction to the previous example.

**Example 2.10.** We consider the last coloring from Example 2.9; we keep the order of equivalence classes and fix

$$a_0 = (0, 0), \quad a_1 = \left(-\frac{3\sqrt{3}}{8}, -\frac{3}{8}\right), \quad a_2 = \left(0, \frac{3}{4}\right), \quad a_3 = \left(\frac{3\sqrt{3}}{8}, -\frac{3}{8}\right),$$

$$b_0 = (0, 0), \quad b_1 = \left(-\frac{1}{2}, \frac{\sqrt{3}}{2}\right), \quad b_2 = \left(\frac{1}{2}, \frac{\sqrt{3}}{2}\right).$$

Then we get the following flexible realization. The flexibility comes from rotating the outer triangles around the vertices of the inner triangle respectively.



Now, we discuss whether all NAC-colorings of a graph are obtained from some curve of realizations compatible with a flexible labeling, or if all flexible labelings of a graph can be expressed in terms of “zigzag” grid construction.

We have seen in Example 2.8 that the active NAC-colorings of the deltoid motion are not all NAC-coloring of the 4-cycle. But every NAC-coloring is active for some algebraic motion. Namely, we show that if we start with a NAC-coloring  $\delta$  of  $G$  and apply the construction  $\Leftarrow$  to get an algebraic motion  $\mathcal{C}$  compatible with a flexible labeling  $\lambda$ , then the construction  $\Rightarrow$  applied on  $\mathcal{C}$  gives back the NAC-coloring  $\delta$ , i.e.,  $\delta$  is an active NAC-coloring of  $\mathcal{C}$ .

Let  $\lambda$  be a labeling and  $\rho_\alpha$  realizations obtained as in the  $\Leftarrow$  part of the proof of Theorem 2.7. The realizations  $\rho_\alpha$  for  $\alpha \in [0, 2\pi)$  give a parametrization of an irreducible curve  $\mathcal{C}$  of realizations compatible with  $\lambda$ . If  $uv \in E_G$  is an edge such that  $\delta(uv) = \text{red}$ , then there are indices  $j, k, l \in \mathbb{N}$  such that  $u \in R_j \cap B_k$  and  $v \in R_j \cap B_{k+l}$ . Hence

$$\begin{aligned} W_{v,u} &= j + k \cos \alpha - (j + (k + l) \cos \alpha) + i(k \sin \alpha - (k + l) \sin \alpha) \\ &= -l(\cos \alpha + i \sin \alpha). \end{aligned}$$

Therefore,  $z = \cos \alpha + i \sin \alpha$  is a transcendental element of the complex function field of  $\mathcal{C}$  and there is a valuation  $\nu$  such that  $\nu(z) = 1$  and  $\nu(\mathbb{C}) = \{0\}$  by Chevalley’s Theorem. Thus,  $\nu(W_e) = 1$  for all  $e \in E_G$  such that  $\delta(e) = \text{red}$ . On the other hand,

if  $u'v' \in E_G$  is such that  $\delta(u'v') = \text{blue}$ , that means  $u' \in R_{j'} \cap B_{k'}$  and  $v' \in R_{j'+l'} \cap B_{k'}$  for some  $j', k', l' \in \mathbb{N}$ , then

$$W_{v',u'} = j' + k' \cos \alpha - ((j' + l') + k' \cos \alpha) + i(k' \sin \alpha - k' \sin \alpha) = -l'.$$

Therefore,  $\nu(W_{e'}) = 0$  for all  $e' \in E_G$  such that  $\delta(e') = \text{blue}$ . We showed that the construction from a flexible labeling  $\lambda$  gives the coloring  $\delta$ , since the valuation of red edges is positive and the valuation of blue edges is zero.

While every NAC-coloring comes from a flexible labeling, there are flexible labelings which cannot be obtained by a “zigzag” grid. This can be seen already on the quadrilateral — the described construction always assigns same lengths to the opposite edges in a 4-cycle, but there are also flexible labelings with different lengths. Another example is  $K_{2,3}$ . A generic labeling of  $K_{2,3}$  is flexible and the realizations are injective, but at least two vertices coincide in the grid construction from any possible NAC-coloring (see Figure 2.3). On the other hand, if there is a NAC-coloring such that  $|B_i \cap R_j| \leq 1$  for all  $i, j$ , then there is a curve of injective realizations compatible with the obtained flexible labeling. We use this observation later in Chapter 3.

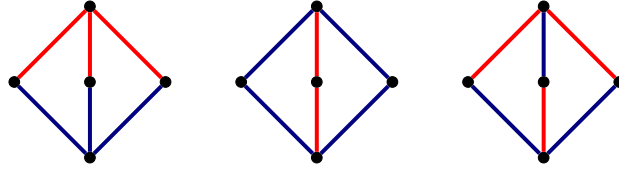


Figure 2.3.: NAC-colorings of  $K_{2,3}$ .

We conclude this section by two technical lemmas. The first one describes independence of active NAC-colorings on the choice of the fixed edge.

**Lemma 2.11.** *Let  $G$  be a graph with a flexible labeling  $\lambda$ . If  $\mathcal{C}_{u',v'}$  and  $\mathcal{C}_{\bar{u},\bar{v}}$  are as in Lemma 1.8, then  $\text{NAC}_G(\mathcal{C}_{u',v'}) = \text{NAC}_G(\mathcal{C}_{\bar{u},\bar{v}})$ .*

*Proof.* Let  $\delta \in \text{NAC}_G(\mathcal{C}_{\bar{u},\bar{v}})$ , i.e., there exists a valuation  $\bar{\nu}$  of  $F(\mathcal{C}_{\bar{u},\bar{v}})$  and  $\alpha \in \mathbb{Q}$  such that  $\delta(uv) = \text{red} \iff \bar{\nu}(W_{u,v}^{\bar{u}\bar{v}}) > \alpha$  for all  $uv \in E_G$ . Let  $\varphi_{u',v'} : \mathcal{C}_{\bar{u},\bar{v}} \rightarrow \mathcal{C}_{u',v'}$  be the birational map from Lemma 1.8. Hence, there is a function field isomorphism  $\phi : F(\mathcal{C}_{u',v'}) \rightarrow F(\mathcal{C}_{\bar{u},\bar{v}})$  given by  $f \mapsto f \circ \varphi_{u',v'}$ . We define a valuation  $\nu'$  of  $F(\mathcal{C}_{u',v'})$  by  $\nu'(f) := \bar{\nu}(\phi(f))$ . If  $W_{u,v}^{u'v'} \in F(\mathcal{C}_{u',v'})$ , then

$$\begin{aligned} W_{u,v}^{u'v'} \circ \varphi_{u',v'} &= \left( (x_v - x_u)(x_{v'} - x_{u'}) + (y_v - y_u)(y_{v'} - y_{u'}) \right) / \lambda(u'v') \\ &\quad + i \left( (y_v - y_u)(x_{v'} - x_{u'}) - (x_v - x_u)(y_{v'} - y_{u'}) \right) / \lambda(u'v') \\ &= \left( (x_v - x_u) + i(y_v - y_u) \right) \cdot \left( (x_{v'} - x_{u'}) - i(y_{v'} - y_{u'}) \right) / \lambda(u'v'). \end{aligned}$$

Therefore,  $\nu'(W_{u,v}^{u'v'}) = \bar{\nu}(W_{u,v}^{\bar{u}\bar{v}}) + \bar{\nu}(Z_{u',v'}^{\bar{u}\bar{v}})$ . This concludes the proof, since

$$\delta(uv) = \text{red} \iff \bar{\nu}(W_{u,v}^{\bar{u}\bar{v}}) > \alpha \iff \nu'(W_{u,v}^{u'v'}) > \alpha + \bar{\nu}(Z_{u',v'}^{\bar{u}\bar{v}}).$$

□

Finally, we show that the set of active NAC-colorings is closed under conjugation.

**Lemma 2.12.** *Let  $\lambda$  be a flexible labeling of a graph  $G$ . Let  $\mathcal{C}$  be an algebraic motion of  $(G, \lambda)$ . If  $\delta, \bar{\delta} \in \text{NAC}_G$  are conjugated, then  $\delta \in \text{NAC}_G(\mathcal{C})$  if and only if  $\bar{\delta} \in \text{NAC}_G(\mathcal{C})$ .*

*Proof.* Let  $\delta$  be an active NAC-coloring of  $G$  w.r.t.  $\mathcal{C}$  given by a valuation  $\nu$  of  $F(\mathcal{C})$  and a threshold  $\alpha$ . Since the algebraic motion  $\mathcal{C}$  is a real algebraic curve, it has complex conjugation defined on its complex points. This induces another valuation  $\bar{\nu}$  of  $F(\mathcal{C})$  given by  $\bar{\nu}(f) := \nu(\bar{f})$  for any  $f \in F(\mathcal{C})$ , where  $\bar{f}$  is given by  $\bar{f}(\rho) := \overline{f(\bar{\rho})}$  for every  $\rho \in \mathcal{C}$ . If  $\beta = \max\{\nu(Z_e) : \nu(Z_e) < -\alpha, e \in E_G\}$ , then  $\bar{\nu}$  and  $\beta$  satisfy (2.3) for  $\bar{\delta}$ , since for every edge  $e \in E_G$ :

$$\begin{aligned} \delta(e) = \text{red} &\iff \alpha < \nu(W_e) \iff -\alpha > \nu(Z_e) \\ &\iff \beta \geq \nu(Z_e) \iff \beta \geq \bar{\nu}(W_e) \iff \bar{\delta}(e) = \text{blue}. \end{aligned}$$

Namely,  $\bar{\delta}$  is in  $\text{NAC}_G(\mathcal{C})$ . □

## 2.2. Graphs with NAC-colorings

At the beginning of this section we explore the fact that every labeling of the triangle graph  $C_3$  is rigid. Hence, it is natural to expect that subgraphs which “consist of triangles” are also always rigid. We give a necessary condition of the existence of a NAC-coloring based on this. Next, we provide some sufficient conditions and prove an upper bound on the number of edges allowing a flexible labeling.

The notion of  $\Delta$ -connected-ness (“triangle-connected-ness”) makes the intuition of “consisting of triangles” precise.

**Definition 2.13.** *Let  $G$  be a graph. Let  $\sim'_\Delta$  be a relation on  $E_G \times E_G$  such that  $e_1 \sim'_\Delta e_2$  if and only if there exists a triangle subgraph  $C_3$  of  $G$  such that  $e_1, e_2 \in E_{C_3}$ . Let  $\sim_\Delta$  be the reflexive-transitive closure of  $\sim'_\Delta$ . The graph  $G$  is called  $\Delta$ -connected if  $e_1 \sim_\Delta e_2$  for all  $e_1, e_2 \in E_G$ . An edge  $e \in E_G$  is called a connecting edge if it belongs to no triangle subgraph.*

Note that the graph consisting of a single edge is therefore  $\Delta$ -connected. Now we can justify the fact that  $\Delta$ -connected subgraphs of a graph are indeed always rigid, since their edges are colored by the same color.



**Lemma 2.14.** *Let  $\delta$  be a NAC-coloring of a graph  $G$ . If  $H$  is a  $\Delta$ -connected subgraph of  $G$ , then  $\delta(e) = \delta(e')$  for all  $e, e' \in E_H$ .*

*Proof.* The claim follows from the fact that  $\sim_\Delta$  is the reflexive-transitive closure of  $\sim'_\Delta$  and all edges of a triangle must have the same color.  $\square$

An immediate consequence of Lemma 2.14 is a necessary condition for the existence of a NAC-coloring.

**Theorem 2.15.** *If a graph  $G$  has a NAC-coloring, then there is no subgraph  $H$  of  $G$  such that  $V_G = V_H$  and  $H$  is  $\Delta$ -connected.*

*Proof.* Assume that there is such a subgraph  $H$ . By Lemma 2.14, all edges of  $H$  must be colored by the same color, let us say red. Since  $H$  spans the whole  $G$ , also the edges in  $E_G \setminus E_H$  must be red according to Lemma 2.2. This contradicts the surjectivity of the NAC-coloring.  $\square$

We remark that the fact that a graph is not spanned by a  $\Delta$ -connected subgraph is a necessary condition, not sufficient. Some counterexamples, i.e., graphs without a NAC-coloring which are not spanned by a  $\Delta$ -connected subgraph, are shown in Figure 2.4. In Section 2.3 we discuss a class of graphs for which this might indeed be a sufficient condition.

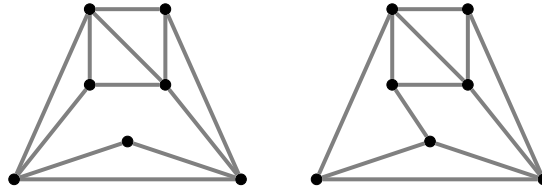


Figure 2.4.: Graphs which are not  $\Delta$ -connected and have no NAC-coloring.

We focus now on some sufficient conditions for the existence of a NAC-coloring. Obviously, if a graph is disconnected in a way that at least two components contain an edge, then a NAC coloring can be obtained by coloring all edges in one of these components to red and the rest to blue. The coloring is surjective and there might be only red cycles or blue cycles.

The following two theorems and corollary construct a NAC-coloring for connected graphs satisfying certain sufficient conditions.

**Theorem 2.16.** *Let  $G$  be a connected graph. If there exists an independent set of vertices  $V_c$  which separates  $G$ , then  $G$  has a NAC-coloring.*

*Proof.* We recall that a set of vertices is independent, if no two vertices of it are connected by an edge. The assumption that  $V_c$  separates  $G$  means that the subgraph  $H$  of  $G$  induced by  $V_G \setminus V_c$  is disconnected. Let  $M$  be a connected component of  $H$ . Set

$$\delta(e) = \begin{cases} \text{red} & \text{if } e \cap V_M \neq \emptyset \\ \text{blue} & \text{otherwise,} \end{cases}$$

for all  $e \in E_G$ . Now if  $uv, u'v \in E_G$  are edges such that  $\delta(uv) \neq \delta(u'v)$ , then  $v \in V_c$ . Hence, there is no almost red cycle or almost blue cycle since vertices of  $V_c$  are nonadjacent by assumption.  $\square$

**Corollary 2.17.** *Let  $G$  be a connected graph such that  $|E_G| \geq 2$ . If there is a vertex  $v$  such that it is not contained in any 3-cycle subgraph of  $G$ , then the graph  $G$  has a NAC-coloring.*

*Proof.* If  $G$  is a star graph, i.e, there is a vertex  $u$  such that  $V_G \setminus \{u\}$  is an independent set, then it has clearly a NAC-coloring. Otherwise, the neighbors of  $v$  separate  $G$  and are nonadjacent by assumption. Thus, there is a NAC-coloring by Theorem 2.16.  $\square$

**Theorem 2.18.** *Let  $G$  be a connected graph,  $|E_G| \geq 2$ . If there is a set  $E_c$  of connecting edges of  $G$  such that  $E_c$  separates  $G$  and the subgraph  $(V_G, E_c)$  contains no path of length four, then  $G$  has a NAC-coloring.*

*Proof.* Let  $E'_c$  be a minimal subset of  $E_c$  which separates  $G$ , i.e.,  $E'_c$  is a minimal subset of  $E_c$  such that  $G' = (V_G, E_G \setminus E'_c)$  is disconnected. Set

$$\delta(e) = \begin{cases} \text{red} & \text{if } e \in E'_c \\ \text{blue} & \text{otherwise,} \end{cases}$$

for all  $e \in E_G$ . The existence of an almost blue cycle with a red edge  $u_r v_r$  contradicts the minimality of  $E'_c$ : since  $u_r$  and  $v_r$  are connected by a blue path, they belong to the same connected component in  $G'$ . Hence,  $E'_c \setminus \{u_r v_r\}$  separates  $G$ .

On the other hand, assume that there exists an almost red cycle  $C$ . Since there is no path of length four in the subgraph  $(V_G, E_c)$ , the length of  $C$  is three or four. The length three contradicts the assumption that the red edges are in  $E_c$ , i.e., they are connecting edges. If  $C$  has length four and the red edges are  $u_1 u_2, u_2 u_3, u_3 u_4$ , then  $G'$  has at least three connected components, since there are no almost blue cycles, i.e.,  $u_1$  and  $u_4$  are in a different component than  $u_2$  and  $u_3$ , and  $u_2$  and  $u_3$  are not in the same component. But the minimality of  $E'_c$  implies that  $G'$  has only two connected components which is a contradiction.

The surjectivity of  $\delta$  follows from minimality of  $E_c$  and the assumption  $|E_G| \geq 2$ .  $\square$

A graph which does not satisfy the assumption of Theorem 2.16 neither Theorem 2.18, but still has a NAC-coloring is shown in Figure 2.5.

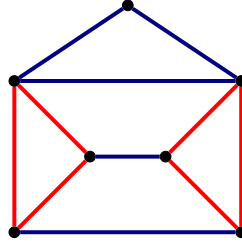


Figure 2.5.: A graph with a NAC-coloring which has no independent separating set of vertices or separating set of connecting edges.

Figure 2.6 shows two graphs with  $n = 6$  vertices and  $\frac{n(n-1)}{2} - (n - 2) = 11$  edges. Both have a flexible labeling according to Corollary 2.17. We show now that this is the maximal number of edges that allows a flexible labeling.

**Theorem 2.19.** *Let  $G$  be a graph,  $n = |V_G|$ . If  $G$  has a flexible labeling, then  $|E_G| \leq \frac{n(n-1)}{2} - (n - 2)$ .*

*Proof.* We can assume that  $G$  is connected, since a disconnected graph has at most  $\frac{n(n-1)}{2} - (n - 1)$  edges. If a graph has a flexible labeling, then it is not  $\Delta$ -connected by Theorem 2.15. Hence, there are two adjacent edges  $vu_1$  and  $vu_2$  such that  $vu_1 \approx_{\Delta} vu_2$ . Thus,  $u_1u_2 \notin E_G$ . Let  $u_3, \dots, u_k$  be the other neighbors of  $v$ . For all  $i \in \{3, \dots, k\}$ , we have  $u_iu_1 \notin E_G$  or  $u_iu_2 \notin E_G$ , otherwise  $vu_1 \sim_{\Delta} vu_2$ . Since the complete graph on  $n$  vertices has  $\frac{n(n-1)}{2}$  edges and  $n - 1 - k$  vertices are not neighbors of  $v$ , we have

$$|E_G| \leq \frac{n(n-1)}{2} - 1 - (k-2) - (n-1-k) = \frac{n(n-1)}{2} - (n-2).$$

□

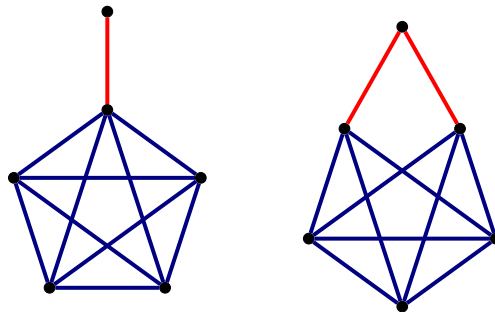


Figure 2.6.: Two examples of graphs with a NAC-coloring on 6 vertices and 11 edges (which is the maximal number).

### 2.3. A Conjecture on Laman graphs

In this section, we give a conjectural characterization of the Laman graphs that have a flexible labeling. By a computer search, we verified the conjecture for all Laman graphs with at most 12 vertices. In order to prove the conjecture, it would suffice to prove it for “problematic cases”, to be defined in Definition 2.21.

**Conjecture 2.20.** *Let  $G$  be a Laman graph. If  $G$  is not  $\Delta$ -connected, then it has a NAC-coloring, i.e., it has a flexible labeling.*

To support the conjecture, we prove it for a large class of Laman graphs in Theorem 2.24 using the Henneberg construction of Laman graphs. The following definition classifies those graphs for which the theorem does not apply. However, for all known examples of such graphs, we can still find a NAC-coloring. One example of such a graph is given in Figure 2.7.

**Definition 2.21.** *A Laman graph  $G$  is called problematic, if the following hold:*

- (i)  $\deg_G v \geq 3$  for all  $v \in V_G$ ,
- (ii) if  $\deg_G v = 3$ , then exactly two neighbors of  $v$  are connected by an edge and both have degree at least 4,
- (iii) all vertices are in some triangle subgraph  $C_3$  of  $G$ .

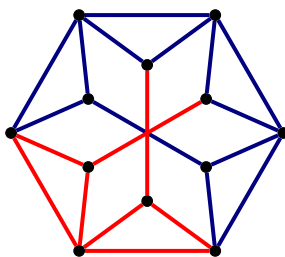


Figure 2.7.: A problematic graph on 12 vertices with a NAC-coloring.

We prove two technical lemmas which are needed in the proof of Theorem 2.24.

**Lemma 2.22.** *Let  $G$  be a Laman graph. Let  $G$  contain a triangle induced by vertices  $u, v, u_1 \in V_G$  such that*

- (i)  $\deg_G u = \deg_G v = 3$  and  $\deg_G u_1 > 3$ ,
- (ii)  $wu_2 \in E_G$ , where  $w \in V_G \setminus \{v, u_1\}$  is the third neighbor of  $u$ , and  $u_2 \in V_G \setminus \{u, u_1\}$  is the third neighbor of  $v$ , and

(iii)  $wu_1, u_1u_2 \notin E_G$ .

Then there is a Laman graph  $G' = (V', E')$  such that  $G$  is constructed from  $G'$  by a Henneberg move IIb by linking the vertex  $v$  to the vertices  $u, u_1, u_2 \in V'$  such that  $uu_1 \in E', uu_2 \notin E'$  and removing the edge  $u_1u_2 \in E'$ , or the situation is symmetric by replacing  $v$  by  $u$  and  $w$  by  $u_2$ .

*Proof.* See Figure 2.8 for the sketch of the situation. According to Theorem 6.4 in [37], we can revert a Henneberg move II by removing the vertex  $v$  and adding the edge between two of its neighbors, namely  $u_1$  and  $u_2$ , if there exists no subgraph  $M$  of  $G \setminus v = (V_G \setminus \{v\}, \{e \in E_G : v \notin e\})$  such that  $u_1, u_2 \in V_M$  and  $|E_M| = 2|V_M| - 3$ . Or the vertex  $u$  can be removed and the edge  $u_1w$  be added if there is no subgraph  $L$  of  $G \setminus u$  such that  $u_1, w \in V_L$  and  $|E_L| = 2|V_L| - 3$ .

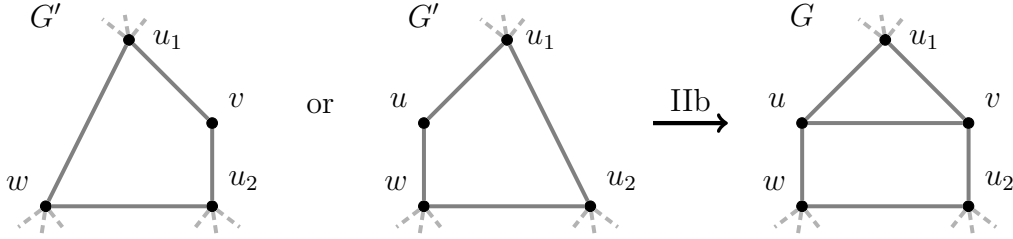


Figure 2.8.: Undoing Henneberg move IIb.

Assume on the contrary that such subgraphs  $M$  and  $L$  exist. Obviously,  $u \notin V_M$ , resp.  $v \notin V_L$ , since otherwise the subgraph  $(V_M \cup \{v\})$ , resp.  $(V_L \cup \{u\})$ , of  $G$  has too many edges. We consider the subgraph  $H$  of  $G$  induced by  $V_H = V_M \cup V_L \cup \{u, v\}$ . If  $V_M \cap V_L = \{u_1\}$ , then

$$\begin{aligned} |E_H| &\geq |E_M| + |E_L| + 6 = 2|V_L| + 2|V_M| = 2(|V_M \cup V_L|) + 2 \\ &= 2(|V_M \cup V_L \cup \{u, v\}|) - 2 = 2|V_H| - 2, \end{aligned}$$

which contradicts Laman's condition. If  $|V_M \cap V_L| \geq 2$ , then the subgraph  $M \cup L$  of  $G$  induced by  $V_M \cup V_L$  satisfies  $|E_{M \cup L}| = 2|V_{M \cup L}| - 3$  by Lemma 6.2 in [37] and we have

$$\begin{aligned} |E_H| &= |E_{M \cup L}| + 5 = 2|V_{M \cup L}| - 3 + 5 = 2(|V_{M \cup L}| + 2) - 2 \\ &= 2(|V_M \cup V_L \cup \{u, v\}|) - 2 = 2|V_H| - 2, \end{aligned}$$

which is also a contradiction. □

**Lemma 2.23.** *If  $T$  is a  $\Delta$ -connected Laman graph, then  $T$  has at least two vertices of degree two.*

*Proof.* The claim is trivial for  $|V_T| \leq 4$ . We proceed by induction on the Henneberg construction. The last Henneberg step in the construction of  $T$  can only be of type Ia

or IIc. If it is Ia, then the number of vertices of degree two obviously remains or increases, because if  $|V_T| \geq 4$ , then there are no adjacent vertices of degree two.

If the step is of type IIc, let  $T$  be constructed from  $T'$  so that a new vertex  $v$  is linked by edges to the vertices  $u, u_1, u_2 \in T_{V'}$ ,  $uu_1, uu_2 \in E_{T'}$  and the edge  $u_1u_2 \in E_{T'}$  is removed. Only the degree of  $u$  increases, so we assume that  $\deg_{T'} u = 2$ . But then  $T'$  is just a triangle, otherwise  $T$  is not  $\Delta$ -connected. Hence, the number of vertices of  $T$  of degree two is still at least two.  $\square$

Now we have all necessary tools to show that the conjecture holds for all Laman graphs which are not constructed by Henneberg steps from problematic ones. We prove even more, namely, the conjecture is true if we could show that all problematic graphs have a NAC-coloring.

**Theorem 2.24.** *Let  $G$  be a Laman graph. If  $G$  is not  $\Delta$ -connected, then it has a NAC-coloring, or there exists a problematic graph  $\tilde{G}$  with no NAC-coloring such that  $G$  can be constructed from  $\tilde{G}$  by Henneberg steps (possibly  $G = \tilde{G}$ ).*

*Proof.* We proceed by induction on the Henneberg construction. Let  $G'$  be a graph such that  $G$  is obtained from  $G' = (V', E')$  by adding a vertex  $v$  by a Henneberg move. We distinguish five cases according to Definition 1.5.

Ia: Let  $v$  be constructed by a Henneberg move of type Ia from vertices  $u, u'$  and  $uu' \in E_G$ . The graph  $G'$  is  $\Delta$ -connected if and only if  $G$  is  $\Delta$ -connected. If  $G'$  has a NAC-coloring  $\delta'$ , then we define a NAC-coloring  $\delta$  of  $G$  by  $\delta|_{E'} = \delta'$  and  $\delta(uv) = \delta(u'v) := \delta'(uu')$ . Otherwise, we have a problematic graph  $\tilde{G}$  from the induction hypothesis.

Ib and IIa: The vertex  $v$  is not in any triangle, so there is a NAC-coloring by Corollary 2.17.

IIc: We may assume that there are no vertices of degree two in  $G$ , otherwise a previous case applies. Let  $v$  be constructed so that it is linked by edges to the vertices  $u, u_1, u_2 \in V'$  such that  $uu_1, uu_2 \in E'$  and the edge  $u_1u_2 \in E'$  is removed. If  $G'$  is not  $\Delta$ -connected, then there is a problematic graph  $\tilde{G}$  without any NAC-coloring, or  $G'$  has a NAC-coloring  $\delta'$  and we define a NAC-coloring  $\delta$  of  $G$  by  $\delta|_{E'} = \delta'$  and  $\delta(uv) = \delta(u_1v) = \delta(u_2v) := \delta'(u_1u_2)$ . Otherwise,  $G'$  has at least two vertices of degree two by Lemma 2.23. But the degrees of vertices in  $G$  and  $G'$  are the same except for  $u$ . Hence, there must be a vertex of degree two in  $G$ , which contradicts our assumption.

IIb: We may assume that there is no  $G'$  from which  $G$  can be constructed by Ia,b or IIa,c, i.e., all vertices of  $G$  have degree at least four or can be constructed by IIb. Note that if  $t$  denotes the number of vertices of degree three, then  $t \geq 6$ :

$$2|V_G| - 3 = |E_G| = \frac{1}{2} \sum_{w \in V_G} \deg_G w \geq \frac{1}{2} \cdot 4(|V_G| - t) + \frac{1}{2} \cdot 3t = 2|V_G| - \frac{t}{2}.$$

If there are three vertices in a triangle in  $G$  such that all of them have degree three, then there is a NAC-coloring by Theorem 2.18.

Let there be a triangle induced by vertices  $u, v, u_1 \in V_G$  such that  $\deg_G u = \deg_G v = 3$  and  $\deg_G u_1 > 3$ . Let  $w \in V_G \setminus \{v, u_1\}$  be the third neighbor of  $u$  and  $u_2 \in V_G \setminus \{u, u_1\}$  be the third neighbor of  $v$ . We remark that the vertices  $w$  and  $u_1$ , resp.  $u_1$  and  $u_2$ , are nonadjacent, otherwise  $u$ , resp.  $v$ , could be constructed by IIc. There are two possibilities: if  $wu_2 \notin E_G$ , then  $\{u_1, u_2, w\}$  separates  $G$  and hence, there is a NAC-coloring by Theorem 2.16.

If  $wu_2 \in E_G$ , then Lemma 2.22 justifies that there is a  $G'$  with the property that the vertex  $v$  is constructed by linking to the vertices  $u, u_1, u_2 \in V'$  such that  $uu_1 \in E'$ ,  $uu_2 \notin E'$  and the edge  $u_1u_2 \in E'$  is removed, or the situation is symmetric by replacing  $v$  by  $u$  and  $w$  by  $u_2$ . Assume the former one, see Figure 2.9. Since the degree of  $u$  in  $G'$  is two,  $G'$  can be obtained from  $G''$  by adding the vertex  $u$  by Henneberg move Ib.

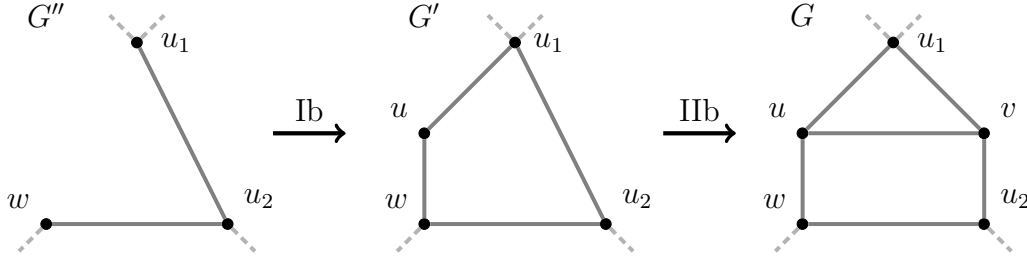


Figure 2.9.: Undoing Henneberg move IIb and Ib (dashed edges illustrate the minimal degrees).

Since  $\deg_G u_1 > 3$ ,  $\deg_G u_2 \geq 3$  and  $\deg_G w \geq 3$ , we have  $\deg_{G''} u_1 \geq 3$ ,  $\deg_{G''} u_2 \geq 3$  and  $\deg_{G''} w \geq 2$ . Assume that  $G''$  is  $\Delta$ -connected. There are at least two vertices of degree two in  $G''$  by Lemma 2.23. Hence, there is a vertex  $v' \in V_{G''} \setminus \{u_1, u_2, w\}$  of degree two. But  $\deg_{G''} v' = \deg_G v'$  which contradicts that all vertices of  $G$  have degree at least three. Thus,  $G''$  is not  $\Delta$ -connected.

By the induction hypothesis, there is a problematic graph  $\tilde{G}$  without any NAC-coloring or  $G''$  has a NAC-coloring  $\delta''$ . If the latter holds, we obtain a NAC-coloring  $\delta$  of  $G$  from  $\delta''$  in the following way:  $\delta|_{E''} = \delta''$ ,  $\delta(uw) := \delta''(wu_2)$  and  $\delta(u_1v) = \delta(u_2v) = \delta(wu_1) = \delta(uv) := \delta''(u_1u_2)$ . There is no almost blue or almost red cycle in  $G$ , since its existence would contradict that  $\delta''$  is a NAC-coloring of  $G''$ .

The remaining graphs are such that all vertices have degree at least three and if  $v$  has degree three, then precisely two neighbors  $u, u_1$  of  $v$  are adjacent and have degree at least four. If  $G$  has a vertex which is not in any triangle, then there is a NAC-coloring by Corollary 2.17. Hence,  $\tilde{G} = G$  is problematic for the remaining cases.  $\square$

## 2.4. Flexible Labelings in Dimension Three

It turns out that the question of existence of a flexible labeling for a given graph is much easier when we consider a straightforward modification of the definitions replacing  $\mathbb{R}^2$  by  $\mathbb{R}^3$ . We get the following result.

**Proposition 2.25.** *If  $G$  is a graph that is not complete, then there exists a labeling with infinitely many non-congruent compatible realizations in  $\mathbb{R}^3$ .*

*Proof.* Let  $u$  and  $v$  be two nonadjacent vertices of  $G$ . Let  $\alpha \in [0, 2\pi]$ . We define a realization  $\rho$  by  $\rho(u) = (1, 0, 0)$ ,  $\rho(v) = (\cos \alpha, 1, \sin \alpha)$  and  $\rho(w) = (0, y_w, 0)$  for  $w \in V_G \setminus \{u, v\}$ , where  $y_w$  are pairwise distinct real numbers. The induced labeling is independent of  $\alpha$  and therefore flexible.  $\square$

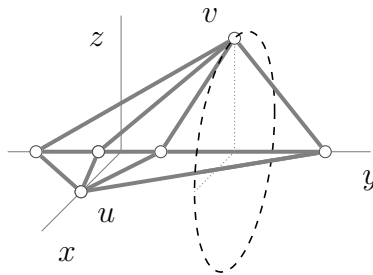


Figure 2.10.: Flexible labeling in  $\mathbb{R}^3$  of a graph with nonadjacent vertices  $u$  and  $v$ .

## Implementation

We briefly describe the parts of the package `FlexRiLoG` that are relevant for this chapter.

### `NACcoloring`

`is_NAC_coloring()` checks whether the coloring is a NAC-coloring using Lemma 2.2.

`grid_coordinates()` returns the coordinates of the vertices in the grid construction described in the proof of Theorem 2.7.

`conjugated()` returns the conjugated NAC-coloring.



## FlexRiGraph

**triangle\_connected\_components()** identifies all maximal  $\Delta$ -connected subgraphs.

**NAC\_colorings()** lists all NAC-colorings of the graph using the following brute force algorithm: by Lemma 2.14, all edges in each  $\Delta$ -connected component obtained by **triangle\_connected\_components()** have the same color. All possible ways of coloring the components are checked by **is\_NAC\_coloring()**. The result is cached in the object.

**has\_NAC\_coloring()** checks if at least one NAC-coloring exists, either from the cache or by running **NAC\_colorings()** until a first NAC-coloring is found (or none).

## GraphMotion/ParametricGraphMotion

**ParametricMotion(*graph*, *parametrization*)** is a factory method creating an instance of **ParametricGraphMotion** for a *graph* with a given *parametrization*.

**Deltoid()** returns the motion of the deltoid in Example 2.8.

**GridConstruction(*graph*, *NAC\_coloring*)** returns the motion of a *graph* coming from a *NAC\_coloring* according to the proof of Theorem 2.7. It supports also the generalized “zigzag” grid construction.

**fix\_edge(*edge*)** sets the *edge* to be fixed according to Lemma 1.8.

## GraphGenerator

**ThreePrismGraph()** returns the 3-prism graph.

**NoNACGraph()** returns the graph in Figure 2.4 on the right.



# 3. Movable Graphs

The focus of this chapter is on the existence of a proper flexible labeling, that is a labeling which has infinitely many non-congruent injective realizations. We call a graph with such a labeling movable.

In Section 3.1 we use the concept of active NAC-colorings from the previous chapter to prove that a graph can be augmented with some edges without changing its algebraic motion, if the active NAC-colorings fulfil a certain condition. Taking all NAC-colorings of the graph instead of only active ones enables us to define a so called constant distance closure of the graph purely combinatorially. The existence of a NAC-coloring of the constant distance closure is then a necessary condition on the movability of the original graph. We list the maximal constant distance closures of all graphs up to 8 vertices that are spanned by a Laman graph and satisfy the necessary condition.

Section 3.2 shows that all listed graphs are actually movable by various constructions of proper flexible labelings. Although this proves that the necessary condition is actually a sufficient one for graphs up to 8 vertices, we show that this is not the case in general.

The content of this chapter was submitted to a journal [29].

## 3.1. Constant Distance Closure

From now on, we are interested only in proper flexible labelings, namely, the question, whether a graph is movable. One of our main tools is introduced in this section: An edge  $uv$  can be added to a graph without changing its algebraic motion, if the vertices  $u$  and  $v$  are connected by a path that is unicolor in every active NAC-coloring. This leads to the notion of constant distance closure — augmenting the graph by edges with the property above, taking into account all NAC-colorings of the graph instead of active ones. Hence, we obtain a necessary combinatorial condition on movability: a graph can be movable only if its constant distance closure has a NAC-coloring. Based on this necessary condition, we show that so called tree-decomposable graphs are not movable. At the end of the section, we list all maximal constant distance closures of graphs up to 8 vertices having a spanning Laman graph that satisfy the necessary condition.

The following statement guarantees that adding an edge  $uv$  with the mentioned property preserves an algebraic motion, since the distance between  $u$  and  $v$  is constant during the motion.

**Lemma 3.1.** *Let  $G$  be a graph,  $\lambda$  a flexible labeling of  $G$  and  $u, v \in V_G$  where  $uv \notin E_G$ . Let  $\mathcal{C}$  be an algebraic motion of  $(G, \lambda)$  such that  $\forall \rho \in \mathcal{C} : \rho(u) \neq \rho(v)$ . If there exists*

a path  $P$  from  $u$  to  $v$  in  $G$  such that  $P$  is unicolor for all  $\delta \in \text{NAC}_G(\mathcal{C})$ , then  $\lambda$  has a unique extension  $\lambda'$  of  $G' = (V_G, E_G \cup \{uv\})$ , such that  $\mathcal{C}$  is an algebraic motion of  $(G', \lambda')$  and  $\text{NAC}_{G'}(\mathcal{C}) = \{\delta' \in \text{NAC}_{G'} : \delta'|_{E_G} \in \text{NAC}_G(\mathcal{C})\}$ .

*Proof.* Let  $S = \{\|\rho(u) - \rho(v)\| \in \mathbb{R}_+ : \rho \in \mathcal{C}\}$ . We first show that  $S$  is finite. By Lemma 2.11, we can assume that the first edge  $e_1$  of the path  $P$  is the fixed one in  $\mathcal{C}$ . If there is any edge  $e_k$  in  $P$  such that  $W_{e_k}$  is transcendental, then there is a valuation  $\nu$  such that  $\nu(W_{e_k}) > 0$  by Chevalley's Theorem. Hence, an active NAC-coloring can be constructed by Lemma 2.5 with  $\nu(W_{e_1}) = 0$ , which contradicts that  $P$  is unicolor. Therefore,  $W_{e_k}$  is algebraic for all  $e_k$  in  $P$ . Then there are only finitely many values for  $W_{e_k}$ . These values correspond to possible angles of the line given by the realization of the vertices of  $e_k$ . Hence, there can only be finitely many elements in  $S$ . Indeed, we can show that  $|S| = 1$ . Assume  $S = \{s_1, \dots, s_\ell\}$ , then

$$\mathcal{C} = \bigcup_{i \in \{1, \dots, \ell\}} \{\rho \in \mathcal{C} : \|\rho(u) - \rho(v)\|^2 = s_i^2\}.$$

Since  $\mathcal{C}$  is irreducible, then  $\ell = 1$ . We define  $\lambda'$  by  $\lambda'|_{E_G} = \lambda$  and  $\lambda'(uv) = s_1$ .

The restriction of any active NAC-coloring  $\delta' \in \text{NAC}_{G'}(\mathcal{C})$  to  $E_G$  is clearly in  $\text{NAC}_G(\mathcal{C})$ . On the other hand, every active NAC-coloring of  $G$  is extended uniquely to an active NAC-coloring of  $G'$ , since the path  $P$  is unicolor.  $\square$

Notice that it is sufficient to check the assumption only for non-conjugated active NAC-colorings due to Lemma 2.12.

Removal of an edge also preserves movability, since edge lengths are assumed to be positive. Together with the fact that  $\text{NAC}_G(\mathcal{C}) \subset \text{NAC}_G$  for any algebraic motion  $\mathcal{C}$ , this gives the following corollary.

**Corollary 3.2.** *Let  $G$  be a graph and  $u, v \in V_G$  be such that  $uv \notin E_G$ . If there exists a path  $P$  from  $u$  to  $v$  in  $G$  such that  $P$  is unicolor for all  $\delta \in \text{NAC}_G$ , then  $G$  is movable if and only if  $G' = (V_G, E_G \cup \{uv\})$  is movable.*

*Proof.* Let  $\lambda'$  be a proper flexible labeling of  $G'$ . Clearly,  $\lambda = \lambda'|_{E_G}$  is a flexible labeling of  $G$ . A realization  $\rho$  of  $G'$  compatible with  $\lambda'$  maps  $u$  and  $v$  to distinct points, since  $\|\rho(u) - \rho(v)\| = \lambda'(uv) \neq 0$ . Clearly,  $\rho$  is also a realization of  $G$  and it is compatible with  $\lambda$ . The other direction follows from Lemma 3.1.  $\square$

Let us point out that there is no specific algebraic motion assumed in the previous corollary. Hence, it can be used for proving that a graph is not movable in a purely combinatorial way. This is demonstrated by the following example.

**Example 3.3.** *The graph  $G$  in Figure 3.1 is not movable: since the vertices 1 and 4 are connected by the path  $(1, 3, 4)$  which is unicolor in every NAC-coloring, and similarly for 2 and 5 with the path  $(2, 3, 5)$ ,  $G$  is movable if and only if  $G' = (V_G, E_G \cup$*

$\{\{1, 4\}, \{2, 5\}\}$ ) is movable. But  $G'$  has no flexible labeling by Theorem 2.7, since it has no NAC-coloring.

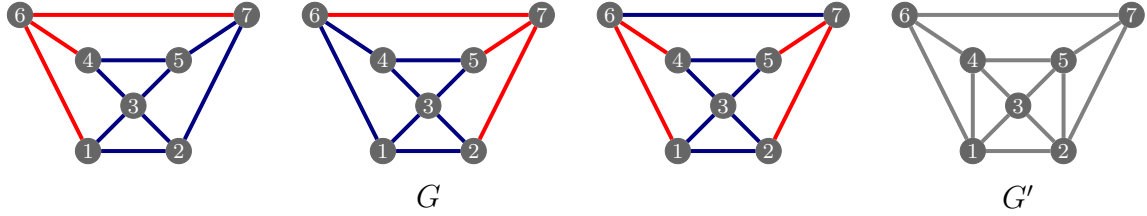


Figure 3.1.: All non-conjugated NAC-colorings of the Laman graph  $G$  in Example 3.3 and the augmented graph  $G'$ , which has no NAC-coloring.

The corollary and example motivate the next definition. The name is inspired by the constant distance between vertices  $u$  and  $v$  in Lemma 3.1 during the motion.

**Definition 3.4.** Let  $G$  be a graph. Let  $U(G)$  denote the set of all pairs  $\{u, v\} \subset V_G$  such that  $uv \notin E_G$  and there exists a path from  $u$  to  $v$  which is unicolor for all  $\delta \in \text{NAC}_G$ . If there exists a sequence of graphs  $G = G_0, \dots, G_n$  such that

- (i)  $G_i = (V_{G_{i-1}}, E_{G_{i-1}} \cup U(G_{i-1}))$  for  $i \in \{1, \dots, n\}$ , and
- (ii)  $U(G_n) = \emptyset$ ,

then the graph  $G_n$  is called the constant distance closure of  $G$ , denoted by  $\text{CDC}(G)$ .

The idea of repetitively augmenting the graph  $G$  by edges in  $U(G)$  is to decrease the number of inequalities guarantying injectivity of compatible realizations — adjacent vertices must be always mapped to different points. This can be seen in Example 3.3 — both constructions of a flexible labeling from a NAC-coloring described in Section 2.1 always coincide the vertices 1 and 4, or 2 and 5. But the edges  $\{1, 4\}$  and  $\{2, 5\}$  are added to the constant distance closure already in the first iteration.

In other words, considering the constant distance closure, while seeking for a proper flexible labeling, utilizes more information from the graph than taking the graph itself. For instance, since  $\text{NAC}_{\text{CDC}(G)} \subset \text{NAC}_G$ , the NAC-colorings of  $G$  that are active only for motions with non-injective realizations might be eliminated. This is summarized by the following statement.

**Theorem 3.5.** A graph  $G$  is movable if and only if the constant distance closure of  $G$  is movable.

*Proof.* The theorem follows by recursive application of Corollary 3.2. □

An immediate consequence is that a graph  $G$  can be movable only if the constant distance closure  $\text{CDC}(G)$  has a flexible labeling, namely, we relax the requirement on the labeling to be proper. By Theorem 2.7, it is equivalent to say that if  $G$  is movable, then  $\text{CDC}(G)$  has a NAC-coloring. We can reformulate this necessary condition using the next two lemmas.

**Lemma 3.6.** *Let  $G$  be a graph. If  $H$  is a subgraph of  $G$ , then the constant distance closure  $\text{CDC}(H)$  is a subgraph of the constant distance closure  $\text{CDC}(G)$ .*

*Proof.* If we show that  $U(H) \subset U(G)$ , then the claim follows by induction. Let a non-edge  $uv$  be in  $U(H)$ , namely, there exists a path  $P$  from  $u$  to  $v$  such that it is unicolor for all NAC-colorings in  $\text{NAC}_H$ . But then  $uv$  is also in  $U(G)$ , since the path  $P$  is unicolor also for all  $\delta \in \text{NAC}_G$ , because  $P$  is a subgraph of  $H$  and  $\delta|_{E_H} \in \text{NAC}_H$ .  $\square$

Now, we can show that having a NAC-coloring and being non-complete is the same for a constant distance closure.

**Lemma 3.7.** *Let  $G$  be a graph. The constant distance closure  $\text{CDC}(G)$  is the complete graph if and only if there exists a spanning subgraph of  $\text{CDC}(G)$  that has no NAC-coloring.*

*Proof.* If  $\text{CDC}(G)$  is the complete graph, then it has clearly no NAC-coloring. For the opposite implication, assume that there is a spanning subgraph  $H$  of  $\text{CDC}(G)$  that has no NAC-coloring. Trivially,  $U(H)$  consists of all nonedges of  $H$ . Hence, the constant distance closure of  $H$  is the complete graph. By Lemma 3.6,  $\text{CDC}(G)$  is also complete.  $\square$

The previous statement clarifies that the necessary condition obtained from Theorem 3.5 can be expressed as follows by relaxing the requirement of a flexible labeling being proper.

**Corollary 3.8.** *Let  $G$  be a graph. If the constant distance closure  $\text{CDC}(G)$  is the complete graph, then  $G$  is not movable.*

Let us use this necessary condition to prove that a certain class of Laman graphs is not movable. We would like to thank Meera Sitharam for pointing us to this class.

**Definition 3.9.** *A graph  $G$  is tree-decomposable if it is a single edge, or there are three tree-decomposable subgraphs  $H_1, H_2$  and  $H_3$  of  $G$  such that  $V_G = V_{H_1} \cup V_{H_2} \cup V_{H_3}$ ,  $E_G = E_{H_1} \cup E_{H_2} \cup E_{H_3}$  and  $V_{H_1} \cap V_{H_2} = \{u\}$ ,  $V_{H_2} \cap V_{H_3} = \{v\}$  and  $V_{H_1} \cap V_{H_3} = \{w\}$  for three distinct vertices  $u, v, w \in V_G$ .*

One could prove geometrically that the tree-decomposable graphs are not movable, but the notion of constant distance closure allows to do it in a combinatorial way.

**Theorem 3.10.** *If a graph is tree-decomposable, then it is not movable.*

*Proof.* Let  $G$  be a tree-decomposable graph. It is sufficient to show that the constant distance closure  $\text{CDC}(G)$  is the complete graph and use Corollary 3.8. We proceed by induction on the tree-decomposable construction. Clearly, the constant distance closure of a single edge is the edge itself which is  $K_2$ . Let  $H_1, H_2$  and  $H_3$  be tree-decomposable subgraphs of  $G$  as in Definition 3.9, with the pairwise common vertices  $u, v$  and  $w$ . By Lemma 3.6 and induction assumption, the subgraphs  $H'_1, H'_2$  and  $H'_3$  of  $\text{CDC}(G)$  induced by  $V_{H_1}, V_{H_2}$  and  $V_{H_3}$  respectively are complete. Thus, there is no NAC-coloring of  $H' = (V_{H_1} \cup V_{H_2} \cup V_{H_3}, E_{H'_1} \cup E_{H'_2} \cup E_{H'_3})$ , since all edges in a complete graph must have the same color and  $H'_1, H'_2$  and  $H'_3$  contain each an edge of the triangle induced by  $u, v, w$ . By Lemma 3.7,  $\text{CDC}(G)$  is complete, since  $H'$  is its spanning subgraph.  $\square$

We remark that the class of so called H1 graphs is a subset of tree-decomposable graphs, hence, they are not movable. A graph is called H1 if it can be constructed from a single edge by a sequence of Henneberg I steps — each step adds a new vertex by linking it to two existing ones. The next statement recalls the known fact that Henneberg I steps do not affect movability.

**Lemma 3.11.** *Let  $G$  be a graph and  $u \in V_G$  be a vertex of degree two. The graph  $G$  is movable if and only if  $G' = G \setminus u$  is movable.*

*Proof.* Let  $v$  and  $w$  be the neighbours of  $u$ . If  $\lambda'$  is a proper flexible labeling of  $G'$ , then  $\lambda : E_G \rightarrow \mathbb{R}_+$  given by  $\lambda'|_{E_{G'}} = \lambda$  and  $\lambda(uv) = \lambda(uw) = L$ , where  $L$  is the maximal distance between  $v$  and  $w$  in all realizations compatible with  $\lambda'$ , is a proper flexible labeling of  $G$ . On the other hand, the restriction of a proper flexible labeling of  $G$  to  $G'$  is a proper flexible labeling, since there are only two possible points where  $u$  can be placed if  $v$  and  $w$  are mapped to distinct points, i.e., there must be infinitely many realization of  $G'$ .  $\square$

Since the previous lemma justifies that the question of movability of a graph with vertices of degree two reduces to a smaller graph with all degrees being different from two, we can provide a list of “interesting” graphs regarding movability. By “interesting”, we mean, besides all vertices having degree at least three, also the fact that they are spanned by a Laman graph. Recall that graphs that are not spanned by a Laman graph are clearly movable, since any labeling induced by a generic realization is proper flexible. So we conclude this section by the list of the “interesting” constant distance closures up to 8 vertices.

**Theorem 3.12.** *Let  $G$  be a graph with at most 8 vertices such that it has a spanning Laman subgraph and  $\text{CDC}(G)$  has no vertex of degree two. If  $G$  satisfies the necessary condition of movability, i.e., the constant distance closure  $\text{CDC}(G)$  is not complete, then  $\text{CDC}(G)$  is one of the graphs  $K_{3,3}, K_{3,4}, K_{3,5}, K_{4,4}, L_1, \dots, L_6, Q_1, \dots, Q_6$ ,*

$S_1, \dots, S_5$ , or a spanning subgraph thereof, where the non-bipartite graphs are given by Figure 3.2.

*Proof.* Using the list of Laman graphs [10], one can compute constant distance closures of all graphs spanned by a Laman graph with at most 8 vertices. The computation (see [40]) shows that each constant distance closure is either a complete graph, or it has a vertex of degree two, or it is a spanning subgraph (or the full graph) of one of  $K_{3,3}, K_{3,4}, K_{3,5}, K_{4,4}$  or the graphs in Figure 3.2.  $\square$

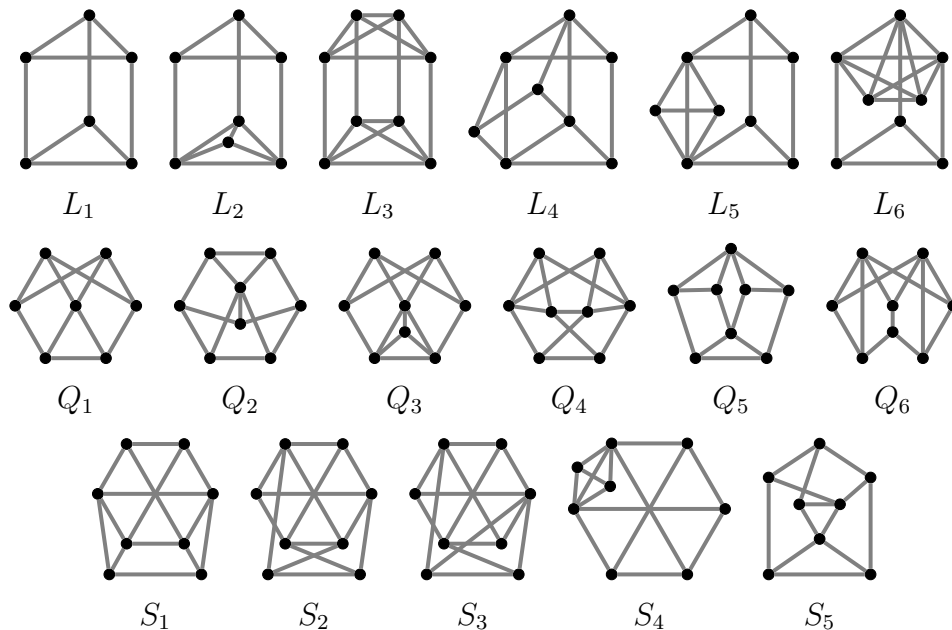


Figure 3.2.: Maximal non-bipartite constant distance closures of graphs with a spanning Laman subgraph, at most 8 vertices and no vertex of degree two.

### 3.2. Constructions

The goal of this section is to prove that all graphs listed in Theorem 3.12 are actually movable. By this we also show that the necessary condition of movability (the constant distance closure is non-complete) is also sufficient for graphs up to eight vertices. Four general ways of constructing a proper flexible labeling are used. The first one is Dixon I motion for bipartite graphs [16], recall Definition 1.9. The second one uses the grid construction from Section 2.1. We describe a new construction that produces an algebraic motion with two active NAC-colorings based on a certain injective embedding of vertices in  $\mathbb{R}^3$ . The fourth method assumes two movable subgraphs whose union spans the whole graph and whose motions coincide on the intersection. We provide a proper



flexible labeling for  $S_5$  ad hoc, since none of the four methods applies. Animations for the movable graphs can be found in [39]. In the conclusion, we give an example showing that the necessary condition is not sufficient for graphs with arbitrary number of vertices.

The proof of the following lemma gives parametrization of Dixon I motion.

**Lemma 3.13.** *Every bipartite graph with at least three vertices is movable.*

*Proof.* Let  $(X, Y)$  be a bipartite partition of a graph  $G$ . Hence, a realization with the vertices of one partition set on the  $x$ -axis, and vertices of the other on the  $y$ -axis induces a proper flexible labeling by Dixon's construction [16, 53]:

$$\rho_t(v) = \begin{cases} (\sqrt{x_v^2 - t^2}, 0), & \text{if } v \in X, \\ (0, \sqrt{y_v^2 + t^2}), & \text{if } v \in Y, \end{cases}$$

where  $x_v, y_v$  are arbitrary nonzero real numbers. Let  $\lambda(uv) := \sqrt{x_v^2 + y_v^2}$  for all  $u \in X$  and  $v \in Y$ . By the Pythagorean Theorem,  $\rho_t$  is compatible with  $\lambda$  for every sufficiently small  $t$ .  $\square$

For certain NAC-colorings, a flexible labeling obtained by the construction in the proof of Theorem 2.7 is actually proper.

**Lemma 3.14.** *Let  $\delta$  be a NAC-coloring of a graph  $G$ . Let  $R_1, \dots, R_m$ , resp.  $B_1, \dots, B_n$ , be the sets of vertices of connected components of the graph obtained from  $G$  by keeping only red, resp. blue, edges. If  $|R_i \cap B_j| \leq 1$  for all  $i, j$ , then  $G$  is movable.*

*Proof.* A flexible labeling is obtained as in Theorem 2.7. The labeling is proper, since the realizations are injective by the assumption  $|R_i \cap B_j| \leq 1$ .  $\square$

The construction yields proper flexible labelings for  $L_1, \dots, L_6$ , since there are NAC-colorings satisfying the assumption, see Figure 3.3. The displayed proper flexible labelings can be obtained by the more general "zigzag" construction.

**Corollary 3.15.** *The graphs  $L_1, \dots, L_6$ , see Figure 3.2 or 3.3, are movable.*

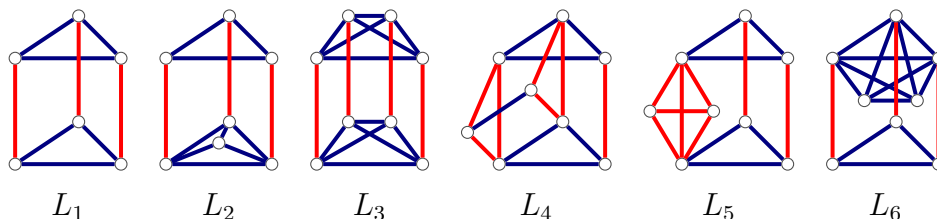


Figure 3.3.: The NAC-colorings inducing a proper flexible labeling.

Now, we present a construction assuming a special injective embedding in  $\mathbb{R}^3$ . The lemma also gives a hint, how existence of such an embedding can be checked (and an embedding found), if we know all NAC-colorings of the given graph.

**Lemma 3.16.** *Let  $G$  be a graph with an injective embedding  $\omega : V_G \rightarrow \mathbb{R}^3$  such that for every edge  $uv \in E_G$ , the vector  $\omega(u) - \omega(v)$  is parallel to one of the four vectors  $(1, 0, 0)$ ,  $(0, 1, 0)$ ,  $(0, 0, 1)$ ,  $(-1, -1, -1)$ , and all four directions are present. Then  $G$  is movable.*

*Moreover, there exists an algebraic motion of  $G$  with exactly two active NAC-colorings modulo conjugation. Two edges are parallel in the embedding  $\omega$  if and only if they receive the same pair of colors in the two active NAC-colorings.*

*Proof.* Assume a proper flexible labeling  $\lambda$  of the 4-cycle  $C_4 = (1, 2, 3, 4)$ , for instance induced by a generic realization. Let  $\rho_t : \{1, 2, 3, 4\} \rightarrow \mathbb{R}^2$  be a parametrization of the algebraic motion of  $(C_4, \lambda)$ . We define three functions from  $\mathbb{R}$  to  $\mathbb{R}^2$  by

$$f_1(t) = \rho_t(2) - \rho_t(1), \quad f_2(t) = \rho_t(3) - \rho_t(2), \quad f_3(t) = \rho_t(4) - \rho_t(3).$$

The norms  $\|f_1\|$ ,  $\|f_2\|$ ,  $\|f_3\|$  and  $\|-f_1(t) - f_2(t) - f_3(t)\|$  are the corresponding values of  $\lambda$ , i.e., they are independent of  $t$ . For each  $t \in \mathbb{R}$ , we define a realization

$$\tilde{\rho}_t : V_G \rightarrow \mathbb{R}^2, \quad u \mapsto \omega_1(u)f_1(t) + \omega_2(u)f_2(t) + \omega_3(u)f_3(t),$$

where  $\omega(u) = (\omega_1(u), \omega_2(u), \omega_3(u))$ . For any edge  $uv$ ,  $\tilde{\rho}_t(u) - \tilde{\rho}_t(v)$  is a multiple of  $f_1, f_2, f_3$  or  $-f_1(t) - f_2(t) - f_3(t)$  by assumption. Thus, the distance  $\|\tilde{\rho}_t(u) - \tilde{\rho}_t(v)\|$  is independent of  $t$  and different from zero. Hence, the set of all  $\rho_t$  is an algebraic motion; this proves the first statement.

In order to construct an algebraic motion with two active NAC-colorings, we take  $\rho_t$  to be the parametrization of the deltoid in Example 2.8. For any edge  $uv$ , the function  $W_{u,v}$  is just a scalar multiple of one of the functions in the example. Hence, there are only two active NAC-colorings modulo conjugation, see Table 2.1.  $\square$

**Remark 3.17.** *Clearly, we can construct also an algebraic motion with three non-conjugated active NAC-colorings by taking  $\rho_t$  from an algebraic motion of the 4-cycle with a general edge lengths, which has three non-conjugated active NAC-colorings. This also shows that if  $\delta_1$  and  $\delta_2$  are the two active NAC-colorings from the second statement of the lemma, then the coloring  $\delta_3$ , given by  $\delta_3(e) = \text{blue}$  if and only if  $\delta_1(e) = \delta_2(e)$ , is also a NAC-coloring of  $G$ . This follows from the fact that there are only three non-conjugated NAC-colorings of a 4-cycle with one chosen edge being always blue and they are related as given above.*

Lemma 3.16 allows to compute algebraic motions with exactly two active NAC-colorings: For any pair of NAC-colorings, try to find an embedding  $\omega : V_G \rightarrow \mathbb{R}^3$

with edge directions  $(1, 0, 0)$ ,  $(0, 1, 0)$ ,  $(0, 0, 1)$  or  $(-1, -1, -1)$  depending on the colors in these two colorings. This leads to a system of linear equations. If it has a nontrivial solution, check if a general solution is injective.

**Example 3.18.** *We illustrate how to find an embedding  $\omega : V_G \rightarrow \mathbb{R}^3$  for the graph  $Q_1$  using the NAC-colorings in Figure 3.4, such that every edge colored with blue/blue is parallel to  $(1, 0, 0)$ , every edge colored with blue/red is parallel to  $(0, 1, 0)$ , every edge colored with red/blue is parallel to  $(0, 0, 1)$ , and every edge colored with red/red is parallel to  $(-1, -1, -1)$ .*

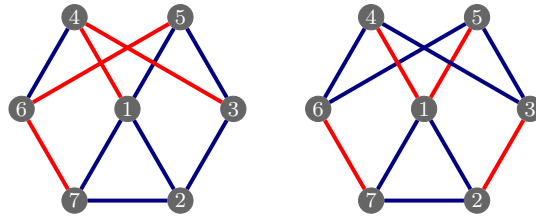


Figure 3.4.: The graph  $Q_1$  with a pair of NAC-colorings giving an embedding in  $\mathbb{R}^3$ .

*We put  $\omega(1)$  to the origin and introduce variables  $x_i, y_i, z_i$  for  $p_i := \omega(i)$ ,  $i = 2, \dots, 7$ . For each edge, we have two linear equations. We obtain the system*

$$\begin{aligned} 0 &= y_7 = z_7 = y_7 - y_2 = z_7 - z_2 = y_2 = z_2 = y_3 - y_5 = z_3 - z_5 = y_4 - y_6, \\ 0 &= z_4 - z_6 = x_5 = z_5 = x_2 - x_3 = z_2 - z_3 = x_3 - x_4 = y_3 - y_4 = x_5 - x_6, \\ 0 &= y_5 - y_6 = x_7 - x_6 - y_7 + y_6 = x_7 - x_6 - z_7 + z_6 = x_4 - y_4 = x_4 - z_4, \end{aligned}$$

*with the general solution parametrized by  $t \in \mathbb{R}$*

$$(p_1, \dots, p_7) = ((0, 0, 0), (t, 0, 0), (t, t, 0), (t, t, t), (0, t, 0), (0, t, t), (-t, 0, 0)).$$

*The solution is injective for  $t \neq 0$ . If we take  $t = 1$  and the parametrization of the deltoid from Example 2.8, then we obtain an algebraic motion of the graph such that its projection to the 4-cycle induced by  $\{1, 2, 3, 4\}$  is precisely the motion of the deltoid. Any other parametrization of the 4-cycle also yields an algebraic motion of the whole graph. Figure 3.5 illustrates using the deltoid and also a general quadrilateral. We remark that the triangle  $\{1, 2, 7\}$  is degenerate independently of the choice of parametrization of the 4-cycle. Moreover, the 4-cycles  $\{1, 2, 3, 5\}$ ,  $\{3, 5, 6, 4\}$  and  $\{1, 4, 6, 7\}$  are always parallelograms.*

By applying the described procedure to all pairs of NAC-colorings for the graphs in the list, we obtain the following:

**Corollary 3.19.** *The graphs  $Q_1, \dots, Q_6$ , see Figure 3.2 or 3.6, are movable.*

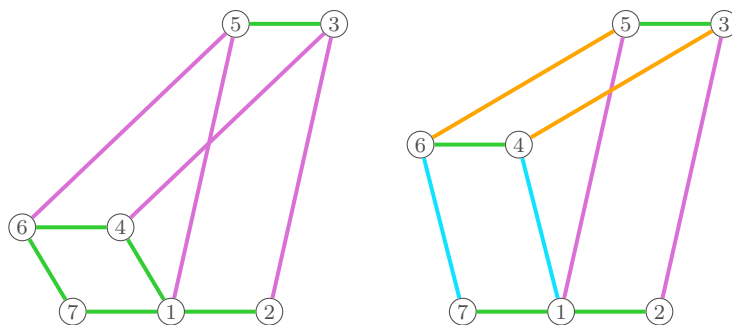


Figure 3.5.: Realizations of the graph  $Q_1$  compatible with proper flexible labelings induced by a deltoid and a general quadrilateral (colors indicate edges with same lengths). Note that the vertices 1,2,7 form a degenerate triangle.

*Proof.* Figure 3.6 shows the pairs of NAC-colorings of the graphs in  $Q_1, \dots, Q_6$  that can be used to construct an injective embedding in  $\mathbb{R}^3$  analogously to Example 3.18. Hence, they are movable by Lemma 3.16.  $\square$

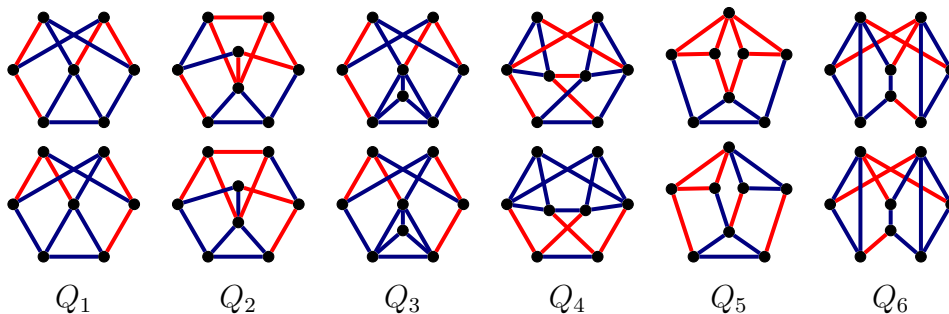


Figure 3.6.: Pairs of NAC-colorings used for construction of injective embeddings in  $\mathbb{R}^3$  satisfying the assumption of Lemma 3.16.

For the graphs  $S_1, \dots, S_4$ , we take advantage of the fact that they contain other graphs in the list as subgraphs. The next lemma formalizes the general construction based on movable subgraphs.

**Lemma 3.20.** *Let  $G$  be a graph. Let  $G_1$  and  $G_2$  be two subgraphs of  $G$  such that  $V_G = V_{G_1} \cup V_{G_2}$ ,  $E_G = E_{G_1} \cup E_{G_2}$  and  $E_{G_1} \cap E_{G_2} \neq \emptyset$ . Let  $W = V_{G_1} \cap V_{G_2}$ . Let  $\lambda_1$  and  $\lambda_2$  be proper flexible labelings of  $G_1$  and  $G_2$  respectively. If there are algebraic motions  $\mathcal{C}_1$  of  $(G_1, \lambda_1)$  and  $\mathcal{C}_2$  of  $(G_2, \lambda_2)$  such that:*

- (i) *the projections of  $\mathcal{C}_1$  and  $\mathcal{C}_2$  to  $W$  are the same, and*
- (ii) *for all  $v_1 \in V_{G_1} \setminus W$  and  $v_2 \in V_{G_2} \setminus W$ , the projections of  $\mathcal{C}_1$  to  $v_1$  and  $\mathcal{C}_2$  to  $v_2$  are different,*

*then there exists a proper flexible labeling of  $G$ .*

*Proof.* We define a labeling  $\lambda$  of  $G$  by  $\lambda|_{E_{G_1}} = \lambda_1$  and  $\lambda|_{E_{G_2}} = \lambda_2$ . This is well-defined, since  $\lambda_1|_{E_{G_1} \cap E_{G_2}} = \lambda_2|_{E_{G_1} \cap E_{G_2}}$  by (i). Now, every realization in the projection of  $\mathcal{C}_1$  to  $W$  can be extended to a realization of  $G$  that is compatible with  $\lambda$ . Hence,  $\lambda$  is flexible. It is also proper, since all extended realizations are injective by the second assumption.  $\square$

Now, we identify the suitable subgraphs and motions for  $S_1, S_2$  and  $S_3$ . Movability of  $S_4$  does not follow from the previous lemma, but it is straightforward.

**Corollary 3.21.** *The graphs  $S_1, S_2, S_3$  and  $S_4$ , see Figure 3.2 or 3.7, are movable.*

*Proof.* Figure 3.7 shows vertex-labelings of the graphs  $S_1, S_2$  and  $S_3$  that are used in the proof. The labelings given by the displayed edge lengths are actually proper flexible. Edges with same lengths have the same color.

Notice that the subgraphs  $G_1$  and  $G_2$  of  $S_1$  induced by the vertices  $\{1, \dots, 6\}$  and  $\{3, \dots, 8\}$  are isomorphic to  $L_1$  and  $K_{3,3}$  respectively. Since  $G_1$  and  $G_2$  satisfy the assumptions of Lemma 3.21, it is sufficient to take proper flexible labelings of  $G_1$  and  $G_2$ , given by Lemma 3.14 and 3.13, such that the quadrilateral  $(3,4,5,6)$  in both graphs moves as a non-degenerate rhombus, i.e.,  $\lambda(3,4) = \lambda(4,5) = \lambda(5,6) = \lambda(3,6)$ .

Recall from Definition 1.9 that a proper flexible labeling of  $K_{4,4}$  according to Dixon II is induced by placing the nodes of the two partition sets to the vertices of two concentric rectangles in orthogonal position. By removing two vertices, one can easily obtain a motion of  $K_{3,3}$ .

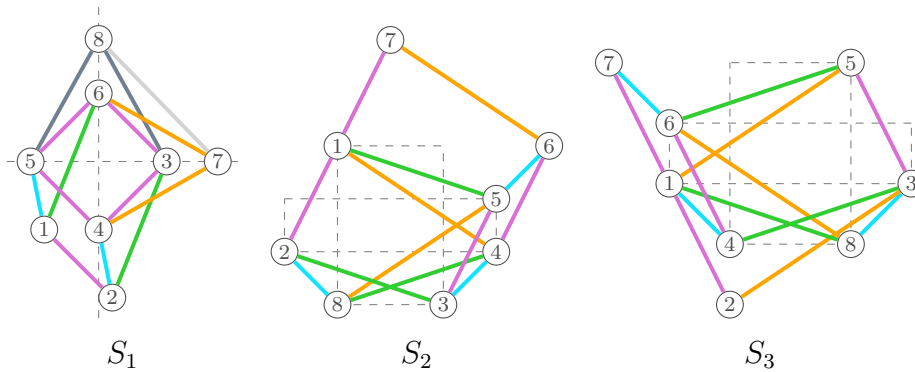


Figure 3.7.: The graphs  $S_1, S_2$  and  $S_3$  with proper flexible labelings (same colors mean same lengths). Note that the vertices 1,2,7 in  $S_2$  and  $S_3$  form a degenerate triangle.

The graph  $S_2$  has a subgraph  $H_{Q_1}$  induced by vertices  $\{1, \dots, 7\}$ , which is isomorphic to  $Q_1$ , and  $H_{K_{3,3}}$  induced by  $\{1, \dots, 5, 8\}$  isomorphic to  $K_{3,3}$ . We consider a proper flexible labeling of the subgraph  $H_{K_{3,3}}$  with an algebraic motion by Dixon II according to Figure 3.7. Now, we can use the motion of the 4-cycle  $\{1, 2, 3, 4\}$  to construct a motion of  $H_{Q_1}$  following Example 3.18. Since the 4-cycle  $\{1, 2, 3, 5\}$  is a parallelogram

in the motions of  $H_{K_{3,3}}$  and  $H_{Q_1}$ , the subgraphs satisfy the assumption of Lemma 3.20. Hence,  $S_2$  is movable.

Similarly, we construct a proper flexible labeling of  $S_3$ , since the vertices  $\{1, \dots, 7\}$  and  $\{1, 3, 4, 5, 6, 8\}$  induce subgraphs isomorphic to  $Q_1$  and  $K_{3,3}$ , respectively. See Figure 3.7 for placing the vertices according to Dixon II. Now, the 4-cycle  $\{1, 4, 3, 5\}$  is used to construct the motion according to Example 3.18.

A proper flexible labeling of  $S_4$  can be clearly obtained by extending a proper flexible labeling of its  $K_{3,3}$  subgraph.  $\square$

Finally, only the graph  $S_5$  is missing to be proved to be movable. Unfortunately, none of the previous constructions applies in this case. Hence, we provide a parametrization of its algebraic motion ad hoc.

**Lemma 3.22.** *The graph  $S_5$  is movable.*

*Proof.* In order to construct a proper flexible labeling for the graph  $S_5$ , we assume the following: the triangles  $(1, 2, 3)$  and  $(1, 4, 5)$  are degenerate into lines, the quadrilaterals  $(1, 4, 6, 2)$  and  $(1, 4, 7, 3)$  are antiparallelograms, the quadrilateral  $(4, 7, 8, 6)$  is a rhombus and the quadrilaterals  $(4, 5, 8, 7)$  and  $(4, 5, 8, 6)$  are deltoids, see Figure 3.8. We scale the lengths so that  $\lambda_{1,4} = 1$  and  $\lambda_{1,2} =: a > 1$ . Now, we define an injective realization  $\rho_\theta$  parametrized by the position of vertex 4. Let

$$\rho_\theta(1) = (0, 0), \quad \rho_\theta(2) = (-a, 0), \quad \rho_\theta(3) = (a, 0), \quad \rho_\theta(4) = (\cos \theta, \sin \theta).$$

Since the coordinates of a missing vertex of an antiparallelogram can be obtained by folding the parallelogram with the same edges along a diagonal, we get

$$\begin{aligned} \rho_\theta(6) &= \left( -\frac{a^3 + (a^2 - 1) \cos \theta - a}{a^2 + 2a \cos \theta + 1}, \frac{(1 - a^2) \sin \theta}{a^2 + 2a \cos \theta + 1} \right), \\ \rho_\theta(7) &= \left( \frac{a^3 - (a^2 - 1) \cos \theta - a}{a^2 - 2a \cos \theta + 1}, \frac{(1 - a^2) \sin \theta}{a^2 - 2a \cos \theta + 1} \right). \end{aligned}$$

The intersection of the line given by  $\rho_\theta(6)$  and  $\rho_\theta(7)$  with the line given by  $\rho_\theta(1)$  and  $\rho_\theta(4)$  gives

$$\rho_\theta(5) = \frac{1 - a^2}{a^2 + 1} (\cos \theta, \sin \theta).$$

The position of 8 can be easily obtained by the fact that  $(4, 7, 8, 6)$  is a rhombus:

$$\rho_\theta(8) = \left( \frac{\left( (a^2 - 1)^2 - 4a^2 (\sin \theta)^2 \right) \cos(\theta)}{(a^2 - 1)^2 + 4a^2 (\sin \theta)^2}, \frac{\left( 3a^4 - 4a^2 (\cos \theta)^2 + 2a^2 - 1 \right) \sin \theta}{(a^2 - 1)^2 + 4a^2 (\sin \theta)^2} \right).$$

One can verify that the induced labeling  $\lambda$  is independent of  $\theta$  and hence it is flexible:

$$\begin{aligned} \lambda_{1,4} = \lambda_{2,6} = \lambda_{3,7} = 1, & \quad \lambda_{2,3} = 2a, \\ \lambda_{1,2} = \lambda_{1,3} = \lambda_{4,6} = \lambda_{4,7} = \lambda_{6,8} = \lambda_{7,8} = a, \\ \lambda_{1,5} = \frac{a^2 - 1}{a^2 + 1}, & \quad \lambda_{4,5} = \lambda_{5,8} = \frac{2a^2}{a^2 + 1} = \lambda_{1,5} + \lambda_{1,4}. \end{aligned}$$

The labeling is proper for a generic  $a$ . □

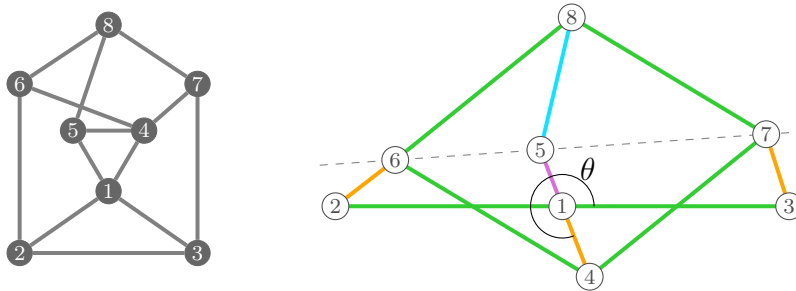


Figure 3.8.: The graph  $S_5$  and its realization inducing a proper flexible labeling. The same colors mean same edge lengths.

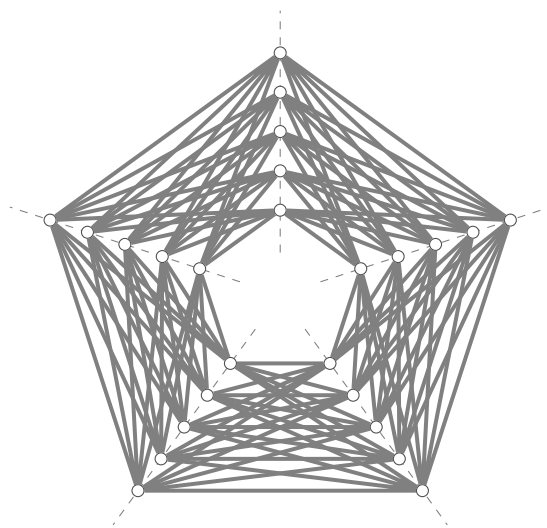
Since all graphs in the list were proved to be movable, we can conclude that the necessary condition is also sufficient up to 8 vertices.

**Corollary 3.23.** *Let  $G$  be a graph with at most 8 vertices. The graph  $G$  is movable if and only if the constant distance closure  $\text{CDC}(G)$  is not complete.*

*Proof.* We can assume that  $G$  is spanned by a Laman graph, otherwise there exists a generic proper flexible labeling. By Lemma 3.11, we can assume that  $G$  has no vertex of degree two. Corollary 3.8 gives the necessary condition for movability. For the opposite implication, Theorem 3.12 lists all constant distance closures that are not complete, Lemma 3.13 and 3.22, and Corollary 3.15, 3.19 and 3.21 show that all these graphs are movable. Hence, also all their subgraphs are movable. □

Based on the previous corollary, one might want to conjecture that the statement holds independently of the number of vertices. Nevertheless, the graph  $G_{25}$  in Figure 3.9 serves as a counter example.

This graph was proposed by Tibor Jordán as a counter example for some conjectures characterizing movable graphs within informal discussions with his students. The constant distance closure of  $G_{25}$  is the graph itself, since there is no unicolor path of length at least two: for every two incident edges  $uv$  and  $vw$ , there exists a NAC-coloring  $\delta$  such that  $\delta(uv) \neq \delta(vw)$ . Namely, we can define  $\delta$  by  $\delta(e) = \text{blue}$  if and only if  $w$  is a vertex

Figure 3.9.: Graph  $G_{25}$ .

of  $e$ . Hence, the necessary condition is satisfied. An explanation that  $G_{25}$  is not movable is the following: it contains five subgraphs isomorphic to the bipartite graph  $K_{5,5}$ , each of them induced by the vertices on two neighboring lines in the figure. The only way to construct a proper flexible labeling of  $K_{5,5}$ , with partition sets  $V_1$  and  $V_2$ , is placing the vertices of  $V_1$  on a line and the vertices of  $V_2$  on another line that is perpendicular to the first one [44]. Therefore, constructing a proper flexible labeling of  $G_{25}$  would require that the vertices on every two neighboring lines in the figure are on perpendicular lines, which is not possible.

## Implementation

The functionality of the package `FlexRiLoG` related to this chapter is summarized below.

### `FlexRiGraph`

`has_injective_grid_construction()` checks whether there is a NAC-coloring such that the assumption of Lemma 3.14 holds.

`spatial_embeddings_four_directions(delta_1, delta_2)` returns an injective spatial embedding satisfying the assumption of Lemma 3.16 with active NAC-colorings  $\delta_1$  and  $\delta_2$  if it exists.

`has_injective_spatial_embedding()` tests whether there is a pair of NAC-coloring such that `spatial_embeddings_four_directions()` yields an embedding.



**unicolor\_pairs(*active\_colorings*)** finds all non-edges that are connected by a path which is unicolor for every NAC-coloring in *active\_colorings*.

**constant\_distance\_closure()** constructs the constant distance closure of the graph by repetitive adding **unicolor\_pairs()** with all NAC-colorings assumed to be active.

**cdc\_is\_complete()** verifies the necessary condition on movability given by Corollary 3.8.

**is\_movable()** verifies **cdc\_is\_complete()** and checks whether there is a proper flexible labeling using **is\_bipartite()**, **has\_injective\_grid\_construction()** or **has\_injective\_spatial\_embedding()**.

## GraphMotion

**SpatialEmbeddingConstruction(*graph*, *active\_NACs*)** creates a parametric motion of a *graph* for two NAC-colorings given by *active\_NACs* according Lemma 3.16 and Remark 3.17, if **spatial\_embeddings\_four\_directions()** returns an embedding. The 4-cycle motion can be specified, **Deltoid()** is used by default.

## GraphGenerator

**Q1Graph()** - **Q6Graph()** return graphs  $Q_1, \dots, Q_6$ , see Figure 3.2.

**S1Graph()** - **S5Graph()** return graphs  $S_1, \dots, S_5$ , see Figure 3.2.



## 4. On the Classification of Motions

The goal of this chapter is to introduce some tools that can be used to classify motions of a graph that is spanned by a Laman graph. We focus on non-degenerate motions, i.e., those with infinitely many injective realizations.

A known example is the classification of the complete bipartite graph  $K_{3,3}$ . Dixon [16] constructed two families of proper flexible labelings of  $K_{3,3}$ . More than a hundred years later, Walter and Husty [60] proved using resultants that these are the only cases. We prove this result in a different way as an example of usage of our techniques.

The first tool, presented in Section 4.1, gives an algebraic constraint on the edge lengths under the assumption that a NAC-coloring satisfying a certain condition is active. It exploits the fact that an algebraic motion can be parametrized by Laurent series, and the leading coefficients must fulfil a system of equations.

In Section 4.2 we compute active NAC-colorings for various cases of edge lengths of a 4-cycle: rhombus, parallelogram, antiparallelogram, deltoid and general quadrilateral. This is an important ingredient for the next section.

Section 4.3 discusses relations between active NAC-colorings of an algebraic motion of the graph and active NAC-colorings of restrictions of the motion to subgraphs. In combination with the knowledge of active NAC-colorings of 4-cycles, it allows to construct a linear system of equations in variables labeled by all NAC-colorings of the graph. The system depends on a given set of NAC-coloring. If this set of NAC-colorings is actually the set of active NAC-colorings of an algebraic motion, then the system has a nontrivial nonnegative solution. This gives a method determining possible sets of active NAC-colorings. In order to restrict the output as much as possible, we combine it also with some other necessary conditions. We illustrate the method on the classification of motions of  $K_{3,3}$ .

In Section 4.4, we classify all proper flexible labelings of the graph  $Q_1$ , which was shown to be movable in the previous chapter (see Figure 3.2). An important part of the classification is the fact that the vertices of the unique triangle in the graph are collinear in every non-degenerate motion. We prove this in two different ways. The classification is done using the developed techniques and the computer algebra system **SageMath**.

The content of this chapter is a joint work with Georg Grasegger and Josef Schicho. It has not been submitted to a journal yet. The material of Section 4.1 and one version of the proof that the triangle in  $Q_1$  is always degenerate were presented at [28].

## 4.1. Leading coefficients system

If a graph  $G$  is spanned by a Laman graph and there is an algebraic motion of  $(G, \lambda)$ , then the edge lengths  $\lambda$  must be non-generic. In this section, we introduce a method deriving some algebraic equation(s) for  $\lambda$ . In general, the method assumes a valuation of the function field of the algebraic motion, but for certain active NAC-colorings, all needed information can be recovered from the NAC-coloring itself.

Let  $\mathcal{C}$  be an algebraic motion. Let  $\nu$  be a valuation yielding an active NAC-coloring of  $\mathcal{C}$ , i.e.  $|\{\nu(W_e) : e \in E_G\}| \geq 2$ . There is a parametrization of  $\mathcal{C}$  such that  $W_{u,v}$  and  $Z_{u,v}$  can be expressed as Laurent series in the parameter  $t$  such that  $\text{ord}(W_{u,v}) = \nu(W_{u,v})$  (see for instance [20]). We denote by  $w_{u,v}$ , resp.  $z_{u,v}$ , the leading coefficients of  $W_{u,v}$ , resp.  $Z_{u,v}$  for all  $uv \in E_G$ .

From the edge equations (2.1) we have

$$\begin{aligned} \lambda_{uv}^2 &= W_{u,v}Z_{u,v} \\ &= (w_{u,v}t^{\text{ord } W_{u,v}} + \text{h.o.t.})(z_{u,v}t^{-\text{ord } W_{u,v}} + \text{h.o.t.}), \end{aligned}$$

where h.o.t. means *higher order terms*. Hence, by comparing leading coefficients, i.e., setting  $t = 0$ , we have

$$w_{u,v}z_{u,v} = \lambda_{uv}^2 \quad \text{for all } uv \in E_G. \quad (4.1)$$

For every cycle  $C = (u_1, \dots, u_n)$  in  $G$ , the cycle condition for the functions  $W_{u,v}$  (see the first equation in (2.2)), gives

$$\sum_{i \in \{1, \dots, n\}} (w_{u_i, u_{i+1}} t^{\text{ord } W_{u_i, u_{i+1}}} + \text{h.o.t.}) = 0,$$

where we use  $u_{n+1} = u_1$ . Comparing leading coefficients gives

$$\sum_{\substack{i \in \{1, \dots, n\} \\ \text{ord } W_{u_i, u_{i+1}} = m}} w_{u_i, u_{i+1}} = 0, \quad (4.2)$$

where  $m = \min\{\text{ord } W_{u_i, u_{i+1}} : i \in \{1, \dots, n\}\}$ . Similarly,

$$\sum_{i \in \{1, \dots, n\}} (z_{u_i, u_{i+1}} t^{-\text{ord } W_{u_i, u_{i+1}}} + \text{h.o.t.}) = 0.$$

Comparing leading coefficients gives

$$\sum_{\substack{i \in \{1, \dots, n\} \\ \text{ord } W_{u_i, u_{i+1}} = M}} z_{u_i, u_{i+1}} = 0, \quad (4.3)$$

where  $M = \max\{\text{ord } W_{u_i, u_{i+1}} : i \in \{1, \dots, n\}\}$ .

The equations for all cycles are not independent. In order to count the number of independent cycles, we choose a spanning tree  $T$  of  $G$ . For every  $uv \in E_G \setminus E_T$ , there is a unique path in  $T$  connecting  $u$  and  $v$ . Hence, we get  $|E_G| - |E_T| = |E_G| - |V_G| + 1$  cycles.

There is also some freedom in the choice of parametrizations, namely, we can assume that they have a certain form. Let  $\bar{u}\bar{v} \in E_G$  be such that  $\nu(W_{\bar{u}\bar{v}}) = \min\{\nu(W_e) : e \in E_G\}$ . The equations (2.1) and (2.2) are satisfied if we replace  $W_{u,v}$  and  $Z_{u,v}$  by  $W_{u,v} \cdot \lambda_{\bar{u},\bar{v}}/W_{\bar{u},\bar{v}}$  and  $Z_{u,v} \cdot W_{\bar{u},\bar{v}}/\lambda_{\bar{u},\bar{v}}$ , respectively. Hence, we assume w.l.o.g. that  $W_{\bar{u},\bar{v}} = Z_{\bar{u},\bar{v}} = \lambda_{\bar{u}\bar{v}}$ . Next, let  $\alpha = \max\{\text{ord}(W_e) : e \in E_G\}$  and  $\hat{u}\hat{v}$  be an edge such that  $\text{ord}(W_{\hat{u},\hat{v}}) = \alpha$ . We can assume that the leading coefficient of  $W_{\hat{u},\hat{v}}$  and  $Z_{\hat{u},\hat{v}}$  is  $\lambda_{\hat{u},\hat{v}}$ , otherwise we reparametrize by taking  $(\lambda_{\hat{u}\hat{v}}/w_{\hat{u},\hat{v}})^{\frac{1}{\alpha}}t$  instead of  $t$ .

For every edge  $uv$ , we have both variables  $w_{u,v}$  and  $w_{v,u}$ . Therefore, we fix an ordering  $\prec$  on  $V_G$  such that  $\bar{u} \prec \bar{v}$  and  $\hat{u} \prec \hat{v}$ . For all  $u, v \in V_G$  such that  $u \succ v$ , we replace all  $w_{u,v}$  and  $z_{u,v}$  in the equations (4.1), (4.2) and (4.3) by  $-w_{v,u}$  and  $-z_{v,u}$  respectively. We also have the equations  $w_{\bar{u},\bar{v}} = z_{\bar{u},\bar{v}} = \lambda_{\bar{u}\bar{v}}$  and  $w_{\hat{u},\hat{v}} = z_{\hat{u},\hat{v}} = \lambda_{\hat{u}\hat{v}}$ .

Assume that  $G$  is spanned by a Laman graph, hence,  $|E_G| \geq 2|V_G| - 3$ . Then we have at least

$$\underbrace{(|E_G| - 2)}_{\text{edge lengths}} + \underbrace{2(|E_G| - |V_G| + 1)}_{\text{cycle equations}} + \underbrace{4}_{\bar{u}\bar{v}, \hat{u}\hat{v}} \geq 2|E_G| + 1$$

equations. We eliminate  $w_{u,v}$  and  $z_{u,v}$  for all  $uv \in E_G, u \prec v$  for instance by Gröbner basis computation taking the  $\lambda_{uv}$  to be variables as well. Since we eliminate  $2|E_G|$  variables out of at least  $2|E_G| + 1$  equations, we expect to get at least one algebraic equation in  $\lambda_{uv}$  for  $uv \in E_G$ .

We illustrate the method on a NAC-coloring satisfying a specific assumption.

**Lemma 4.1.** *Let  $H = (v_1, v_2, v_3, v_4)$  be a 4-cycle in a graph  $G$  with a flexible labeling  $\lambda$  and  $\mathcal{C}$  be an algebraic motion of  $(G, \lambda)$ . Let  $\delta \in \text{NAC}_G(\mathcal{C})$  be an active NAC-coloring such that the 4-cycle  $H$  is blue and there exist a red path  $P_1$  from  $v_1$  to  $v_3$  and a red path  $P_2$  from  $v_2$  to  $v_4$ . Then  $\lambda_{12}^2 + \lambda_{34}^2 = \lambda_{23}^2 + \lambda_{14}^2$ . In particular, the 4-cycle  $H$  has perpendicular diagonals in every injective realization in  $\mathcal{C}$ .*

*Proof.* To simplify the notation, we write  $W_{i,j}$  for  $W_{v_i,v_j}$  and similarly for  $w_{v_i,v_j}$  and  $z_{v_i,v_j}$ . Let  $\nu$  be the valuation yielding  $\delta$ . If a sum in a function field is zero, then there are at least two summands with the same valuation, namely the minimal one. Therefore, we have that  $\nu(W_{1,2}) = \nu(W_{2,3})$  due to the cycle consisting of  $P_1$  and the edges  $v_1v_2$  and  $v_2v_3$ . Remember that blue edges have lower valuation than red ones in active NAC-colorings. Similarly we get  $\nu(W_{1,4}) = \nu(W_{4,3})$ ,  $\nu(W_{2,1}) = \nu(W_{1,4})$  and  $\nu(W_{2,3}) = \nu(W_{3,4})$ . Therefore, the equations (4.2) and (4.3) give

$$\begin{aligned} w_{1,2} + w_{2,3} &= w_{1,4} - w_{3,4} = w_{2,3} + w_{3,4} = w_{1,2} - w_{1,4} = 0 \\ z_{1,2} + z_{2,3} + z_{3,4} - z_{1,4} &= 0. \end{aligned}$$

In combination with (4.1), we get  $\lambda_{12}^2 + \lambda_{34}^2 = \lambda_{23}^2 + \lambda_{14}^2$ .

Perpendicularity of diagonals follows from the fact that a quadrilateral has orthogonal diagonals if and only if the sums of squares of opposite sides are equal.  $\square$

We assume now that the valuation  $\nu$  yields only one active NAC-coloring  $\delta$ . This assumption implies that  $\{\nu(W_{u,v}) : uv \in E_G\} = \{0, \alpha\}$ . Then the equations (4.2) and (4.3) have the form

$$\sum_{\substack{i \in \{1, \dots, n\} \\ \delta(u_i u_{i+1}) = \text{blue}}} w_{u_i, u_{i+1}} = 0 \quad \text{and} \quad \sum_{\substack{i \in \{1, \dots, n\} \\ \delta(u_i u_{i+1}) = \text{red}}} z_{u_i, u_{i+1}} = 0 \quad (4.4)$$

for every cycle  $C = (u_1, \dots, u_n)$  in  $G$  that is not unicolor. For unicolor cycles, the sums are over all edges in the cycle.

Notice that if  $\nu$  yields another active NAC-coloring  $\delta'$  for another threshold, then the set  $\{(\delta(e), \delta'(e)) : e \in E_G\}$  has 3 elements. This motivates the following definition.

**Definition 4.2.** *Let  $G$  be a graph and  $N \subset \text{NAC}_G$  be a subset of its NAC-colorings. A NAC-coloring  $\delta$  is called singleton w.r.t.  $N$  if  $|\{(\delta(e), \delta'(e)) : e \in E_G\}| \neq 3$  for all  $\delta' \in N$ . We say just singleton if  $N = \text{NAC}_G$ .*

Therefore, if  $\mathcal{C}$  is an algebraic motion of  $(G, \lambda)$  and an active NAC-coloring  $\delta \in \text{NAC}_G(\mathcal{C})$  is a singleton w.r.t.  $\text{NAC}_G(\mathcal{C})$ , then we can apply the procedure described in this section using equation (4.4) instead of (4.2) and (4.3).

We remark that it does not matter whether we apply the procedure with a NAC-coloring or its conjugate, since taking the conjugate corresponds to renaming  $z_{u,v}$  by  $w_{u,v}$  and vice versa. Hence, the elimination returns the same equation.

**Example 4.3.** *The NAC-coloring  $\eta$  of the graph  $Q_1$ , see Figure 4.1, is a singleton, so the procedure can be applied. Hence, if  $\mathcal{C}$  is an algebraic motion of  $Q_1$  compatible with a flexible labeling  $\lambda$  such that  $\eta \in \text{NAC}_{Q_1}(\mathcal{C})$ , then we have the following equation for  $\lambda$ :*

$$\lambda_{57}^2 (\lambda_{24}^2 - \lambda_{23}^2)^2 + \lambda_{67}^2 (\lambda_{14}^2 - \lambda_{13}^2)^2 + (\lambda_{56}^2 - \lambda_{57}^2 - \lambda_{67}^2) (\lambda_{24}^2 - \lambda_{23}^2) (\lambda_{14}^2 - \lambda_{13}^2) = 0.$$

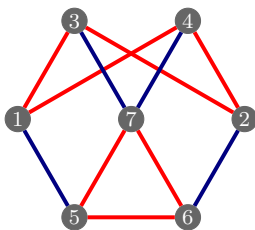


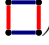
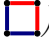
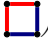
Figure 4.1.: The NAC-coloring  $\eta$  of the graph  $Q_1$ .

## 4.2. Active NAC-colorings of quadrilaterals

In this section, we describe the active NAC-colorings of an algebraic motion of a 4-cycle with various flexible labelings. We will see that active NAC-colorings determine whether the labeling satisfies some equations, for instance opposite edge lengths being equal. Moreover, it determines also a specific motion — a quadrilateral with same opposite edge lengths can form a parallelogram, but also an antiparallelogram. This is used in Section 4.3 to identify possible active NAC-colorings of graphs containing 4-cycles.

For the rest of this chapter, by notation  $(v_1, v_2, v_3, v_4)$  for a 4-cycle, we fix also the order of vertices. This allows to define types of active NAC-colorings of a 4-cycle.

**Definition 4.4.** *Let  $C_4 = (v_1, v_2, v_3, v_4)$  be a 4-cycle. The type of a NAC-coloring  $\delta \in \text{NAC}_{C_4}$  is*

- *O (opposite, ) if  $\delta(v_1v_2) = \delta(v_3v_4) \wedge \delta(v_2v_3) = \delta(v_1v_4)$ , or*
- *L (left, ) if  $\delta(v_1v_2) = \delta(v_1v_4) \wedge \delta(v_2v_3) = \delta(v_3v_4)$ , or*
- *R (right, ) if  $\delta(v_1v_2) = \delta(v_2v_3) \wedge \delta(v_3v_4) = \delta(v_1v_4)$ .*

We remark that the terminology comes from the edge with the same color as the bottom one if the vertices of the 4-cycle are numbered counterclockwise starting with the bottom left, see Figure 4.2.

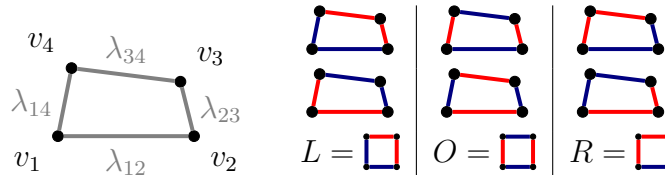


Figure 4.2.: Labeling of the 4-cycle  $C_4$  and notation for conjugated NAC-colorings.

Let  $\mathcal{C}$  be an algebraic motion of a 4-cycle graph  $C_4 = (v_1, v_2, v_3, v_4)$  with a flexible labeling  $\lambda$  (see Figure 4.2). Table 4.1 classifies the motions according to the types of active NAC-colorings. The computations showing how motions determine NAC-colorings are at the end of this section. Since the table is complete we also know that active NAC-colorings do imply a motion.

Notice that there might be different algebraic motions compatible with the same  $\lambda$ , namely, the solution set of the equation (1.1) is not necessarily irreducible. In the case of *odd*, resp. *even*, deltoid, there is also a degenerate component, where the vertices  $v_1$  and  $v_3$ , resp.  $v_2$  and  $v_4$ , coincide. If the opposite edge lengths are equal, then there are

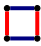
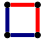
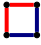
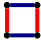
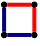

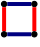

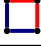
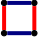



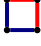

Quadrilateral	Motion	Types of $\text{NAC}_{C_4}(\mathcal{C})$	Equations	
Rhombus	parallel		$O$	$\left\{ \begin{array}{l} \lambda_{12} = \lambda_{23} = \\ = \lambda_{34} = \lambda_{14} \end{array} \right\}$
	degenerate	 resp. 	$L$ resp. $R$	
Parallelogram	parallel		$O$	$\left\{ \begin{array}{l} \lambda_{12} = \lambda_{34}, \\ \lambda_{23} = \lambda_{14} \end{array} \right\}$
Antiparallelogram	antiparallel	 	$L, R$	
Deltoid (even)	non-degenerate	 	$O, R$	$\left\{ \begin{array}{l} \lambda_{12} = \lambda_{14}, \\ \lambda_{23} = \lambda_{34} \end{array} \right\}$
	degenerate		$L$	
Deltoid (odd)	non-degenerate	 	$O, L$	$\left\{ \begin{array}{l} \lambda_{12} = \lambda_{23}, \\ \lambda_{34} = \lambda_{14} \end{array} \right\}$
	degenerate		$R$	
General		  	$O, L, R$	otherwise


Table 4.1.: Active NAC-colorings of possible motions of a  $(C_4, \lambda)$ .

two non-degenerate motions: parallel and antiparallel. The rhombus has two degenerate components corresponding to two pairs of opposite vertices that can coincide.

In order to find a classification of motions of a graph, we use restrictions of active NAC-colorings to 4-cycle subgraphs. Indeed, assuming an algebraic motion  $\mathcal{C}$  of a graph  $G$ , the active NAC-colorings of the projection of  $\mathcal{C}$  to a 4-cycle subgraph of  $G$  are precisely the restrictions of the active NAC-colorings of  $\mathcal{C}$ . A formal proof is given later in Corollary 4.9 as consequence of a more general theory.

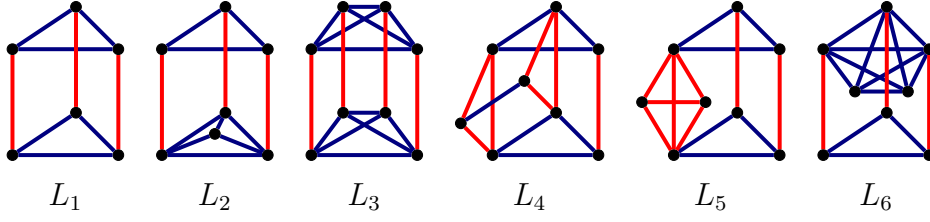
It is well known that the graphs  $L_i$  are movable by making the vertical edges in Figure 3.2 parallel and same lengths. Looking at 4-cycles gives easily that this is the only option:

**Corollary 4.5.** *Let  $i \in \{1, \dots, 6\}$ . If  $\lambda$  is a proper flexible labeling of  $L_i$ , then every 4-cycle that is colored nontrivially by  $\delta_i$  (see Figure 4.3), is a parallelogram.*

*Proof.* Since  $\delta_i$  is the only NAC-coloring of  $L_i$  modulo conjugation, it is the only active NAC-coloring in every algebraic motion. As we see in Figure 4.3 the restriction of  $\delta_i$  to each nontrivially colored 4-cycle is of type O (). According to Table 4.1 it must be in a parallel motion.  $\square$

We conclude the section by the computations proving Table 4.1. We again write  $W_{i,j}$  for  $W_{v_i,v_j}$  etc. Assume that  $v_1v_2$  is the fixed edge. We determine the valuations  $\nu$  such that  $\nu(W_{1,2}) = 0$  and  $\nu(W_e) > 0$  is positive for some other edge  $e$ . Namely,  $\nu$  yields an active NAC-coloring by taking the threshold  $\alpha = 0$ . Hence, the fixed edge  $v_1v_2$  is always blue. The conjugated NAC-colorings are automatically active by Lemma 2.12.




 Figure 4.3.: The only NAC-colorings  $\delta_1, \dots, \delta_6$  of  $L_1, \dots, L_6$  modulo conjugation.

The system of the equations (2.2) has the form

$$\begin{aligned} W_{1,2} = Z_{1,2} = \lambda_{12}, \quad W_{2,3}Z_{2,3} = \lambda_{23}^2, \quad W_{3,4}Z_{3,4} = \lambda_{34}^2, \quad W_{4,1}Z_{4,1} = \lambda_{14}^2, \\ W_{1,2} + W_{2,3} + W_{3,4} + W_{4,1} = 0, \quad Z_{1,2} + Z_{2,3} + Z_{3,4} + Z_{4,1} = 0. \end{aligned}$$

We express  $W_{3,4}$  as a Laurent series in  $s = W_{4,1}$ , unless stated differently. A valuation is then given by the order. Hence, we obtain active NAC-colorings such that  $v_1 v_4$  is red. By substituting

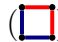


$$\begin{aligned} W_{1,2} = \lambda_{12}, \quad Z_{1,2} = \lambda_{12}, \quad W_{2,3} = -s - W_{1,2} - W_{3,4}, \\ Z_{3,4} = \frac{\lambda_{34}^2}{W_{3,4}}, \quad Z_{4,1} = \frac{\lambda_{14}^2}{s}, \quad Z_{2,3} = -\frac{\lambda_{14}^2}{s} - Z_{1,2} - Z_{3,4} \end{aligned}$$

into  $W_{2,3}Z_{2,3} = \lambda_{23}^2$ , we obtain the following equation:

$$(\lambda_{14}^2 + \lambda_{12}s)W_{3,4}^2 + (\lambda_{12}\lambda_{14}^2 + \lambda_{12}^2s - \lambda_{23}^2s + \lambda_{34}^2s + \lambda_{14}^2s + \lambda_{12}s^2)W_{3,4} + \lambda_{12}\lambda_{34}^2s + \lambda_{34}^2s^2 = 0 \quad (4.5)$$

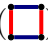


We solve the equation for  $W_{3,4}$  for various cases:

## Rhombus


If  $\lambda_{12} = \lambda_{23} = \lambda_{34} = \lambda_{14}$ , then (4.5) simplifies to  $(W_{3,4} + \lambda_{12})(W_{3,4} + s)(\lambda_{12} + s)\lambda_{12} = 0$ . If  $-\lambda_{12} = s = W_{4,1} = -x_4 - iy_4$ , then  $x_4 = \lambda_{12}$  and  $y_4 = 0$ , i.e., the rhombus is degenerate so that vertices  $v_2$  and  $v_4$  coincide. Since  $s = W_{4,1}$  is not transcendental in this case, we choose  $W_{2,3}$  to have a positive valuation. Hence, the type of the NAC-coloring is L () . If  $W_{3,4} = -s = -W_{4,1}$ , then the rhombus degenerates so that  $v_1$  and  $v_3$  coincide and the type of the NAC-coloring is R () . Finally, if  $W_{3,4} = -\lambda_{12}$ , then we have the type O () . Note that only one factor of the equation can vanish, since vanishing any two factors contradicts a motion.

## Parallelogram and Antiparallelogram

If  $\lambda_{12} = \lambda_{34}$  and  $\lambda_{23} = \lambda_{14}$ , then (4.5) simplifies to  $(W_{3,4}\lambda_{23}^2 + W_{3,4}\lambda_{12}s + \lambda_{12}^2s + \lambda_{12}s^2)(W_{3,4} + \lambda_{12}) = 0$ . If  $W_{3,4} = -\lambda_{12}$ , then the type of the active NAC-coloring of the

parallel motion of the parallelogram is O . Otherwise, we have  $W_{3,4} = -\frac{\lambda_{12}^2 s + \lambda_{12} s^2}{\lambda_{23}^2 + \lambda_{12} s}$ ; the parallelogram moves along the antiparallel irreducible component and by symmetry we have R  and L .

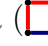
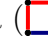


## Deltoid

Assume that the quadrilateral is an even deltoid, i.e.,  $\lambda_{12} = \lambda_{14}$  and  $\lambda_{23} = \lambda_{34}$ . The equation (4.5) has the form  $(W_{3,4}^2 \lambda_{12} + W_{3,4} \lambda_{12}^2 + W_{3,4} \lambda_{12} s + \lambda_{23}^2 s)(\lambda_{12} + s) = 0$ . If  $s = -\lambda_{12}$ , then the deltoid degenerates,  $s$  is not transcendental and by choosing  $W_{2,3}$  to have a positive valuation, we get a NAC-coloring of type L . The solutions corresponding to the non-degenerate motion are

$$W_{3,4} = -\frac{\lambda_{12}^2 + \lambda_{12} u \pm \sqrt{\lambda_{12}^4 + \lambda_{12}^2 u^2 + 2(\lambda_{12}^3 - 2\lambda_{12}\lambda_{23}^2)u}}{2\lambda_{12}}.$$

Using  $\sqrt{1+t} = 1 + \frac{t}{2} - \frac{t^2}{8} + O(t^3)$ , they can be expressed as Laurent series:




$$W_{3,4} = -\frac{\lambda_{23}^2}{\lambda_{12}^2} s + O(s^2) \quad \text{and} \quad W_{3,4} = -\lambda_{12} + \frac{\lambda_{23}^2 - \lambda_{12}^2}{\lambda_{12}^2} s + O(s^2).$$

This gives active NAC-colorings of type R  and O . The types of active NAC-colorings of an odd deltoid are L  and O .

## General case

If the lengths are general, then (4.5) has the following solutions:

$$W_{3,4} = -\frac{\lambda_{34}^2}{\lambda_{14}^2} s + O(s^2) \quad \text{and} \quad W_{3,4} = -\lambda_{12} + \left( \frac{\lambda_{23}^2 - \lambda_{14}^2}{\lambda_{14}^2} \right) s + O(s^2).$$

Since we can also choose  $W_{2,3}$  to have a positive valuation, we get altogether NAC-colorings of all three types L , O  and R .

### 4.3. Determining active NAC-colorings

In this section, we exploit how valuations giving active NAC-colorings behave when we restrict an algebraic motion to the vertices of a subgraph, in particular a 4-cycle. This allows to implement an algorithm which provides possible motion types of 4-cycles, as described in the previous section, with possible sets of active NAC-coloring.

We start the section with introducing a new notation — a so called  $\mu$ -number assigns a nonnegative integer to a NAC-coloring of a graph  $G$  and an algebraic motion of  $G$ .

The  $\mu$ -number is nonzero if and only if the NAC-coloring is active. The main theorem of this section provides a formula which relates  $\mu$ -numbers for the whole graph with the  $\mu$ -numbers of a subgraph of  $G$ . Computing  $\mu$ -numbers for all types of motions of a 4-cycle allows to construct a linear system determined by a set of NAC-colorings, resp. motion types of 4-cycles, which has a nonnegative integer solution if the set of NAC-colorings form a set of active NAC-colorings of an algebraic motion. Based on this, we implement an algorithm listing possible motion types of 4-cycles, resp. sets of active NAC-colorings. Besides ramification of valuations, we introduce also some other necessary conditions on the consistency of motion types of 4-cycles based on the requirement of having injective realizations or geometric arguments like orthogonality of diagonals. We illustrate the method on the well known classification of motions of  $K_{3,3}$ . We define  $\mu$ -numbers now.

**Definition 4.6.** *Let  $\lambda$  be a flexible labeling of a graph  $G$ . Let  $\mathcal{C}$  be an algebraic motion of  $(G, \lambda)$ . For  $\delta \in \text{NAC}_G$  and a valuation  $\nu$  of  $F(\mathcal{C})$ , we define*

$$\text{gap}(\delta, \nu) := \max \left\{ 0, \min_{e \in E_G} \{ \nu(W_e) : \delta(e) = \text{red} \} - \max_{e \in E_G} \{ \nu(W_e) : \delta(e) = \text{blue} \} \right\}.$$

We also define a  $\mu$ -number

$$\mu(\delta, \mathcal{C}) := \sum_{\nu \in \text{Val}(\mathcal{C})} \text{gap}(\delta, \nu),$$

where  $\text{Val}(\mathcal{C})$  denotes all valuations of the function field  $F(\mathcal{C})$  that are surjective on  $\mathbb{Z}$  and trivial on  $\mathbb{C}$ .

Given  $X \in F(\mathcal{C}), X \neq 0$ , there are only finitely many valuations  $\nu \in \text{Val}(\mathcal{C})$  such that  $\nu(X) \neq 0$  (see for instance [14, Lecture 6]). Therefore, there are only finitely many valuations  $\nu \in \text{Val}(\mathcal{C})$  such that  $\text{gap}(\delta, \nu) \neq 0$ . Hence,  $\mu(\delta, \mathcal{C}) \in \mathbb{N}_0$ .

If  $\delta$  is an active NAC-coloring due to a valuation  $\nu$  and threshold  $\alpha$ , then we have  $\nu(W_e) > \alpha \geq \nu(W_{e'})$  for all  $e, e'$  such that  $\delta(e) = \text{red}$  and  $\delta(e') = \text{blue}$ . Therefore,  $\text{gap}(\delta, \nu)$  is positive. On the other hand, if  $\nu$  does not yield  $\delta$  for any threshold  $\alpha$ , then there must be edges  $e, e'$  such that  $\delta(e) = \text{red}$ ,  $\delta(e') = \text{blue}$  and  $\nu(W_e) < \nu(W_{e'})$ . Then  $\text{gap}(\delta, \nu) = 0$ . These observations give the following remark.

**Remark 4.7.** *The set of active NAC-colorings of an algebraic motion  $\mathcal{C}$  satisfies*

$$\text{NAC}_G(\mathcal{C}) = \{ \delta \in \text{NAC}_G : \mu(\delta, \mathcal{C}) \neq 0 \}.$$

Let  $\mathcal{C}$  be an algebraic motion of a graph  $G$  and  $G'$  be a subgraph of  $G$ . We consider the projection  $f: \mathcal{C} \rightarrow \mathcal{C}'$  to the vertices of  $G'$  and assume that  $\mathcal{C}'$  is an algebraic motion of  $G'$ . If  $\nu \in \text{Val}(\mathcal{C})$ , then  $\nu(F(\mathcal{C}')) = r\mathbb{Z}$  for some positive integer  $r$  and there is a valuation  $\nu' \in \text{Val}(\mathcal{C}')$  surjective on  $\mathbb{Z}$  such that  $\nu(x) = r\nu'(x)$  for all  $x \in F(\mathcal{C}')$ . We say

that  $\nu$  extends  $\nu'$ . The number  $r$  is called *ramification index* of  $\nu$  over  $F(\mathcal{C}')$ , denoted by  $\text{ram}_{F(\mathcal{C})/F(\mathcal{C}')}(\nu)$ . We have the following

$$\sum_{\substack{\nu \in \text{Val}(\mathcal{C}) \\ \nu \text{ ext. } \nu'}} \text{ram}_{F(\mathcal{C})/F(\mathcal{C}')}(\nu) = \deg(f). \quad (4.6)$$

where  $\nu'$  is a valuation of  $F(\mathcal{C}')$ ; see Appendix A.3. Now we are ready to prove the main theorem of this section.

**Theorem 4.8.** *Let  $\mathcal{C}$  be an algebraic motion of  $(G, \lambda)$ . Let  $G'$  be a subgraph of  $G$  and  $f : \mathcal{C} \rightarrow \mathcal{C}'$  be the projection of  $\mathcal{C}$  into realizations of  $G'$ , where  $\mathcal{C}'$  is an algebraic motion of  $G'$ . Let  $\delta'$  be a NAC-coloring of  $G'$ . If  $\{\delta_1, \dots, \delta_k\} = \{\delta \in \text{NAC}_G : \delta|_{E_{G'}} = \delta'\}$ , then*

$$\sum_{i=1}^k \mu(\delta_i, \mathcal{C}) = \mu(\delta', \mathcal{C}') \cdot \deg(f).$$

*Proof.* First, we prove that for every  $\nu \in \text{Val}(\mathcal{C})$  we have

$$\text{gap}(\delta', \nu|_{F(\mathcal{C}')} ) = \sum_{i=1}^k \text{gap}(\delta_i, \nu). \quad (4.7)$$

If  $\text{gap}(\delta', \nu|_{F(\mathcal{C}')} ) = 0$ , then there exist edges  $e_1, e_2 \in E_{G'}$  such that  $\delta'(e_1) = \text{red}$ ,  $\delta'(e_2) = \text{blue}$  and  $\nu|_{F(\mathcal{C}')} (W_{e_1}) \leq \nu|_{F(\mathcal{C}')} (W_{e_2})$ . Hence,  $\text{gap}(\delta_i, \nu) = 0$  for all  $i$  since

$$\min_{e \in E_G} \{\nu(W_e) : \delta_i(e) = \text{red}\} \leq \nu(W_{e_1}) \leq \nu(W_{e_2}) \leq \max_{e \in E_G} \{\nu(W_e) : \delta_i(e) = \text{blue}\},$$

and the claim holds. Otherwise, let

$$\begin{aligned} \alpha &:= \max_{e \in E_{G'}} \{\nu(W_e) : \delta'(e) = \text{blue}\}, \\ \beta &:= \min_{e \in E_{G'}} \{\nu(W_e) : \delta'(e) = \text{red}\}. \end{aligned}$$

Let  $\alpha = \alpha_0 < \alpha_1 < \dots < \alpha_n = \beta$  be such that  $\{\alpha_0, \dots, \alpha_n\} = [\alpha, \beta] \cap \{\nu(W_e) : e \in E_G\}$ . For  $i \in \{0, \dots, n-1\}$ , let  $\gamma_i$  be the active NAC-coloring obtained from  $\nu$  with threshold  $\alpha_i$  using Lemma 2.5. All NAC-colorings  $\gamma_i$  are extensions of  $\delta'$ , thus  $\{\gamma_0, \dots, \gamma_{n-1}\} \subset \{\delta_1, \dots, \delta_k\}$ . On the other hand, we have for all  $j \in \{1, \dots, k\}$  that either  $\text{gap}(\delta_j, \nu) = 0$ , or  $\text{gap}(\delta_j, \nu) = \alpha_{i_j+1} - \alpha_{i_j} = \text{gap}(\gamma_{i_j}, \nu)$  for some  $i_j \in \{0, \dots, n-1\}$ . In the latter case,  $\delta_j = \gamma_{i_j}$ . Figure 4.4 illustrates the two cases.

By this we get

$$\sum_{j=1}^k \text{gap}(\delta_j, \nu) = \sum_{i=0}^{n-1} \text{gap}(\gamma_i, \nu) = \sum_{i=0}^{n-1} (\alpha_{i+1} - \alpha_i) = \beta - \alpha = \text{gap}(\delta', \nu|_{F(\mathcal{C}')} ).$$

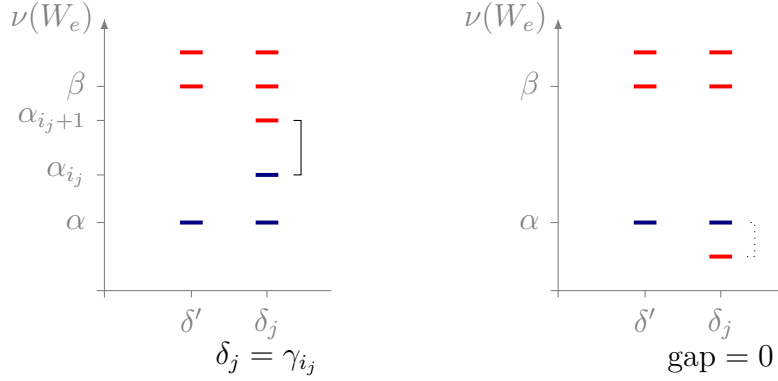


Figure 4.4.: Gaps for different settings of the edge colorings  $\delta_j$  for edges in  $G$  (right column) that are not in  $G'$  (left column). Horizontal bars represent edges in their color at the level of their valuation.

We can conclude the proof now.

$$\begin{aligned}
 \sum_{j=1}^k \mu(\delta_j, \mathcal{C}) &= \sum_{j=1}^k \sum_{\nu \in \text{Val}(\mathcal{C})} \text{gap}(\delta_j, \nu) = \sum_{\nu \in \text{Val}(\mathcal{C})} \sum_{j=1}^k \text{gap}(\delta_j, \nu) \\
 &\stackrel{(4.7)}{=} \sum_{\nu \in \text{Val}(\mathcal{C})} \text{gap}(\delta', \nu|_{F(\mathcal{C}')} ) = \sum_{\nu' \in \text{Val}(\mathcal{C}')} \sum_{\substack{\nu \in \text{Val}(\mathcal{C}) \\ \nu \text{ ext. } \nu'}} \text{gap}(\delta', \nu|_{F(\mathcal{C}')} ) \\
 &= \sum_{\nu' \in \text{Val}(\mathcal{C}')} \sum_{\substack{\nu \in \text{Val}(\mathcal{C}) \\ \nu \text{ ext. } \nu'}} \text{gap}(\delta', \text{ram}_{F(\mathcal{C})/F(\mathcal{C}')}(\nu) \cdot \nu') \\
 &= \sum_{\nu' \in \text{Val}(\mathcal{C}')} \text{gap}(\delta', \nu') \sum_{\substack{\nu \in \text{Val}(\mathcal{C}) \\ \nu \text{ ext. } \nu'}} \text{ram}_{F(\mathcal{C})/F(\mathcal{C}')}(\nu) \\
 &\stackrel{(4.6)}{=} \sum_{\nu' \in \text{Val}(\mathcal{C}')} \text{gap}(\delta', \nu') \cdot \deg(f) = \deg(f) \cdot \mu(\delta', \mathcal{C}').
 \end{aligned}$$

□

As an immediate consequence we get that active NAC-colorings of a subgraph are the restrictions of active NAC-colorings of the whole graph.

**Corollary 4.9.** *Let  $G, G', \mathcal{C}, \mathcal{C}'$  and  $\delta'$  be as in Theorem 4.8. Then*

$$\text{NAC}_{G'}(\mathcal{C}') = \{\delta|_{E_{G'}} : \delta \in \text{NAC}_G(\mathcal{C})\}.$$

*Proof.* From Remark 4.7, we know

$$\delta' \notin \text{NAC}_{G'}(\mathcal{C}') \iff \mu(\delta', \mathcal{C}') = 0.$$

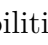

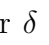
By Theorem 4.8 and the fact that  $\mu$  is nonnegative, this implies  $\delta \notin \text{NAC}_G(\mathcal{C})$  for all  $\delta \in \text{NAC}_G$  extending  $\delta'$ . For the other direction we know

$$\delta' \in \text{NAC}_{G'}(\mathcal{C}') \iff \mu(\delta', \mathcal{C}') \neq 0 \xrightarrow{4.8} \exists \delta \text{ extending } \delta': \mu(\delta, \mathcal{C}) \neq 0.$$

□

Since we want to use the formula from Theorem 4.8 to construct a system of equations based on restrictions to 4-cycles, we need to compute the  $\mu$ -numbers for active NAC-colorings of a 4-cycle.

**Theorem 4.10.** *Let  $C_4$  be a 4-cycle graph with an algebraic motion  $\mathcal{C}$ . If  $\delta \in \text{NAC}_{C_4}(\mathcal{C})$ , then  $\mu(\delta, \mathcal{C}) = 1$ .*

*Proof.* There are three possible NAC-colorings of  $C_4 = (v_1, v_2, v_3, v_4)$  modulo conjugation. W.l.o.g., we assume that the edge  $v_1v_2$  is fixed and  $\delta(v_1v_2) = \text{blue}$ . Let  $\delta_O, \delta_L$  and  $\delta_R$  be the three possibilities for  $\delta$  with types ,  and  respectively (see Figure 4.2). We set  $\mu_O := \mu(\delta_O, \mathcal{C})$ ,  $\mu_L := \mu(\delta_L, \mathcal{C})$  and  $\mu_R := \mu(\delta_R, \mathcal{C})$ . We want to show that if  $\mu_O, \mu_L$  or  $\mu_R$  is nonzero, i.e., the corresponding NAC-coloring is active for  $\mathcal{C}$ , then it equals 1.

Let  $f: \mathcal{C} \rightarrow \mathcal{C}_f$ , resp.  $g: \mathcal{C} \rightarrow \mathcal{C}_g$ , be the projection of  $\mathcal{C}$  into realizations of the subgraph of  $C_4$  induced by removing vertex  $v_3$ , resp.  $v_4$ . For these two subgraphs, we set  $\mu_f := \mu(\underline{\text{red}}, \mathcal{C}_f)$  and  $\mu_g := \mu(\underline{\text{red}}, \mathcal{C}_g)$ . Theorem 4.8 gives the following equations:

$$\mu_O + \mu_R = \mu_f \cdot \deg(f), \quad \mu_O + \mu_L = \mu_g \cdot \deg(g) \quad (4.8)$$

Assuming that in  $\mathcal{C}_g$  the vertices  $v_1$  and  $v_3$  do not coincide (this is equivalent to  $\mathcal{C}_g$  being a curve not just a point) we show that  $\mu_g = 1$ . Since  $v_1v_2$  is fixed,  $\rho(v_1) = (0, 0)$  and  $\rho(v_2) = (\lambda(v_1v_2), 0)$ . By the definition of  $W_{2,3}$  and  $Z_{2,3}$ , we have  $2(x_3 - \lambda(v_1v_2)) = W_{2,3} + Z_{2,3} = W_{2,3} + \lambda(v_2v_3)^2/W_{2,3}$ . Hence,  $x_3 \in \mathbb{C}(W_{2,3})$ . Similarly,  $y_3 \in \mathbb{C}(W_{2,3})$ . Thus, the rational function field  $\mathbb{C}(W_{2,3})$  is the function field of  $\mathcal{C}_g$ . But there are only two valuations  $\nu_1, \nu_2$  of  $\mathbb{C}(W_{2,3})$  trivial on  $\mathbb{C}$  such that  $\nu_i(W_{2,3}) \neq 0$  (compare [14, Lecture 3]). Those valuations yield  $\nu_1(W_{2,3}) = 1$  and  $\nu_2(W_{2,3}) = -1$ . We know that  $\nu_i(W_{1,2}) = \nu_i(\lambda(v_1v_2)) = 0$ . Hence,  $\mu_g = \text{gap}(\underline{\text{red}}, \nu_1) + \text{gap}(\underline{\text{red}}, \nu_2) = 1 + 0 = 1$ . Analogously, if vertices  $v_2$  and  $v_4$  do not coincide in  $\mathcal{C}_f$ , we get  $\mu_f = 1$ . Under these assumptions equations (4.8) simplify to

$$\begin{aligned} \mu_O + \mu_R &= \deg(f) \\ \mu_O + \mu_L &= \deg(g). \end{aligned}$$

The degree of  $g$ , is the cardinality of the fibre  $g^{-1}(P) \subset \mathcal{C}$ , where  $P$  is a generic point of  $\mathcal{C}_g$ . In other words, we count how many possibilities we have for extending a

realization of a subgraph to a realization of  $C_4$ . Note that, vertex  $v_4$  in  $\mathcal{C}$  has to have coordinates on the intersection of two circles (coming from the edge lengths to vertices  $v_1$  and  $v_3$ ). It might happen that one point of the intersection does not lie in  $\mathcal{C}$ . Hence,  $\deg(g) \in \{1, 2\}$ . Similarly we get this information for  $f$ .

We treat the different motions separately (we still assume non-coinciding vertices).

- If the motion  $\mathcal{C}$  is antiparallel, then  $\mu_L > 0, \mu_R > 0$  and  $\mu_O = 0$ . The coordinates of vertex  $v_4$  in the fibre of  $g$  lie on the intersection of two circles but only one of the intersection points is in  $\mathcal{C}$ , i.e. actually yields an antiparallelogram, whereas the other corresponds to a parallel motion. The same argument works for  $v_3$  and the fibre of  $f$ . Therefore, we have  $\deg(f) = \deg(g) = 1$ , and hence  $\mu_R = \mu_L = 1$ .
- If the motion  $\mathcal{C}$  is parallel, then  $\mu_L = 0, \mu_R = 0$  and  $\mu_O > 0$ . Since one of the points of intersection lies on the antiparallel component, we have  $\deg(f) = \deg(g) = 1$  and thus  $\mu_O = 1$ .
- Similarly for a rhombus where one of the intersection points lies on a degenerate component.
- If the motion  $\mathcal{C}$  of  $C_4$  is general, then  $\deg(f) = \deg(g) = 2$  since the coordinates of the missing vertex both lie on the curve  $\mathcal{C}$ . Since all possible NAC-colorings are active, we know that  $\mu_O, \mu_L$  and  $\mu_R$  are non-zero and therefore  $\mu_O = \mu_L = \mu_R = 1$ .
- If the motion  $\mathcal{C}$  of  $C_4$  is an odd deltoid, then  $\mu_L > 0, \mu_O > 0$  and  $\mu_R = 0$  (see Table 4.1). The degree of  $g$  is two, since the coordinates of  $v_4$  both lie on the curve  $\mathcal{C}$ . Hence,  $\mu_O = \mu_L = 1$ . The equations imply  $\deg(f) = 1$  which is indeed the case, since one point of the intersection does not lie on  $\mathcal{C}$ , but on the degenerate component. Similarly,  $\mu_O = \mu_R = 1$  for an even deltoid.

Finally, if the motion is the degenerate component of an odd deltoid, then  $\mu_L = 0, \mu_O = 0$  and  $\mu_R > 0$ . Hence, only the first equation in (4.8) plays a role, namely,  $\mu_R = \mu_f \cdot \deg(f)$ . We already proved that  $\mu_f = 1$ . The degree of  $f$  is one since the coordinates of  $v_3$  are the same as the coordinates of  $v_1$ . Therefore,  $\mu_R = 1$ . The proofs for an even deltoid and also for the degenerate components of rhombus are analogous.  $\square$

Assuming an algebraic motion, the  $\mu$ -numbers for the valuations of the motion satisfy the formula given by Theorem 4.8 for restrictions to subgraphs. The main step of our classification approach is to find possible sets of active NAC-coloring, which are consistent with the formula for restrictions to 4-cycles. The following definition introduces a consistency condition without assuming an algebraic motion.

**Definition 4.11.** *Let  $H_1, \dots, H_k$  be some 4-cycles of a graph  $G$  such that for each  $H_i$  there exists a NAC-coloring  $\delta \in \text{NAC}_G$  with  $\delta(E_i) = \{\text{red}, \text{blue}\}$ . A subset  $N$  of the*

NAC-colorings of  $G$  is called consistent with the 4-cycles  $H_1, \dots, H_k$  if there exists a vector of nonnegative integers  $(\mu_\delta)_{\delta \in \text{NAC}_G}$  such that:

- (i)  $\mu_\delta \neq 0$  if and only if  $\delta \in N$ , and
- (ii) for each 4-cycle  $H_i$ , there exists a positive integer  $d_i$  such that

$$\sum_{\substack{\delta \in \text{NAC}_G \\ \delta|_{E_{H_i}} = \delta'}} \mu_\delta = d_i$$

for all  $\delta' \in \{\delta|_{E_{H_i}} : \delta \in N\}$ .

We say just consistent with 4-cycles if  $H_1, \dots, H_k$  are all possible 4-cycles of  $G$  satisfying the assumption.

The following corollary proves that the set of active NAC-colorings of an algebraic motion is indeed consistent with the 4-cycles. Therefore, the sets of NAC-colorings consistent with 4-cycles form a superset of actual sets of active NAC-colorings.

**Corollary 4.12.** *Let  $\mathcal{C}$  be an algebraic motion of a graph  $G$ . Let  $H_1, \dots, H_k$  be some 4-cycles of  $G$ . Let  $\mathcal{C}_1, \dots, \mathcal{C}_k$  be the images of  $\mathcal{C}$  by the projections to the realizations of  $H_1, \dots, H_k$ . If  $\mathcal{C}_1, \dots, \mathcal{C}_k$  are curves, then the set of active NAC-colorings  $\text{NAC}_G(\mathcal{C})$  is consistent with the 4-cycles  $H_1, \dots, H_k$ ,*

*Proof.* We set  $\mu_\delta := \mu(\delta, \mathcal{C})$ . The first condition of Definition 4.11 follows immediately from Remark 4.7.

For every  $i \in \{1, \dots, k\}$ , if  $\delta' \in \{\delta|_{E_{H_i}} : \delta \in \text{NAC}_G(\mathcal{C})\} \stackrel{4.9}{=} \text{NAC}_{H_i}(\mathcal{C}_i)$ , then

$$\sum_{\substack{\delta \in \text{NAC}_G \\ \delta|_{E_{H_i}} = \delta'}} \mu_\delta = \mu(\delta', \mathcal{C}_i) \cdot \deg(f_i) = \deg(f_i) > 0$$

by Theorem 4.8 and Theorem 4.10. □

Corollary 4.12 justifies that if there is an algebraic motion of  $(G, \lambda)$ , then the set of active NAC-colorings is consistent with 4-cycles. In order to classify proper flexible labelings, we want to determine all possible candidate sets of active NAC-colorings. One possible approach would be to check for each subset of  $\text{NAC}_G$ , whether it is consistent with 4-cycles of  $G$ . Namely, one would determine the motions of the 4-cycles, construct the system of equations according to Definition 4.11 and check if it has a nonnegative solution.

We choose a slightly modified approach: instead of assuming a set of NAC-colorings, we make an assumption on the motions of quadrilaterals, construct the system and check possible solutions. We also say “motion types consistent with 4-cycles”, since the



assumption of a motion type defines the equation (ii) in Definition 4.11. The nonzero entries of a solution give us a possible set of active NAC-colorings. This seems to be more efficient since some combinations of types can be excluded. Namely, if some combination is not consistent with a subset of 4-cycles, then all extensions of this combination to all 4-cycles can be skipped. Hence, we proceed iteratively — having combinations for some 4-cycles, we extend it for one more 4-cycle and check the consistency.

We describe the procedure in detail now. First, we explain checking consistency for given types of motion of 4-cycles (see Algorithm 1). Let  $H_1, \dots, H_k$  be 4-cycles of  $G$  such that there exists a NAC-coloring  $\delta \in \text{NAC}_G$  with  $\delta(E_i) = \{\text{red}, \text{blue}\}$ . Since we are interested only in proper flexible labelings, the types of NAC-coloring  $m_i$  of a 4-cycle  $H_i$  are allowed to be one of the following motion types (compare with Table 4.1):

- $\mathfrak{p} = \{\square\} = \{O\}$  (parallelogram/rhombus),
- $\mathfrak{a} = \{\square, \square\} = \{L, R\}$  (antiparallelogram),
- $\mathfrak{o} = \{\square, \square\} = \{O, L\}$  (odd deltoid),
- $\mathfrak{e} = \{\square, \square\} = \{O, R\}$  (even deltoid), or
- $\mathfrak{g} = \{\square, \square, \square\} = \{O, L, R\}$  (general).

Having an ansatz  $(m_1, \dots, m_k) \in \{\mathfrak{p}, \mathfrak{a}, \mathfrak{o}, \mathfrak{e}, \mathfrak{g}\}^k$  of motions types of the 4-cycles, we construct the set of equations in variables  $\mu_\delta$  for all  $\delta \in \text{NAC}_G$ . According to Corollary 4.9,  $\mu_\delta = 0$  for all  $\delta \in \text{NAC}_G$  such that the type of  $\delta|_{E_{H_i}}$  is not in  $m_i$  for some  $H_i$ . For each  $H_i$ , the equations from (ii) in Definition 4.11 are added for  $\delta \in \text{NAC}_G$  whose restriction has a type in  $m_i$ . Since we do not know the  $d_i$ , we consider the equations with  $d_i$  eliminated. In particular, there is no equation added if  $m_i = \mathfrak{p}$ . If the obtained system of equations allows a nontrivial nonnegative solution, then  $(m_1, \dots, m_k)$  is consistent with 4-cycles. Example 4.15 shows the system of equations for a specific assumption of motion types of 4-cycles of  $K_{3,3}$ .

We remark that if  $(m_1, \dots, m_k)$  are motion types of an algebraic motion with a flexible labeling  $\lambda$ , then all  $m_i \in \{\mathfrak{p}, \mathfrak{a}, \mathfrak{e}, \mathfrak{o}\}$  enforce some edge lengths to be equal, e.g. if  $m_i \in \{\mathfrak{a}, \mathfrak{p}\}$ , then the opposite edges of  $H_i$  have the same lengths.

In order to find all combinations of motion types consistent with 4-cycles (see Algorithm 2), let  $H_1, \dots, H_\ell$  be all nontrivially colored 4-cycles of  $G$ . In the  $i$ -th iteration, we extend all consistent motion types for  $H_1, \dots, H_{i-1}$  by all  $m_i \in \{\mathfrak{g}, \mathfrak{p}, \mathfrak{a}, \mathfrak{e}, \mathfrak{o}\}$  and check by Algorithm 1.

**Remark 4.13.** *Moreover, we check also the following necessary conditions:*

---

**Algorithm 1** Check consistency

---

**Input:** Motion types  $(m_1, \dots, m_k) \in \{\mathbf{g}, \mathbf{p}, \mathbf{a}, \mathbf{e}, \mathbf{o}\}^k$  for 4-cycle subgraphs  $H_1, \dots, H_k$

**Output:** Consistency of the motion types with the 4-cycles

- 1:  $R := \emptyset$
- 2: **for**  $\delta \in \text{NAC}_G$  **do**
- 3:     **if**  $\exists i \in \{1, \dots, k\} : \text{type of } \delta|_{E_{H_i}} \notin m_i$  **then**
- 4:         Add the equation  $\mu_\delta = 0$  into  $R$ .
- 5:     **end if**
- 6: **end for**
- 7: **for**  $i \in \{1, \dots, k\}$  **do**
- 8:     Add the equations

$$\sum_{\substack{\delta \in \text{NAC}_G \\ \text{type of } \delta|_{E_i} = t_1}} \mu_\delta = \dots = \sum_{\substack{\delta \in \text{NAC}_G \\ \text{type of } \delta|_{E_i} = t_{s_i}}} \mu_\delta$$

into  $R$ , where  $\{t_1, \dots, t_{s_i}\} = m_i$ .

9: **end for**

10: **return** Boolean value whether  $R$  has a nonzero solution with nonnegative entries

---

- (i) Let  $\lambda$  be edge lengths enforced by  $(m_1, \dots, m_k)$ . The edge lengths of the 4-cycles with the motion type  $\mathbf{g}$  must be general, i.e., pairs of opposite, resp. incident, edges cannot have the same length.
- (ii) For  $\lambda$  as in (i), the subgraphs isomorphic to  $K_{2,3}$  cannot have all edge lengths to be the same. Otherwise, two vertices have to coincide.
- (iii) If there are two 4-cycles sharing two incident edges, we assume their orders to be  $(v_1, v_2, v_3, v_4)$  and  $(v_1, v_2, v_5, v_4)$ , then they are not allowed to have motion types  $\mathbf{aa}$ ,  $\mathbf{pp}$ ,  $\mathbf{eo}$  or  $\mathbf{ae}$ . The first two cases would coincide vertices, the third one would imply that one of the deltoids is actually a rhombus, which violates the assumption of motion type, and the last one would force the antiparallelogram to have all lengths equal.

The conditions suggest that a heuristic to reduce the number of checked cases in Algorithm 2 is to sort the 4-cycles so that  $H_{i+1}$  shares some edges with  $H_i$ , if possible.

Having the set of possible motion types from Algorithm 2, we consider only non-isomorphic cases. Namely, motion types  $(m_1, \dots, m_\ell)$  and  $(m'_1, \dots, m'_\ell)$  are isomorphic if there exists an element of the group of automorphisms of the graph such that the sets of edges with the same lengths enforced by  $(m_1, \dots, m_\ell)$  are the images of the sets of edges with the same lengths enforced by  $(m'_1, \dots, m'_\ell)$ . In other words, 4-cycles with general, resp. antiparallel, resp. parallel, resp. deltoid motion are mapped to 4-cycles

---

**Algorithm 2** Find sets of NAC-colorings consistent with 4-cycles

---

**Input:** All 4-cycle subgraphs  $H_1, \dots, H_\ell$

```

1:  $S_{\text{prev}} := \emptyset$ 
2: for  $i \in \{1, \dots, \ell\}$  do
3:    $S := \emptyset$ 
4:   for  $(m_1, \dots, m_{i-1}) \in S_{\text{prev}}$  do
5:     for  $m_i \in \{\mathbf{g}, \mathbf{p}, \mathbf{a}, \mathbf{e}, \mathbf{o}\}$  do
6:       if  $(m_1, \dots, m_i)$  consistent with  $H_1, \dots, H_i$  and (i)–(iii) in 4.13 hold then
7:         Add  $(m_1, \dots, m_i)$  to  $S$ 
8:       end if
9:     end for
10:     $S_{\text{prev}} := S$ 
11:  end for
12: end for

```

**Output:** Set  $S$  of possible motion types of 4-cycles.

---

of the same type. One has to be careful with odd and even deltoids — the order of a 4-cycle can change when an automorphism is applied.

For a representative of each isomorphism class, we consider the system of equations from Algorithm 1. For each nonnegative solution of the system, a set of possible active NAC-colorings consistent with 4-cycles is given by (i) in Definition 4.11. Clearly, the solutions with the same nonzero entries give the same sets of active NAC-colorings.

**Remark 4.14.** *For each set of active NAC-colorings for motion types  $M = (m_1, \dots, m_\ell)$ , we check if there are any 4-cycles with perpendicular diagonals. This is the case of the deltoid, but also if there is an active NAC-coloring satisfying the assumption of Lemma 4.1. Some diagonals might be orthogonal also as a consequence of these two cases. Assume now that  $H_i$  has orthogonal diagonals:*

- (i) *If  $m_i = \mathbf{a}$ , then  $M$  is not valid, since an antiparallelogram cannot have orthogonal diagonals.*
- (ii) *If  $m_i = \mathbf{p}$ , then all edges of  $H_i$  have the same lengths. The conditions (i) and (ii) in Remark 4.13 have to be verified for edge lengths enforced by  $M$  and this extra condition.*
- (iii) *If  $m_i = \mathbf{g}$  and two incident edges of  $H_i$  are enforced by  $M$  to have the same lengths, then also the lengths of the other two edges are equal, which contradicts that  $H_i$  is general.*

Here is a summary how to get pairs of motion types and a set of active NAC-colorings that are possible for non-degenerate motions of the graph, modulo graph automorphism:

- (i) Find all motion types consistent with 4-cycles (Algorithm 2) such that also the conditions of Remark 4.13 hold.
- (ii) Identify isomorphism class of the consistent motion types.
- (iii) For a representative of each class, determine all possible sets of active NAC-colorings.
- (iv) Determine orthogonality of diagonals due to deltoids and special active NAC-coloring and check the conditions of Remark 4.14.

We provide our implementation of the method in [26], see also the section at the end of this chapter.

**Example 4.15.** *We illustrate our method on the well know example of  $K_{3,3}$  by describing all proper flexible labelings. Dixon [16] showed that there are two ways to construct a proper flexible labeling of  $K_{3,3}$ , see Definition 1.9. Walter and Husty [60] proved that these are the only two cases. We prove the same using our method. Let  $V_{K_{3,3}} = \{1, \dots, 6\}$  and  $E_{K_{3,3}} = \{ij : i \in \{1, 3, 5\}, j \in \{2, 4, 6\}\}$ , see Figure 4.5.*

*There are only two NAC-colorings of  $K_{3,3}$  up to symmetries and conjugation, see Figure 4.5. We denote them by  $\omega_k$  for  $k \in V_{K_{3,3}}$  and  $\epsilon_{kl}$  for  $kl \in E_{K_{3,3}}$ , where for an edge  $ij \in E_{K_{3,3}}$ :*

$$\begin{aligned} \omega_k(ij) = \text{blue} &\iff k \in \{i, j\}, \\ \epsilon_{kl}(ij) = \text{blue} &\iff \{k, l\} = \{i, j\} \text{ or } \{k, l\} \cap \{i, j\} = \emptyset. \end{aligned}$$

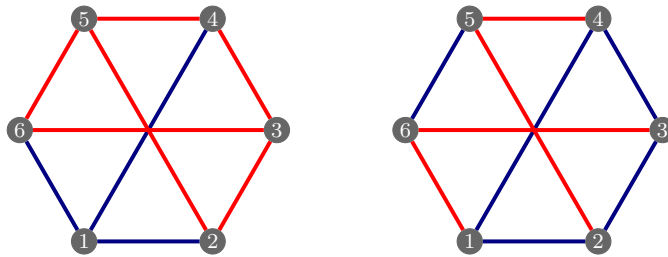


Figure 4.5.:  $K_{3,3}$  with NAC-colorings  $\omega_1$  and  $\epsilon_{56}$ .

*Let  $H_1, \dots, H_9$  be the 4-cycles  $(1, 2, 3, 4)$ ,  $(1, 2, 3, 6)$ ,  $(1, 4, 3, 6)$ ,  $(1, 2, 5, 6)$ ,  $(2, 3, 6, 5)$ ,  $(2, 3, 4, 5)$ ,  $(3, 4, 5, 6)$ ,  $(1, 4, 5, 6)$ ,  $(1, 2, 5, 4)$  respectively. To illustrate Algorithm 1, we*

assume motion types of the 4-cycles and construct the equations:

$$\begin{aligned}
 H_1 : \mathbf{e} \quad & \mu_{\omega_3} = \mu_{\omega_1} = \mu_{\epsilon_{36}} = \mu_{\epsilon_{16}} = 0 \\
 & \mu_{\epsilon_{34}} + \mu_{\epsilon_{14}} + \mu_{\epsilon_{23}} + \mu_{\epsilon_{12}} = \mu_{\omega_4} + \mu_{\epsilon_{45}} + \mu_{\omega_2} + \mu_{\epsilon_{25}} , \\
 H_2 : \mathbf{p} \quad & \mu_{\omega_3} = \mu_{\omega_1} = \mu_{\epsilon_{34}} = \mu_{\epsilon_{14}} = \mu_{\omega_6} = \mu_{\epsilon_{56}} = \mu_{\omega_2} = \mu_{\epsilon_{25}} = 0 , \\
 H_3 : \mathbf{a} \quad & \mu_{\epsilon_{36}} = \mu_{\epsilon_{16}} = \mu_{\epsilon_{34}} = \mu_{\epsilon_{14}} = 0 , \\
 & \mu_{\omega_3} + \mu_{\omega_1} + \mu_{\epsilon_{23}} + \mu_{\epsilon_{12}} = \mu_{\omega_6} + \mu_{\epsilon_{56}} + \mu_{\omega_4} + \mu_{\epsilon_{45}} , \\
 H_4 : \mathbf{g} \quad & \mu_{\omega_5} + \mu_{\omega_1} + \mu_{\epsilon_{45}} + \mu_{\epsilon_{14}} = \mu_{\epsilon_{56}} + \mu_{\epsilon_{16}} + \mu_{\epsilon_{25}} + \mu_{\epsilon_{12}} = \mu_{\omega_6} + \mu_{\epsilon_{36}} + \mu_{\omega_2} + \mu_{\epsilon_{23}} , \\
 H_5 : \mathbf{g} \quad & \mu_{\omega_6} + \mu_{\epsilon_{16}} + \mu_{\omega_2} + \mu_{\epsilon_{12}} = \mu_{\epsilon_{56}} + \mu_{\epsilon_{36}} + \mu_{\epsilon_{25}} + \mu_{\epsilon_{23}} = \mu_{\omega_5} + \mu_{\omega_3} + \mu_{\epsilon_{45}} + \mu_{\epsilon_{34}} , \\
 H_6 : \mathbf{o} \quad & \mu_{\omega_5} = \mu_{\omega_3} = \mu_{\epsilon_{56}} = \mu_{\epsilon_{36}} = 0 , \\
 & \mu_{\omega_4} + \mu_{\epsilon_{14}} + \mu_{\omega_2} + \mu_{\epsilon_{12}} = \mu_{\epsilon_{45}} + \mu_{\epsilon_{34}} + \mu_{\epsilon_{25}} + \mu_{\epsilon_{23}} , \\
 H_7 : \mathbf{g} \quad & \mu_{\omega_5} + \mu_{\omega_3} + \mu_{\epsilon_{25}} + \mu_{\epsilon_{23}} = \mu_{\epsilon_{56}} + \mu_{\epsilon_{36}} + \mu_{\epsilon_{45}} + \mu_{\epsilon_{34}} = \mu_{\omega_6} + \mu_{\epsilon_{16}} + \mu_{\omega_4} + \mu_{\epsilon_{14}} , \\
 H_8 : \mathbf{g} \quad & \mu_{\omega_5} + \mu_{\omega_1} + \mu_{\epsilon_{25}} + \mu_{\epsilon_{12}} = \mu_{\epsilon_{56}} + \mu_{\epsilon_{16}} + \mu_{\epsilon_{45}} + \mu_{\epsilon_{14}} = \mu_{\omega_6} + \mu_{\epsilon_{36}} + \mu_{\omega_4} + \mu_{\epsilon_{34}} , \\
 H_9 : \mathbf{p} \quad & \mu_{\omega_5} = \mu_{\omega_1} = \mu_{\epsilon_{56}} = \mu_{\epsilon_{16}} = \mu_{\omega_4} = \mu_{\epsilon_{34}} = \mu_{\omega_2} = \mu_{\epsilon_{23}} = 0 .
 \end{aligned}$$

The summands that are immediately zero are colored gray. We can see that  $\mu_{\epsilon_{45}}$  and  $\mu_{\epsilon_{12}}$  must be also zero. Hence, these motion types are not consistent with 4-cycles since there is no nontrivial solution.

The output of the whole method described in Section 4.3 obtained by computer is summarized in Table 4.2 (see [26, 40]). The motion types consistent with  $H_1, \dots, H_9$  and the corresponding sets of active NAC-colorings are in the first and second column. The third column indicates the number of motion types isomorphic to the chosen representative.

Motions types of $(H_1, \dots, H_7)$	Active NAC-colorings	# isomorphic	Type of motion
$\mathbf{g} \mathbf{g} \mathbf{g} \mathbf{g} \mathbf{g} \mathbf{g} \mathbf{g} \mathbf{g} \mathbf{g} \mathbf{g}$	$\text{NAC}_{K_{3,3}}$	1	
$\mathbf{o} \mathbf{o} \mathbf{o} \mathbf{g} \mathbf{g} \mathbf{g} \mathbf{g} \mathbf{g} \mathbf{g} \mathbf{g}$	$\{\epsilon_{12}, \epsilon_{23}, \epsilon_{34}, \epsilon_{14}, \epsilon_{16}, \epsilon_{36}, \omega_1, \omega_3\}$	6	Dixon I
$\mathbf{p} \mathbf{o} \mathbf{o} \mathbf{g} \mathbf{g} \mathbf{o} \mathbf{g} \mathbf{g} \mathbf{e}$	$\{\epsilon_{12}, \epsilon_{23}, \epsilon_{34}, \epsilon_{14}\}$	9	
$\mathbf{p} \mathbf{g} \mathbf{g} \mathbf{g} \mathbf{a} \mathbf{g} \mathbf{g} \mathbf{a} \mathbf{g}$	$\{\epsilon_{12}, \epsilon_{34}, \omega_5, \omega_6\}$	18	Dixon II

Table 4.2.: Consistent motion types and active NAC-colorings of  $K_{3,3}$ .

We show that the first three lines are of Dixon I type. Since  $\epsilon_{12}, \epsilon_{23}, \epsilon_{34}$  are active, we have that the 4-cycles  $(3, 4, 5, 6)$ ,  $(1, 4, 5, 6)$  and  $(1, 2, 5, 6)$  have perpendicular diagonals by Lemma 4.1. It immediately follows that 1, 3 and 5, resp. 2, 4 and 6 are collinear and these two lines are orthogonal. We remark that the second and third line are special cases when some 4-cycles are deltoids. The 4-cycle  $H_1$  in the third line is actually a rhombus.

To show that the last line is a Dixon II motion, consider a realization compatible with edge lengths enforced by the motion types. The positions of the vertices of the antiparallelogram  $(2, 3, 6, 5)$  together with the edge lengths determine the position of the vertex 4, since the 4-cycle  $(3, 4, 5, 6)$  has perpendicular diagonals due the active NAC-coloring  $\epsilon_{12}$ . The position of 1 is then determined since  $(1, 2, 3, 4)$  is a parallelogram. Since  $(1, 4, 5, 6)$  is an antiparallelogram, it follows that the vertices lie on the two rectangles as required, see Figure 4.6.

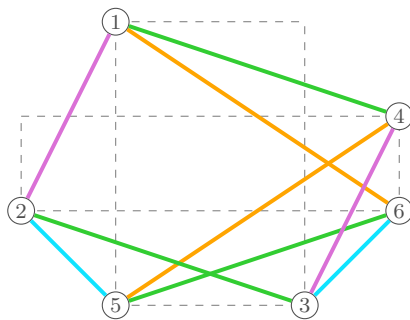


Figure 4.6.: Dixon II motion of  $K_{3,3}$  (same colors indicate same edge lengths).

#### 4.4. Classification of motions of $Q_1$

The goal of this section is to classify all proper flexible labelings of the graph  $Q_1$  using the tools developed in the previous sections. At the beginning, we show that certain active NAC-colorings force the vertices of the unique triangle in  $Q_1$  to be collinear, or some edge lengths must be equal.

Next, we determine consistent motion types and active NAC-colorings by the method from Section 4.3. These are obtained by computer using our implementation of the method [26]. It appears that the triangle is actually degenerate for every consistent motion types. Then we obtain necessary algebraic conditions on  $\lambda$  from singleton NAC-colorings by the technique from Section 4.1. Using the computer algebra system SageMath [57], we identify six types of motion, containing altogether eight families of proper flexible labelings (see [40] for the computations). Animations of these motions can be found in [39].

At the end of this section, we give a proof that the triangle is degenerate for every proper flexible labeling without using the consistent motion types, i.e., in computer-free manner. The proof was presented in [28].

Let  $\Lambda \subset \mathbb{R}^{E_{Q_1}}$  be the set of all proper flexible labelings  $\lambda : E_{Q_1} \rightarrow \mathbb{R}_+$  of  $Q_1$ . By *classification of motions*, or *proper flexible labelings* of  $Q_1$  we mean the decomposition

of the Zariski closure of  $\Lambda$  into irreducible algebraic sets  $\Lambda_1, \dots, \Lambda_k$ . We recall that the Zariski closure of  $\Lambda$  is the smallest algebraic set containing  $\Lambda$ .

Clearly, every proper flexible labeling is in some  $\Lambda_i$ , but not every  $\lambda \in \Lambda_i$  is flexible — for instance, it is not guaranteed that it is realizable over  $\mathbb{R}$ , since this would require also inequalities. Notice also that a labeling in  $\Lambda_i$  does not have all edge lengths necessarily positive, but as long as they are not zero, the system (1.1) does not change due to taking squares, with the exception of the fixed edge — switching the sign of the fixed edge rotates the compatible realizations around the origin by  $180^\circ$ . There also might be a proper subvariety containing flexible labelings that are not proper.

Our goal is to provide equations defining the irreducible varieties and an instance for each of them that is proper flexible, namely, it has infinitely many non-congruent injective real realizations. The examples might have negative edge lengths of the degenerate triangle in order to handle all three possible arrangements of the collinear points using only one equation.

The NAC-colorings of  $Q_1$ , modulo conjugation, are shown in Figure 4.7. The figure also depicts the vertex labels we use in this section.

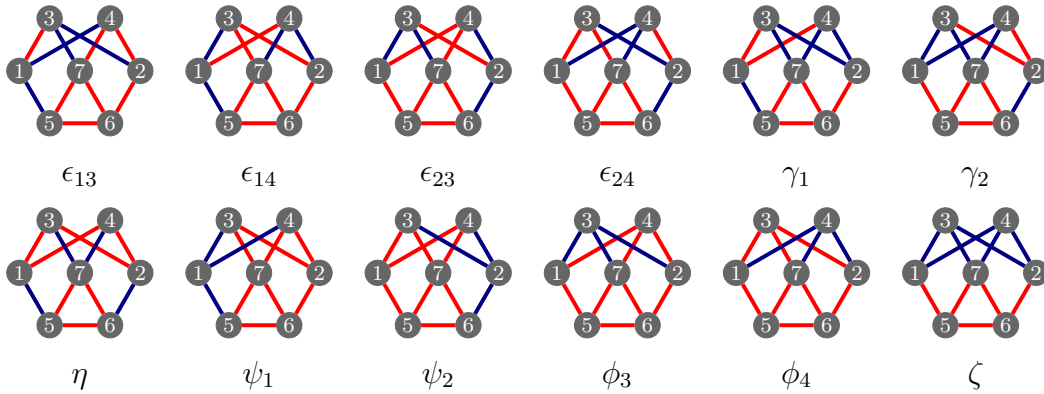


Figure 4.7.: NAC-colorings of the graph  $Q_1$ .

We start with the following lemma which states that the triangle  $(5, 6, 7)$  is degenerate, or some edge lengths must be equal if a certain NAC-coloring is active.

**Lemma 4.16.** *Let  $\mathcal{C}$  be an algebraic motion of  $(Q_1, \lambda)$ . If  $\eta \in \text{NAC}_{Q_1}(\mathcal{C})$ , resp.  $\epsilon_{13} \in \text{NAC}_{Q_1}(\mathcal{C})$ , then the vertices of the triangle  $(5, 6, 7)$  are collinear, or  $\lambda_{24} = \lambda_{23}$  and  $\lambda_{14} = \lambda_{13}$ , resp.  $\lambda_{26} = \lambda_{67}$  and  $\lambda_{24} = \lambda_{47}$ .*

*Proof.* The leading coefficient technique described in Section 4.1 can be used, since the NAC-colorings  $\eta$  and  $\epsilon_{13}$  are singletons. In case  $\eta \in \text{NAC}_{Q_1}(\mathcal{C})$ , the equation

$$\lambda_{57}^2 r^2 + \lambda_{67}^2 s^2 + (\lambda_{56}^2 - \lambda_{57}^2 - \lambda_{67}^2) rs = 0$$

is obtained (see also Example 4.3), where  $r = \lambda_{24}^2 - \lambda_{23}^2$  and  $s = \lambda_{14}^2 - \lambda_{13}^2$ . Considering the equation as a polynomial in  $r$ , the discriminant is

$$(\lambda_{56} + \lambda_{57} + \lambda_{67})(\lambda_{56} + \lambda_{57} - \lambda_{67})(\lambda_{56} - \lambda_{57} + \lambda_{67})(\lambda_{56} - \lambda_{57} - \lambda_{67})s^2.$$

But this is always negative or zero from the triangle inequality. Hence, the triangle must be degenerate, or  $s = 0$ . If  $s = 0$ , then also  $r = 0$  and the statement follows. The proof for  $\epsilon_{13} \in \text{NAC}_{Q_1}(\mathcal{C})$  is similar, since the obtained equation is

$$\lambda_{57}^2 \underbrace{(\lambda_{26}^2 - \lambda_{67}^2)}_r^2 + \lambda_{67}^2 \underbrace{(\lambda_{24}^2 - \lambda_{47}^2)}_s^2 + (\lambda_{56}^2 - \lambda_{57}^2 - \lambda_{67}^2) \underbrace{(\lambda_{26}^2 - \lambda_{67}^2)}_r \underbrace{(\lambda_{24}^2 - \lambda_{47}^2)}_s.$$

□

Table 4.3 summarizes the output of the computation of consistent motion types using our implementation [26, 40]. The consistent motion types of 4-cycles and active NAC-coloring are given. The 4-cycles  $H_1, \dots, H_7$  are  $(1, 3, 2, 4)$ ,  $(1, 3, 7, 4)$ ,  $(2, 3, 7, 4)$ ,  $(1, 3, 7, 5)$ ,  $(1, 4, 7, 5)$ ,  $(2, 4, 7, 6)$ ,  $(2, 3, 7, 6)$  respectively. The number of isomorphic motion types is also indicated in the table. The column ‘‘Type of motion’’ indicates to which family of proper flexible labelings of  $Q_1$  a particular row belongs. The next column gives information about the dimension of this family. The last column provides the reference to the section where a particular type of motion is elaborated.

	<b>Motions types of <math>(H_1, \dots, H_7)</math></b>	<b>Active NAC-colorings</b>	<b># isom.</b>	<b>Type of motion</b>	<b>Dim.</b>	<b>Sec.</b>
(a)	<b>p g g p g p g</b>	$\{\epsilon_{13}, \epsilon_{24}, \eta\}$	2	I	4	
(b)	<b>p o a p o p e</b>	$\{\epsilon_{13}, \eta\}$	4	$\subset$ I, IV <sub>-</sub> , V, VI	2	4.4.1
(c)	<b>p e e p a p a</b>	$\{\epsilon_{13}, \epsilon_{24}\}$	2	$\subset$ I, II, III	2	
(d)	<b>o g g g g g g</b>	$\{\epsilon_{ij}, \gamma_1, \gamma_2, \psi_1, \psi_2\}$	1	II <sub>-</sub> $\cup$ II <sub>+</sub>	5	
(e)	<b>p e e g g g g</b>	$\{\epsilon_{13}, \epsilon_{14}, \epsilon_{23}, \epsilon_{24}\}$	1	$\subset$ II <sub>-</sub> , II <sub>+</sub>	4	4.4.2
(f)	<b>o g g p g g a</b>	$\{\epsilon_{13}, \epsilon_{24}, \gamma_1, \psi_2\}$	4	$\subset$ II <sub>-</sub>	3	
(g)	<b>o g g e g g e</b>	$\{\epsilon_{13}, \epsilon_{23}, \gamma_1, \gamma_2\}$	2	$\subset$ II <sub>-</sub> , deg.	2	
(h)	<b>o g g g a g a</b>	$\{\epsilon_{13}, \epsilon_{24}, \psi_1, \psi_2, \zeta\}$	2	III	3	4.4.3
(i)	<b>g g a p g g g</b>	$\{\epsilon_{13}, \eta, \phi_4, \psi_2\}$	4	IV <sub>-</sub> $\cup$ IV <sub>+</sub>	4	4.4.4
(j)	<b>g g a e g p e</b>	$\{\epsilon_{13}, \eta, \gamma_2, \phi_3\}$	4	V	3	4.4.5
(k)	<b>p g g e g g e</b>	$\{\epsilon_{13}, \epsilon_{23}, \eta, \zeta\}$	2	VI	3	4.4.6

Table 4.3.: The cases of consistent motion types and active NAC-colorings of  $Q_1$ .



### 4.4.1. Motion type I

We prove that Case (a) gives a 4-dimensional family of proper flexible labelings, with (b) and (c) being special cases. Although it might be seen rather easily that the triangle  $(5, 6, 7)$  is degenerate, since the 4-cycles  $(1, 3, 2, 4)$ ,  $(1, 3, 7, 5)$  and  $(2, 4, 7, 6)$  are parallelograms, and that the proper flexible labelings can be actually constructed by Lemma 3.16 (see also Figure 4.9), we illustrate an approach that allows to deal also with the other cases.

In Case (a), the motion types enforce the following equalities of edge lengths:

$$\lambda_{13} = \lambda_{24} = \lambda_{57} = \lambda_{67}, \quad \lambda_{14} = \lambda_{23}, \quad \lambda_{15} = \lambda_{37}, \quad \lambda_{26} = \lambda_{47}.$$

They are also depicted by the same colors in Figure 4.8.

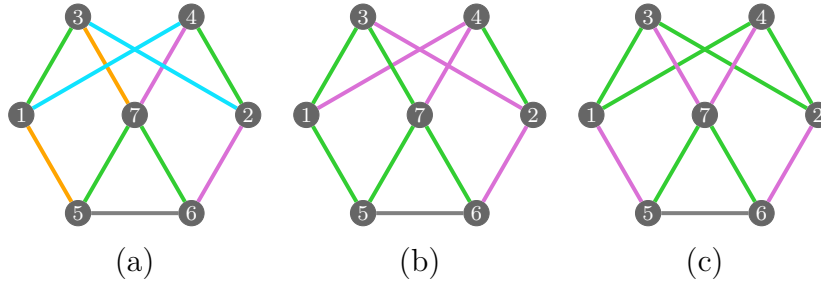


Figure 4.8.: Edge lengths enforced by motion types (a)–(c): same color indicates equality of edge lengths.

Since the NAC-colorings  $\epsilon_{13}$ ,  $\epsilon_{24}$  and  $\eta$  are singletons, we can use the method of comparing leading coefficients described in Section 4.1 to obtain the following equations for  $\lambda$ :

$$\begin{aligned} (\lambda_{56} - 2\lambda_{67})(\lambda_{56} + 2\lambda_{67})(\lambda_{47} - \lambda_{67})(\lambda_{47} + \lambda_{67}) &= 0 && (\epsilon_{13} \text{ active}), \\ (\lambda_{56} - 2\lambda_{67})(\lambda_{56} + 2\lambda_{67})(\lambda_{37} - \lambda_{67})(\lambda_{37} + \lambda_{67}) &= 0 && (\epsilon_{24} \text{ active}), \\ (\lambda_{56} - 2\lambda_{67})(\lambda_{56} + 2\lambda_{67})(\lambda_{23} - \lambda_{67})(\lambda_{23} + \lambda_{67}) &= 0 && (\eta \text{ active}). \end{aligned} \tag{4.9}$$

The second and fourth factor cannot vanish by the assumption that edge lengths are positive. If the first factor does not vanish, then  $\lambda_{13} = \lambda_{24} = \lambda_{57} = \lambda_{67} = \lambda_{14} = \lambda_{23} = \lambda_{15} = \lambda_{37} = \lambda_{26} = \lambda_{47}$ , which contradicts injective realizations (for instance the  $K_{2,3}$  subgraph induced by 1, 2, 3, 4 and 7 has no injective realizations). Hence, we have that  $\lambda_{56} = 2\lambda_{67} = \lambda_{57} + \lambda_{67}$ , i.e., the triangle  $(5, 6, 7)$  is degenerate. We remark that instead of taking the factorizations, we could also argue by Lemma 4.17.

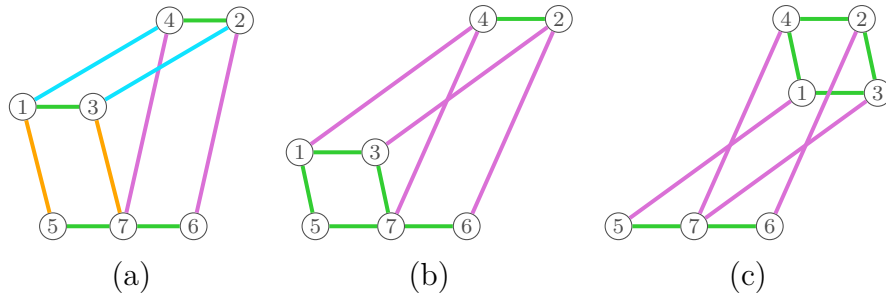


Figure 4.9.: Realizations of  $Q_1$  compatible with proper flexible labelings of type I.

If we fix the vertices 5 and 6, then the system (1.1) has the following form

$$\begin{aligned}
 (x_1 - x_3)^2 + (y_1 - y_3)^2 &= (x_2 - x_4)^2 + (y_2 - y_4)^2 = \lambda_{67}^2 \\
 (x_5 - x_7)^2 + (y_5 - y_7)^2 &= (x_6 - x_7)^2 + (y_6 - y_7)^2 = \lambda_{67}^2 \\
 (x_1 - x_4)^2 + (y_1 - y_4)^2 &= (x_2 - x_3)^2 + (y_2 - y_3)^2 = \lambda_{23}^2 \\
 (x_1 - x_5)^2 + (y_1 - y_5)^2 &= (x_3 - x_7)^2 + (y_3 - y_7)^2 = \lambda_{37}^2 \\
 (x_2 - x_6)^2 + (y_2 - y_6)^2 &= (x_4 - x_7)^2 + (y_4 - y_7)^2 = \lambda_{47}^2 \\
 x_5 = y_5 = y_6 &= 0, \quad x_6 = 2\lambda_{67}.
 \end{aligned}$$

Considering  $\lambda_{67}$ ,  $\lambda_{23}$ ,  $\lambda_{37}$  and  $\lambda_{47}$  also as variables, the zero set has dimension 5, as one can check by Gröbner basis computation. There are only 4 parameters, therefore if we fix  $\lambda_{67}$ ,  $\lambda_{23}$ ,  $\lambda_{37}$  and  $\lambda_{47}$ , then there is a curve of solutions. Hence, the labeling is flexible whenever it is realizable. If the parameters are general enough, for instance pairwise distinct, then the labeling is proper flexible. A realization compatible with such an instance is shown in Figure 4.9.

In Case (b) and (c), the equations from comparing leading coefficients for corresponding active NAC-colorings always have the form of the first equation in 4.9. By the same reasons as before, the triangle (5, 6, 7) is degenerate for every proper flexible labeling. Any flexible labeling enforced by motion types (b) or (c) and having the degenerate triangle satisfy also the equations of (a), i.e., (b) and (c) are subcases of (a). Figure 4.9 shows some examples.

#### 4.4.2. Motion type II

If  $\gamma_1$ , resp.  $\gamma_2$  is active, then the 4-cycle  $H_3 = (2, 3, 7, 4)$ , resp.  $H_2 = (1, 3, 7, 4)$  has orthogonal diagonals by Lemma 4.1. Together with the motion types of  $H_1$ ,  $H_2$  and  $H_3$ , this implies that the vertices 1, 2 and 7 are collinear in all Cases (d)–(g).

The motion types in Cases (d)–(g) enforce  $\lambda_{13} = \lambda_{23}$  and  $\lambda_{14} = \lambda_{24}$  (see Figure 4.10). Assuming that the triangle (5, 6, 7) is not degenerate, Lemma 4.17 for  $\epsilon_{13}$  gives  $\lambda_{24} = \lambda_{47}$ .

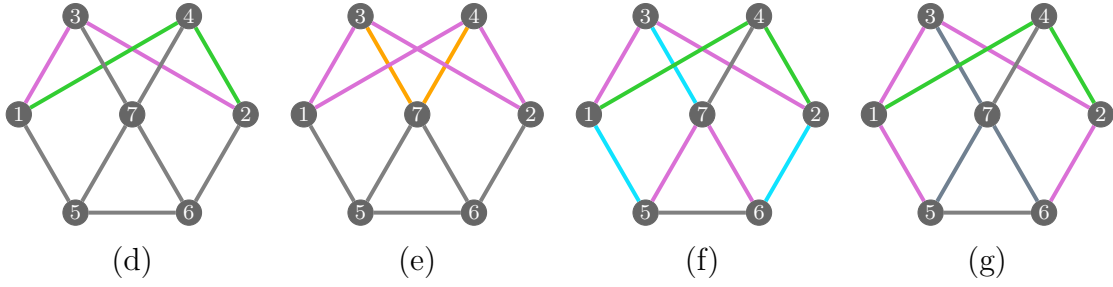


Figure 4.10.: Edge lengths enforced by motion types (d)–(g): same color (except for gray) indicates equality of edge lengths.

But this is a contradiction, since three distinct collinear points 1, 2 and 7 cannot have the same distance to vertex 4. Hence, the triangle (5, 6, 7) is degenerate. In order to avoid distinguishing the cases of which vertex is the middle one, we allow edge lengths in the triangle to be also negative. Then we can cover all three cases by the equation  $\lambda_{56} = \lambda_{57} + \lambda_{67}$ .

We focus now on Case (d). The active NAC-colorings  $\epsilon_{13}, \epsilon_{14}, \epsilon_{23}, \epsilon_{24}, \gamma_1$  and  $\gamma_2$  are singletons ( $\psi_1$  and  $\psi_2$  are not). The system of equations they provide together with the enforced edge lengths by the motion types has Gröbner basis:

$$\begin{aligned} & \left( \lambda_{26}^2 \lambda_{57}^2 - \lambda_{15}^2 \lambda_{67}^2 \right) \cdot A(\lambda_{15}, \lambda_{24}, \lambda_{26}, \lambda_{47}, \lambda_{56}, \lambda_{57}, \lambda_{67}) = 0, \\ & \left( \lambda_{26}^2 \lambda_{57}^2 - \lambda_{15}^2 \lambda_{67}^2 \right) \cdot B(\lambda_{15}, \lambda_{24}, \lambda_{26}, \lambda_{47}, \lambda_{57}, \lambda_{67}) = 0, \\ & D(\lambda_{15}, \lambda_{24}, \lambda_{47}, \lambda_{56}, \lambda_{57}, \lambda_{67}) = 0, \\ & E(\lambda_{24}, \lambda_{26}, \lambda_{47}, \lambda_{56}, \lambda_{57}, \lambda_{67}) = 0, \\ & \lambda_{13} = \lambda_{23}, \quad \lambda_{14} = \lambda_{24}, \quad \lambda_{24}^2 + \lambda_{37}^2 = \lambda_{23}^2 + \lambda_{47}^2 \end{aligned}$$

where  $A, B, C, D, E$  are polynomials in  $\lambda_{ij}$ . Assume that the first factor vanishes. We introduce a new variable  $u$ , add the equations  $\lambda_{56} = \lambda_{57} + \lambda_{67}$  and  $(\lambda_{26}^2 \lambda_{57}^2 - \lambda_{15}^2 \lambda_{67}^2) \cdot u = 1$  and eliminate the variable  $u$ . Then the ideal is  $\langle 1 \rangle$ , namely it is not possible that  $(\lambda_{26}^2 \lambda_{57}^2 - \lambda_{15}^2 \lambda_{67}^2)$  does not vanish. Therefore, we add the factor and the equation for the degenerate triangle to the Gröbner basis. After eliminating the case  $\lambda_{67} = 0$ , we obtain:

$$\begin{aligned} & -\lambda_{24}^4 + \lambda_{15}^2 \lambda_{26}^2 + 2\lambda_{24}^2 \lambda_{47}^2 - \lambda_{47}^4 - 2\lambda_{15}^2 \lambda_{67}^2 + \lambda_{57}^2 \lambda_{67}^2 = 0, \\ & \lambda_{24}^2 \lambda_{57} - \lambda_{47}^2 \lambda_{57} + \lambda_{15}^2 \lambda_{67} - \lambda_{57}^2 \lambda_{67} = 0, \\ & \lambda_{26}^2 \lambda_{57} + \lambda_{24}^2 \lambda_{67} - \lambda_{47}^2 \lambda_{67} - \lambda_{57} \lambda_{67}^2 = 0, \\ & \lambda_{13} = \lambda_{23}, \quad \lambda_{14} = \lambda_{24}, \quad \lambda_{24}^2 + \lambda_{37}^2 = \lambda_{23}^2 + \lambda_{47}^2, \quad \lambda_{57} + \lambda_{67} = \lambda_{56}. \end{aligned}$$

The zero set of these equations is not irreducible. The two irreducible components are

given by the following equations for  $\alpha \in \{-1, 1\}$ :

$$\begin{aligned} -\lambda_{24}^2 + \alpha\lambda_{15}\lambda_{26} + \lambda_{47}^2 + \lambda_{57}\lambda_{67} &= 0, \\ \lambda_{26}\lambda_{57} + \alpha\lambda_{15}\lambda_{67} &= 0, \\ \lambda_{13} = \lambda_{23}, \quad \lambda_{14} = \lambda_{24}, \quad \lambda_{24}^2 + \lambda_{37}^2 &= \lambda_{23}^2 + \lambda_{47}^2, \quad \lambda_{57} + \lambda_{67} = \lambda_{56}. \end{aligned}$$

To indicate  $\alpha$ , we denote the components by  $\text{II}_-$  and  $\text{II}_+$ . We recall that the second equation is consistent also in  $\text{II}_+$ , since we allow negative edge lengths for the edges in the triangle  $(5, 6, 7)$ . The dimension of both varieties is 5. If we construct the system of equations for vertex coordinates, taking the  $\lambda_{ij}$  as variables, the dimension is 6. Therefore, a generic fibre of the projection from the whole zero set to  $\text{II}_-$ , resp.  $\text{II}_+$ , has positive dimension. Hence, a generic  $\lambda$  in  $\text{II}_- \cup \text{II}_+$  that is realizable is flexible.

Before we provide an example of a proper flexible labeling for  $\text{II}_-$  and  $\text{II}_+$ , let us remark that using an analogous approach, one can show that Case (e) gives also two irreducible components, each of them being a subcase of  $\text{II}_-$  or  $\text{II}_+$ . Case (f) yields an irreducible component, which is a subvariety of  $\text{II}_-$ . This is the case also for (c). Labelings which satisfy equations given by motion types, active NAC-colorings and the degenerate triangle in Case (g) form a subvariety of  $\text{II}_-$ . Nevertheless, they are not proper. Assuming a non-degenerate motion, the deltoids and active NAC-colorings  $\gamma_1$  and  $\gamma_2$  imply that  $1, 2, 7$  and  $3, 4, 5, 6$  are collinear, respectively. These line are perpendicular, but since there is also for instance an edge between 5 and 6, no motion is possible.

Case (g) shows that not all labelings in  $\text{II}_-$  are proper. The labelings which are not proper form a subset of an algebraic variety. Theoretically, the equations for this variety can be obtained by adding the equations for coordinates of coinciding vertices into the system (1.1) and eliminating the coordinate variables. Since,  $\text{II}_-$ , resp.  $\text{II}_+$ , are irreducible, giving an example of a proper flexible labeling implies that the subvariety of non-proper labelings is strict. In particular, a generic realizable labeling in  $\text{II}_-$ , resp.  $\text{II}_+$ , is proper. An example of a proper flexible labeling in  $\text{II}_+$  is

$$\begin{aligned} \lambda_{13} = \lambda_{23} = 14, \quad \lambda_{15} = 9, \quad \lambda_{26} = 12, \quad \lambda_{37} = 10, \quad \lambda_{47} = 5, \\ \lambda_{14} = \lambda_{24} = 11, \quad \lambda_{56} = 1, \quad \lambda_{57} = -3, \quad \lambda_{67} = 4. \end{aligned}$$

The algebraic motion can be parametrized by

$$\begin{aligned} (x_1, y_1) &= \left( -\frac{9(t^2 - 1)}{t^2 + 1}, \frac{18t}{t^2 + 1} \right), \\ (x_2, y_2) &= \left( \frac{13t^2 - 44}{t^2 + 4}, -\frac{48t}{t^2 + 4} \right), \\ (x_3, y_3) &= \left( \frac{2t^4 - 3s(t)_1 t - 29t^2 - 4}{t^4 + 5t^2 + 4}, -\frac{15t^3 + (t^2 - 2)s(t)_1 - 12t}{t^4 + 5t^2 + 4} \right), \end{aligned}$$

$$(x_4, y_4) = \left( \frac{2t^4 - 3s(t)_2t - 29t^2 - 4}{t^4 + 5t^2 + 4}, -\frac{15t^3 + (t^2 - 2)s(t)_2 - 12t}{t^4 + 5t^2 + 4} \right),$$

$$(x_5, y_5) = (0, 0), \quad (x_6, y_6) = (1, 0), \quad (x_7, y_7) = (-3, 0),$$

where

$$s_1(t) = \pm\sqrt{3(5t^2 + 32)(5t^2 + 4)} \quad \text{and} \quad s_2(t) = \pm\sqrt{165t^2 + 84}.$$

There are two connected components, one is parametrized by taking  $(+, +)$  and  $(+, -)$  for  $s_1$  and  $s_2$ , the other by taking  $(-, -)$  and  $(-, +)$ . They are symmetric by reflection w.r.t. the line of the degenerate triangle. Figure 4.11 illustrates a part of the motion, with positive  $s_1$  and  $s_2$ .

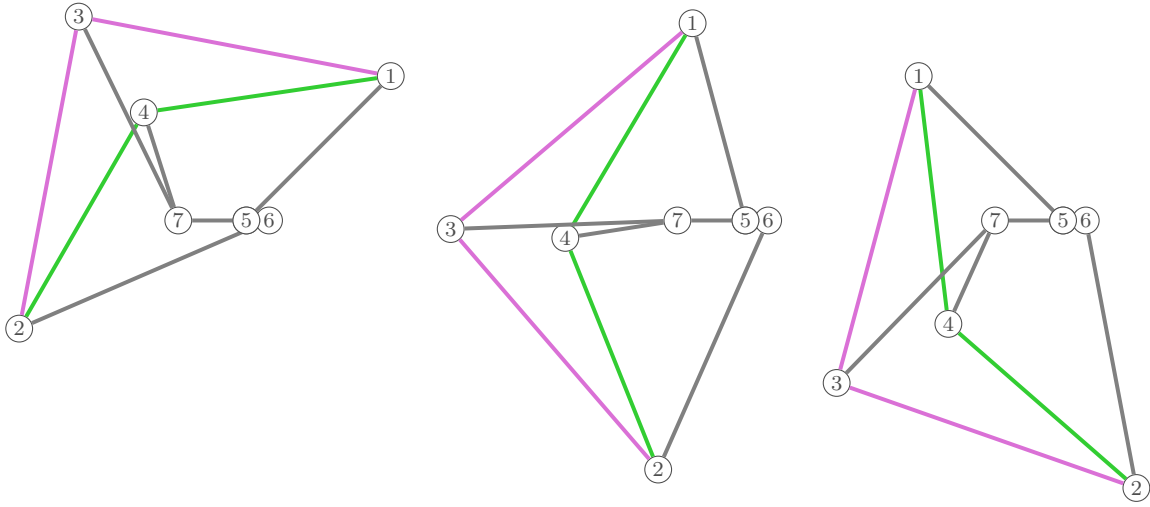


Figure 4.11.: Example of a motion of type  $II_+$ .

An example of a proper flexible labeling in  $II_-$  is

$$\begin{aligned} \lambda_{13} = \lambda_{23} = 10, & \quad \lambda_{15} = 9, & \quad \lambda_{26} = 12, & \quad \lambda_{37} = 14, & \quad \lambda_{47} = 11, \\ \lambda_{14} = \lambda_{24} = 5, & \quad \lambda_{56} = 7, & \quad \lambda_{57} = 3, & \quad \lambda_{67} = 4. \end{aligned}$$

A parametrization of the motion is

$$(x_1, y_1) = \left( -\frac{9(t^2 - 1)}{t^2 + 1}, \frac{18t}{t^2 + 1} \right),$$

$$(x_2, y_2) = \left( -\frac{20t^2 - 19}{4t^2 + 1}, \frac{48t}{4t^2 + 1} \right),$$

$$(x_3, y_3) = \left( -\frac{28t^4 + 3s_1(t)t - 13t^2 - 14}{4t^4 + 5t^2 + 1}, \frac{60t^3 - (2t^2 - 1)s_1(t) + 33t}{4t^4 + 5t^2 + 1} \right),$$

$$(x_4, y_4) = \left( -\frac{28t^4 + 3s_2(t)t^2 - 13t^2 - 14}{4t^4 + 5t^2 + 1}, \frac{60t^3 - (2t^3 - t)s_2(t) + 33t}{4t^4 + 5t^2 + 1} \right),$$

$$(x_5, y_5) = (0, 0), \quad (x_6, y_6) = (7, 0), \quad (x_7, y_7) = (3, 0),$$

where

$$s_1(t) = \pm\sqrt{3(32t^2 + 5)(4t^2 + 5)} \quad \text{and} \quad s_2(t) = \pm\sqrt{84t^2 + 165}.$$

There are again two connected components, which are symmetric to each other by reflection. Figure 4.12 illustrates a part of the motion, with positive  $s_1$  and negative  $s_2$ .

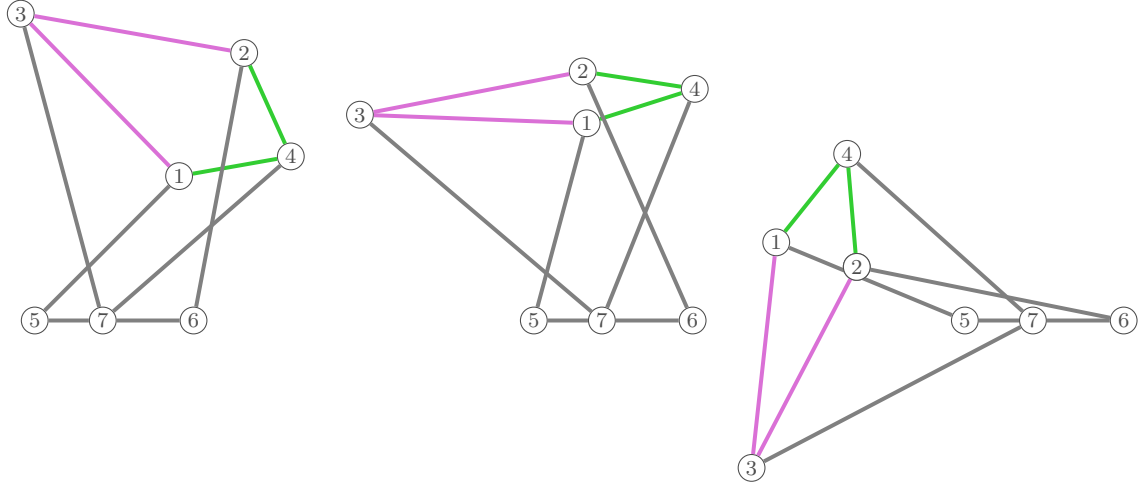


Figure 4.12.: Example of a motion of type II<sub>-</sub>.

### 4.4.3. Motion type III

The edge lengths enforced by the motion types in Case (h) are depicted in Figure 4.13 (h). The triangle (5, 6, 7) is degenerate, otherwise the active NAC-coloring  $\epsilon_{13}$  implies that  $\lambda_{26} = \lambda_{67}$  by Lemma 4.16. But this contradicts that the 4-cycle  $H_7 = (2, 3, 7, 6)$  is an antiparallelogram.

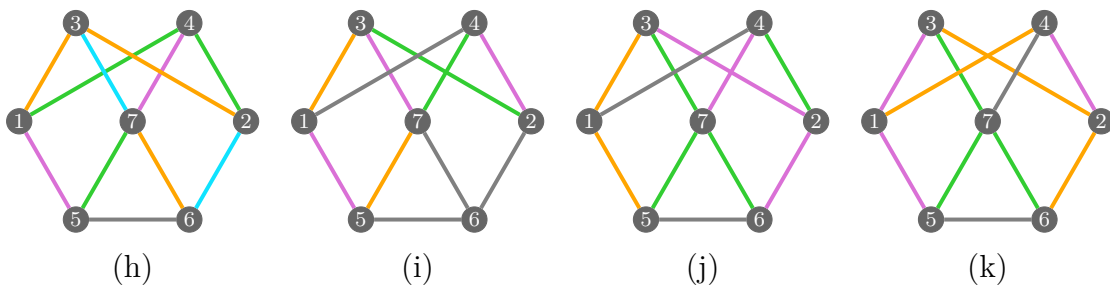


Figure 4.13.: Edge lengths enforced by Cases (h)–(k): same color (except for gray) indicates equality of edge lengths.

We consider the ideal generated by the edge lengths equalities, active NAC-colorings  $\epsilon_{13}$ ,  $\epsilon_{24}$  and  $\zeta$ , which are singletons w.r.t. all active NAC-colorings and the equation for

the degenerate triangle. Notice that  $\zeta$  is not singleton in general. The ideal has the following Gröbner basis:

$$(\lambda_{37}^2 \lambda_{57} - \lambda_{47}^2 \lambda_{67} + \lambda_{57}^2 \lambda_{67} - \lambda_{57} \lambda_{67}^2)^2 = 0,$$

$$\lambda_{23} = \lambda_{13} = \lambda_{67}, \quad \lambda_{24} = \lambda_{14} = \lambda_{57}, \quad \lambda_{15} = \lambda_{47}, \quad \lambda_{26} = \lambda_{37}, \quad \lambda_{56} = \lambda_{57} + \lambda_{67}.$$

Clearly, we can skip taking the square in the first equation. Then the ideal is prime, i.e., the variety is irreducible. It has dimension 3, whereas the system for vertex coordinates enriched with the equations above has dimension 4. Hence, a generic realizable labeling is flexible. An example of a proper flexible labeling is

$$\begin{aligned} \lambda_{23} = \lambda_{13} = \lambda_{67} = 10, & & \lambda_{15} = \lambda_{47} = 2, & & \lambda_{56} = 18, \\ \lambda_{24} = \lambda_{14} = \lambda_{57} = 8, & & \lambda_{26} = \lambda_{37} = 5. \end{aligned}$$

The motion can be parametrized by

$$\begin{aligned} (x_1, y_1) &= \left( -\frac{2(t^2 - 1)}{t^2 + 1}, \frac{4t}{t^2 + 1} \right), \\ (x_2, y_2) &= \left( \frac{68125t^4 - 25ts(t) + 39675t^2 + 4734}{8(625t^4 + 325t^2 + 36)}, -\frac{5(875t^3 - (25t^2 + 6)s(t) + 75t)}{8(625t^4 + 325t^2 + 36)} \right), \\ (x_3, y_3) &= \left( \frac{675t^4 - 2s(t)t + 1208t^2 + 405}{4(25t^4 + 34t^2 + 9)}, \frac{50t^3 - (5t^2 + 3)s(t) - 78t}{4(25t^4 + 34t^2 + 9)} \right), \\ (x_4, y_4) &= \left( \frac{30(5t^2 + 3)}{25t^2 + 9}, -\frac{60t}{25t^2 + 9} \right), \\ (x_5, y_5) &= (0, 0), \quad (x_6, y_6) = (18, 0), \quad (x_7, y_7) = (8, 0), \end{aligned}$$

where  $s(t) = \pm\sqrt{(125t^2 + 189)(75t^2 + 11)}$ . Each sign determines one connected component of the motion. Figure 4.14 shows three realizations of the component for positive  $s$ .

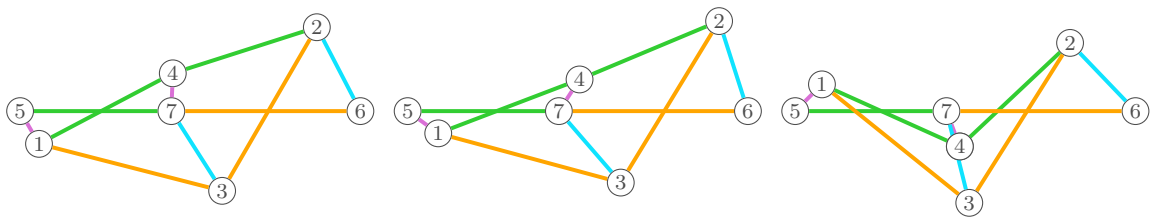


Figure 4.14.: Example of a motion of type III.

#### 4.4.4. Motion type IV

The edge lengths enforced by the motion types in Case (i) are depicted in Figure 4.13. The triangle  $(5, 6, 7)$  is degenerate, otherwise the active NAC-coloring  $\epsilon_{13}$  implies that

$\lambda_{24} = \lambda_{47}$  by Lemma 4.16. But this contradicts that the 4-cycle  $H_3 = (2, 3, 7, 4)$  is an antiparallelogram.

The irreducible components  $IV_-$  and  $IV_+$  of the zero set of the ideal generated by the equalities of edge lengths, triangle equality and the equations implied by the active NAC-colorings  $\epsilon_{13}, \eta, \phi_4$  and  $\psi_2$ , which are all singletons w.r.t. themselves, are described by

$$\begin{aligned} \lambda_{37}^2 \lambda_{57} - \lambda_{47}^2 \lambda_{57} + \lambda_{14}^2 \lambda_{67} - \lambda_{57}^2 \lambda_{67} &= 0, \\ \lambda_{47}^2 + \alpha \lambda_{14} \lambda_{26} - \lambda_{37}^2 + \lambda_{57} \lambda_{67} &= 0, \\ \lambda_{26} \lambda_{57} + \alpha \lambda_{14} \lambda_{67} &= 0, \\ \lambda_{13} = \lambda_{57}, \quad \lambda_{24} = \lambda_{15} = \lambda_{37}, \quad \lambda_{23} = \lambda_{47}, \quad \lambda_{56} = \lambda_{57} + \lambda_{67}, \end{aligned}$$

where  $\alpha \in \{-1, 1\}$ . The dimension of  $IV_-$  and  $IV_+$  is 4, whereas the dimension of the systems for vertex coordinates is 5, which again proves that a generic realizable  $\lambda$  is flexible. Computation shows that Case (b) is a subvariety of  $IV_-$ . An example of a proper flexible labeling in  $IV_-$  is

$$\begin{aligned} \lambda_{15} = \lambda_{24} = \lambda_{37} = 8, \quad \lambda_{14} = 14, \quad \lambda_{26} = 10, \quad \lambda_{56} = 12, \\ \lambda_{13} = \lambda_{57} = 7, \quad \lambda_{23} = \lambda_{47} = 13, \quad \lambda_{67} = 5. \end{aligned}$$

A parametrization of the motion is

$$\begin{aligned} (x_1, y_1) &= \left( -\frac{8(t^2 - 1)}{t^2 + 1}, \frac{16t}{t^2 + 1} \right), \\ (x_2, y_2) &= \left( \frac{2(689t^4 - 320t^2s(t) + 1338t^2 + 9)}{169t^4 + 178t^2 + 9}, \frac{40(20t^3 - (13t^3 - 3t)s(t) - 12t)}{169t^4 + 178t^2 + 9} \right), \\ (x_3, y_3) &= \left( -\frac{t^2 - 15}{t^2 + 1}, \frac{16t}{t^2 + 1} \right), \\ (x_4, y_4) &= \left( \frac{2(45t^4 - 448t^2s(t) + 938t^2 - 3)}{225t^4 + 226t^2 + 1}, \frac{8(198t^3 - 7(15t^3 - t)s(t) - 26t)}{225t^4 + 226t^2 + 1} \right), \\ (x_5, y_5) &= (0, 0), \quad (x_6, y_6) = (12, 0), \quad (x_7, y_7) = (7, 0), \end{aligned}$$

where  $s(t) = \pm\sqrt{9t^2 + 13}$ . It has only one connected component. Figure 4.15 shows three realizations from the motion. An example of a proper flexible labeling in  $IV_+$  is

$$\begin{aligned} \lambda_{15} = \lambda_{24} = \lambda_{37} = 13, \quad \lambda_{14} = 14, \quad \lambda_{26} = 10, \quad \lambda_{56} = 2, \\ \lambda_{13} = \lambda_{57} = 7, \quad \lambda_{23} = \lambda_{47} = 8, \quad \lambda_{67} = -5. \end{aligned}$$



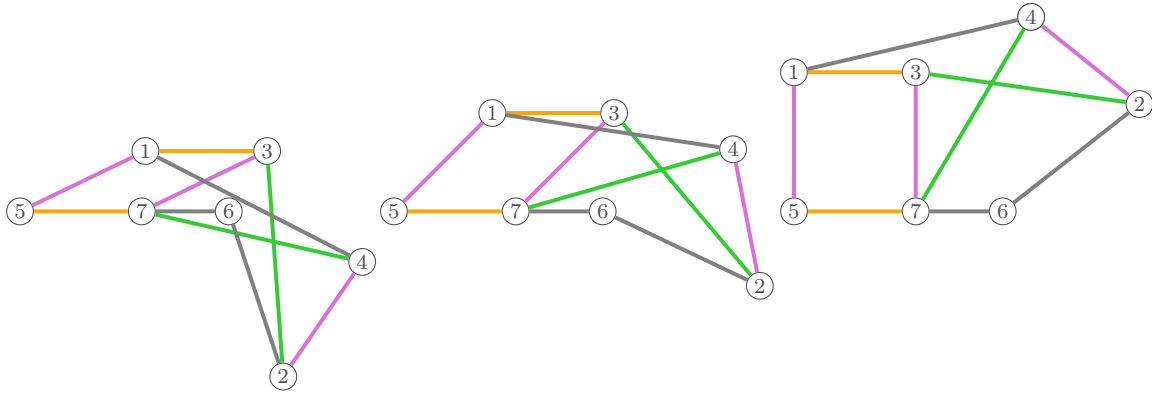


Figure 4.15.: Example of a motion of type IV<sub>-</sub>.

A parametrization of the motion is

$$\begin{aligned} (x_1, y_1) &= \left( -\frac{13(t^2 - 1)}{t^2 + 1}, \frac{26t}{t^2 + 1} \right), \\ (x_2, y_2) &= \left( -\frac{68t^4 + 65s(t)t^2 - 59t^2 - 972}{16t^4 + 97t^2 + 81}, \frac{5(65t^3 - (4t^3 - 9t)s(t) + 234t)}{16t^4 + 97t^2 + 81} \right), \\ (x_3, y_3) &= \left( -\frac{2(3t^2 - 10)}{t^2 + 1}, \frac{26t}{t^2 + 1} \right), \\ (x_4, y_4) &= \left( \frac{30t^4 + 91s(t)t^2 + 1204t^2 - 9}{100t^4 + 109t^2 + 9}, \frac{871t^3 + 7(10t^3 - 3t)s(t) - 312t}{100t^4 + 109t^2 + 9} \right), \\ (x_5, y_5) &= (0, 0), \quad (x_6, y_6) = (2, 0), \quad (x_7, y_7) = (7, 0), \end{aligned}$$

where  $s(t) = \pm\sqrt{39t^2 + 208}$ . Figure 4.16 shows three realizations from the motion.

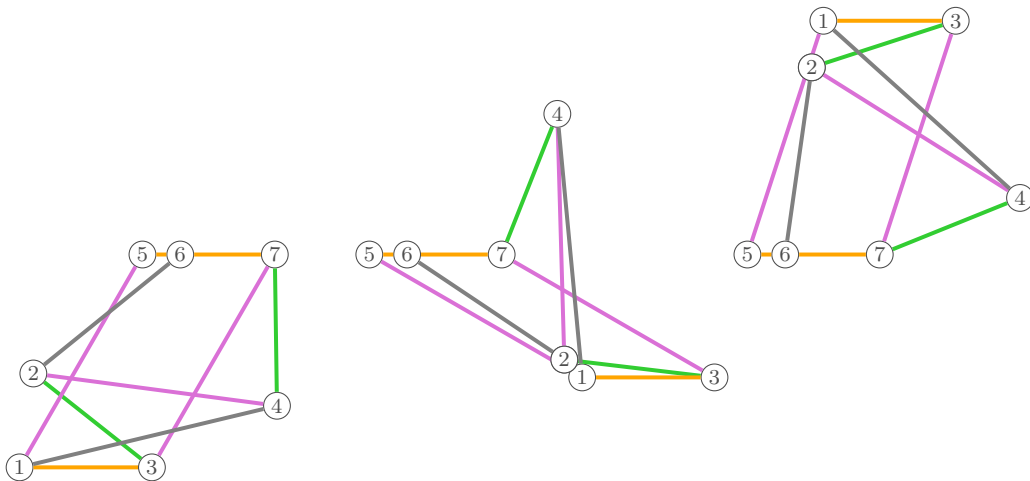


Figure 4.16.: Example of a motion of type IV<sub>+</sub>.

### 4.4.5. Motion type V

Case (j) has the triangle degenerate by the same reason as (i). The obtained system of equations for edge lengths is

$$\lambda_{15}^2 + \lambda_{47}^2 = \lambda_{14}^2 + \lambda_{67}^2,$$

$$\lambda_{13} = \lambda_{15}, \quad \lambda_{23} = \lambda_{26} = \lambda_{47}, \quad \lambda_{24} = \lambda_{57} = \lambda_{37} = \lambda_{67}, \quad \lambda_{56} = 2\lambda_{67}.$$

The dimension is 3. A generic realizable labeling is flexible, since the dimension of the system for coordinates is one higher. Case (b) is again a subcase. An example of a proper flexible labeling is

$$\lambda_{13} = \lambda_{15} = 6, \quad \lambda_{14} = 9, \quad \lambda_{23} = \lambda_{26} = \lambda_{47} = 7, \quad \lambda_{24} = \lambda_{37} = \lambda_{57} = \lambda_{67} = 2, \quad \lambda_{56} = 4.$$

The motion is parametrized by

$$(x_1, y_1) = \left( -\frac{6(t^2 - 1)}{t^2 + 1}, \frac{12t}{t^2 + 1} \right),$$

$$(x_2, y_2) = \left( \frac{8t^4 + 9s(t)t + 28t^2 + 2}{4t^4 + 5t^2 + 1}, \frac{3(4t^3 + (2t^2 - 1)s(t) - 2t)}{4t^4 + 5t^2 + 1} \right),$$

$$(x_3, y_3) = \left( \frac{36t^2}{4t^4 + 5t^2 + 1}, \frac{12(2t^3 - t)}{4t^4 + 5t^2 + 1} \right),$$

$$(x_4, y_4) = \left( \frac{9(s(t)t + 2t^2)}{4t^4 + 5t^2 + 1}, \frac{3(4t^3 + (2t^2 - 1)s(t) - 2t)}{4t^4 + 5t^2 + 1} \right),$$

$$(x_5, y_5) = (0, 0), \quad (x_6, y_6) = (4, 0), \quad (x_7, y_7) = (2, 0),$$

where  $s(t) = \pm\sqrt{(5t^2 + 1)(4t^2 + 5)}$ . Figure 4.17 shows three realizations of one of the two connected components.

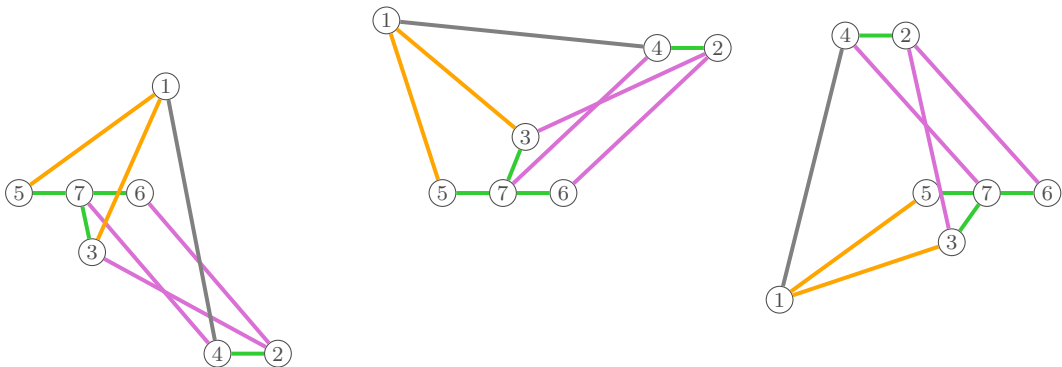


Figure 4.17.: Example of a motion of type V.

### 4.4.6. Motion type VI

The edge lengths enforced by the motion types in Case (k) are depicted in Figure 4.13. The triangle  $(5, 6, 7)$  is degenerate, otherwise the active NAC-coloring  $\epsilon_{13}$  implies that  $\lambda_{26} = \lambda_{67}$  by Lemma 4.16. But this contradicts that the 4-cycle  $H_7 = (2, 3, 7, 6)$  is an even deltoid.

In order to get the system of equations for  $\lambda$ , we again take the equalities of edge lengths, equations from the active NAC-colorings and triangle equality. The case  $\lambda_{67} = 0$  must be excluded using elimination. By taking the radical ideal, we get a prime ideal generated by

$$\begin{aligned} & -\lambda_{24}^2 - \lambda_{26}^2 + \lambda_{47}^2 + \lambda_{67}^2 = 0, \\ \lambda_{13} = \lambda_{15} = \lambda_{24}, \quad \lambda_{14} = \lambda_{23} = \lambda_{26}, \quad \lambda_{57} = \lambda_{37} = \lambda_{67}, \quad \lambda_{56} = 2\lambda_{67}. \end{aligned}$$

The dimension is 3, a generic realizable labeling is flexible and Case (b) is a subcase. An instance of VI is

$$\lambda_{13} = \lambda_{15} = \lambda_{24} = 7, \quad \lambda_{14} = \lambda_{23} = \lambda_{26} = 6, \quad \lambda_{57} = \lambda_{37} = \lambda_{67} = 2, \quad \lambda_{47} = 9, \quad \lambda_{56} = 4.$$

The motion can be parametrized by

$$\begin{aligned} (x_1, y_1) &= \left( -\frac{7(t^2 - 1)}{t^2 + 1}, \frac{14t}{t^2 + 1} \right), \\ (x_2, y_2) &= \left( \frac{2(81t^4 + 28s(t)t + 302t^2 + 25)}{81t^4 + 106t^2 + 25}, \frac{4(63t^3 + (9t^2 - 5)s(t) - 35t)}{81t^4 + 106t^2 + 25} \right), \\ (x_3, y_3) &= \left( \frac{784t^2}{81t^4 + 106t^2 + 25}, \frac{56(9t^3 - 5t)}{81t^4 + 106t^2 + 25} \right), \\ (x_4, y_4) &= \left( -\frac{405t^4 - 56s(t)t - 212t^2 - 225}{81t^4 + 106t^2 + 25}, \frac{2(441t^3 + 2(9t^2 - 5)s(t) + 245t)}{81t^4 + 106t^2 + 25} \right), \\ (x_5, y_5) &= (0, 0), \quad (x_6, y_6) = (4, 0), \quad (x_7, y_7) = (2, 0), \end{aligned}$$

where  $s(t) = \pm\sqrt{(18t^2 + 25)(9t^2 + 2)}$ . It has two connected components. One of them is illustrated in Figure 4.18.

To conclude the classification, we also have to check that the varieties I, ..., VI are not subvarieties of each other. To see that none of them is a subvariety of  $\text{II}_- \cup \text{II}_+$ , we directly check ideal containment using the equations from the previous sections, since Case (d) has no isomorphic motion types (see [40]). Motion types III–VI are not special cases of I because they do not have three parallelograms. Clearly, III, V and VI are not contained in each other due to irreducibility and same dimension. To check that they are not subcases of  $\text{IV}_- \cup \text{IV}_+$ , we check ideal containment for all isomorphic cases of IV (see [40]).

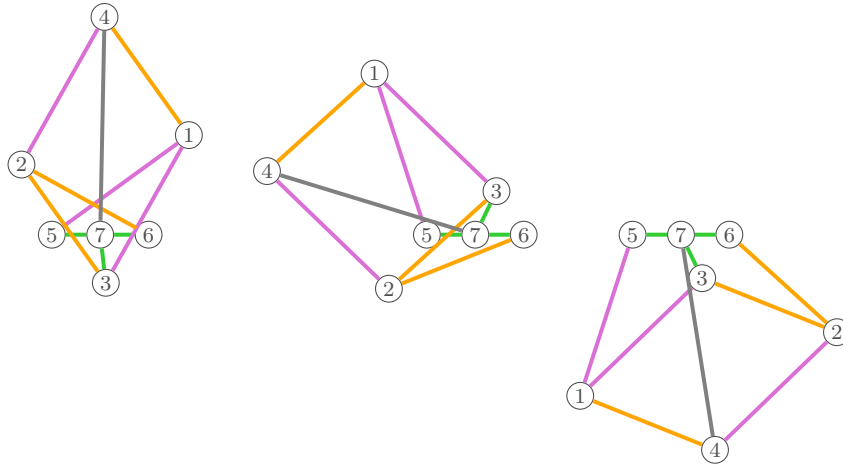


Figure 4.18.: Example of a motion of type VI.

#### 4.4.7. Degenerate triangle (5, 6, 7)

Interestingly, we can prove that the triangle (5, 6, 7) is degenerate for every proper flexible labeling of  $Q_1$  even without the method deriving possible active NAC-colorings. The following approach was presented in [28].

Lemma 4.16 allows to give some conditions on active NAC-colorings of motions with injective realizations, under the assumption that the triangle (5, 6, 7) is not degenerate. Then, we conclude that this assumption actually always yields a contradiction.

**Lemma 4.17.** *Let  $\mathcal{C}$  be an algebraic motion of  $(Q_1, \lambda)$  such that  $\lambda$  is a proper flexible labeling and the vertices 5, 6, 7 are not collinear. If  $\epsilon_{13} \in \text{NAC}_{Q_1}(\mathcal{C})$ , then*

- (i)  $\epsilon_{14}, \gamma_1, \gamma_2, \psi_1, \psi_2, \phi_4, \zeta \notin \text{NAC}_{Q_1}(\mathcal{C})$ ,
- (ii) either  $\epsilon_{23} \in \text{NAC}_{Q_1}(\mathcal{C})$  or  $\epsilon_{24} \in \text{NAC}_{Q_1}(\mathcal{C})$ , and
- (iii)  $\eta \in \text{NAC}_{Q_1}(\mathcal{C})$ .

*Proof.* By the assumption and Lemma 4.16, if  $\epsilon_{13} \in \text{NAC}_{Q_1}(\mathcal{C})$ , then  $\lambda_{26} = \lambda_{67}$  and  $\lambda_{24} = \lambda_{47}$ . But then the 4-cycle (2, 4, 7, 6) is an odd deltoid or rhombus. Hence, the restriction of any active NAC-coloring to (2, 4, 7, 6) cannot be of type R (recall Table 4.1), i.e.,  $\epsilon_{14}, \gamma_1, \phi_4, \zeta \notin \text{NAC}_{Q_1}(\mathcal{C})$  by Table 4.4. Since the 4-cycle (2, 3, 7, 4) cannot be an antiparallelogram, there must be an active NAC-coloring whose restriction is of type O, namely,  $\epsilon_{23} \in \text{NAC}_{Q_1}(\mathcal{C})$  or  $\epsilon_{24} \in \text{NAC}_{Q_1}(\mathcal{C})$ . Since  $\epsilon_{13}$  excludes  $\epsilon_{14}$  to be active,  $\epsilon_{23}$  excludes  $\epsilon_{24}$  by graph symmetry. This gives (ii). By the symmetric approach to the fact that  $\epsilon_{13}$  excludes  $\gamma_1$ , we also get that both  $\epsilon_{23}$  and  $\epsilon_{24}$  prohibit  $\gamma_2$  to be active. Since the 4-cycle (2, 4, 7, 6), resp. (2, 3, 7, 6), is not an antiparallelogram, there must be an active NAC-coloring restricting to O, namely  $\epsilon_{24}$  or  $\eta$ , resp.  $\epsilon_{23}$  or  $\eta$  ( $\gamma_2$  is already excluded).

In the combination with the previous, we get (iii). Therefore,  $\lambda_{24} = \lambda_{23}$  and  $\lambda_{14} = \lambda_{13}$  by Lemma 4.16. This shows that the 4-cycle  $(1, 3, 2, 4)$  is an even deltoid or rhombus which prohibits L. Thus,  $\psi_1, \psi_2 \notin \text{NAC}_{Q_1}(\mathcal{C})$ , which finishes (i).  $\square$

4-cycle	$\epsilon_{13}$	$\epsilon_{14}$	$\epsilon_{23}$	$\epsilon_{24}$	$\gamma_1$	$\gamma_2$	$\eta$	$\psi_1$	$\psi_2$	$\phi_3$	$\phi_4$	$\zeta$
$H_1 = (1, 3, 2, 4)$	O	O	O	O	L	L	S	L	L	R	R	S
$H_2 = (1, 3, 7, 4)$	O	O	R	R	L	S	L	L	S	R	R	S
$H_3 = (2, 3, 7, 4)$	R	R	O	O	S	L	L	S	L	R	R	S
$H_4 = (1, 3, 7, 5)$	O	L	R	S	O	R	O	L	S	R	S	R
$H_5 = (1, 4, 7, 5)$	L	O	S	R	O	R	O	L	S	S	R	R
$H_6 = (2, 4, 7, 6)$	S	R	L	O	R	O	O	S	L	S	R	R
$H_7 = (2, 3, 7, 6)$	R	S	O	L	R	O	O	S	L	R	S	R

Table 4.4.: Types of NAC-colorings of  $Q_1$  restricted to 4-cycles using the notation from Figure 4.2 and S meaning all edges have the same color.

We conclude that the triangle  $(5, 6, 7)$  in  $Q_1$  is always degenerate.

**Theorem 4.18.** *If  $\mathcal{C}$  is an algebraic motion of  $Q_1$  with infinitely many injective realization, then the vertices 5, 6 and 7 are always collinear.*

*Proof.* If no  $\epsilon_{ij}$  is active, then the 4-cycles  $(1, 3, 2, 4)$ ,  $(1, 3, 7, 4)$  and  $(2, 3, 7, 4)$  are all antiparallelograms. But this is not possible for injective realizations. Hence, by symmetry we can assume w.l.o.g. that  $\epsilon_{13}$  is active. Suppose by contradiction that the triangle  $(5, 6, 7)$  is not degenerate. By Lemma 4.17 (and its symmetric version for  $\epsilon_{24}$ ), the only possibilities for  $\text{NAC}_{Q_1}(\mathcal{C})$  are  $\{\epsilon_{13}, \epsilon_{23}, \eta\}$ ,  $\{\epsilon_{13}, \epsilon_{23}, \eta, \phi_3\}$  and  $\{\epsilon_{13}, \epsilon_{24}, \eta\}$ . In all cases, the motion types of 4-cycles given by the active NAC-colorings and Lemma 4.16 enforce the edge lengths to be the same for all edges in the  $K_{2,3}$  subgraph induced by the vertices 1, 2, 3, 4 and 7. This contradicts a non-degenerate motion.  $\square$

## Implementation

Most of the functionality of this chapter is implemented in the class `MotionClassifier`.

### NACcoloring

`cycle_has_orthogonal_diagonals(cycle)` checks whether the NAC-coloring implies orthogonal diagonals for a given *cycle* according to Lemma 4.1.

`is_singleton(NACs)` returns whether the NAC-coloring is a singleton w.r.t. *NACs*. If no set is provided, then all NAC-colorings of the graph are considered.

## MotionClassifier

**four\_cycles\_ordered()** returns 4-cycles of the graph sorted so that two consecutive 4-cycles share some edge, if possible.

**ramification\_formula(*cycle*, *motion\_type*)** returns the equations for a given *motion\_type* of a *cycle* according to Definition 4.11.

**consistent\_motion\_types()** returns consistent motion types of 4-cycles by Algorithm 2.

**check\_orthogonal\_diagonals(*motion\_types*, *active\_NACs*)** checks the conditions in Remark 4.14 for given *motion\_types* and *active\_NACs*.

**motion\_types\_equivalent\_classes(*motion\_types\_list*)** splits the motion types in *motion\_types\_list* into equivalence classes w.r.t. the graph automorphism group.

**possible\_motion\_types\_and\_active\_NACs()** outputs symmetry classes of consistent motion types with their sets of active NAC-coloring (if uniquely determined) by calling `consistent_motion_types()`, `check_orthogonal_diagonals()` and `motion_types_equivalent_classes()`. Optionally returns also a formatted table, similar for instance to Table 4.3.

**equations\_from\_leading\_coefs(*delta*)** gives algebraic constraints on edge lengths for a singleton NAC-coloring *delta* according to the method described in Section 4.1.

**motion\_types2same\_lengths\_equations(*motion\_types*)** returns equations between edge lengths enforced by *motion\_types* of 4-cycles.

**motion\_types2equations(*motion\_types*)** wraps `equations_from_leading_coefs()` and `motion_types2same_lengths_equations()` for given *motion\_types* under the assumption that the set of active NAC-colorings is uniquely determined by the motion types, otherwise it has to be explicitly specified.

**edge\_equations\_ideal(*fixed\_edge*)** returns the ideal of the system of equations (1.1) with *fixed\_edge* and symbolic edge lengths satisfying given constraints.

**edge\_lengths\_dimension(*eqs\_lambdas*)** computes the dimension of the algebraic variety of edge lengths satisfying *eqs\_lambdas*.

The package FlexRiLoG is used in Jupyter notebooks with the computation of motion classification of  $Q_1$ , which can be found in [40].

# 5. Number of Real Realizations compatible with a Rigid Labeling

Contrary to the previous, this chapter is focused on rigid labelings of minimally rigid graphs in both  $\mathbb{R}^2$  and  $\mathbb{R}^3$ . The goal is to specify edge lengths such that there are as many non-congruent real realizations as possible.

A general approach is to consider in general complex solutions of the algebraic system (1.1) and try to find parameters such that these solutions are actually real. This has been done for Laman graphs up to 7 vertices [7, 17] and Geiringer graphs up to 6 vertices [19]. The precise numbers of complex solutions were given up to 12, resp. 10, vertices in [25]. We specify edge lengths with many real realizations for certain graphs up to 10, resp. 8 vertices.

Before the combinatorial algorithm for computing the number of complex realizations of a Laman graph was presented [9], the mixed volume techniques had been used to bound the number of complex solutions. The mixed volume of a well-constrained polynomial system is a number given by the Newton polytopes of the system, see for instance [11]. The so called BKK bound (Bernstein, Kushnirenko, Khovanskii) states that the number of solutions with no zero entry is at most the mixed volume [5].

Computation of the mixed volume of a given system is implemented for instance in the package `phcpy` by Verschelde [59]. We use this package extensively also to solve the systems numerically. The program constructs a family of polynomial systems (homotopy) containing a starting system and the target system. The starting system is based on the Newton polytopes of the target system and has known solutions, whose number equals the mixed volume. Then, the solutions are tracked numerically along the homotopy to the solutions of the target system. Therefore, the computation time strongly depends on the mixed volume. In Section 5.1, we recall a known trick [19, 54] decreasing the mixed volume for systems corresponding to minimally rigid graphs.

We provide edge lengths with many real realizations for the Laman graph up to 10 vertices with the maximum number of complex solutions in Section 5.2 using sampling around unit lengths.

In Section 5.3, we study the Geiringer graphs with 7 and 8 vertices that have the maximum number of complex solutions. In order to provide edge lengths such that all solutions are real in the 7-vertex case, we developed a new method inspired by coupler curves and approach of Borcea and Streinu in the plane [7]. The method gives edge lengths with many real solutions also for the 8-vertex graph.

For both Laman and Geiringer graphs we use the obtained bounds on the number

of real realizations of small graphs to improve the lower asymptotic bounds on the maximum number of real realizations among  $n$ -vertex graphs. The bounds are  $2.3003^n$  and  $2.6553^n$  respectively. Compare that the known upper bound on the number of realizations are  $\binom{2n-4}{n-2}$  and  $\frac{2^{n-3}}{n-2} \binom{2n-6}{n-3}$  respectively [7]. The upper bounds behave approximately as  $2^{dn}$ ,  $d \in \{2, 3\}$ .

The content of this chapter is a joint work with Elias Tsigaridas, Vangelis Bartzos and Ioannis Emiris. Our conference paper [2] presented at ISSAC'18 covers the part about Geiringer graphs. We have submitted also an extended version containing the case of Laman graphs [1]. Moreover, it discusses another algebraic formulation based on distance geometry, namely Cayley-Menger matrices, and realizations of Laman graphs on sphere.

## 5.1. Algebraic formulation

The zero set of the algebraic system (1.1) describes the realizations of a Laman graph  $G$  in plane compatible with a given edge lengths. Nevertheless, the system is not suitable for numerical solving using polyhedral homotopy continuation, since PHC creates a starting system with the number of solutions equal to the mixed volume of the target system, and this is usually much higher than the actual number of solutions in the case of minimally rigid graphs. The mixed volume can be significantly lowered by introducing a new variable  $s_v$  for each vertex  $v$ , see [19, 54]. The variable  $s_v$  corresponds to the squared distance of  $v$  from the origin:

$$\begin{aligned} s_u + s_v - 2(x_u x_v + y_u y_v) &= \lambda_{uv}^2, \quad \forall uv \in E_G \setminus \{v_1 v_2\} \\ x_v^2 + y_v^2 &= s_v, \quad \forall v \in V_G \setminus \{v_1, v_2\}. \end{aligned} \tag{5.1}$$

As in (1.1), we fix the coordinates of an edge  $v_1 v_2$  to remove rotations and translations. For a Geiringer graph  $G$  with a triangle  $(v_1, v_2, v_3)$ , we have analogous equations

$$\begin{aligned} s_u + s_v - 2(x_u x_v + y_u y_v + z_u z_v) &= \lambda_{uv}^2, \quad \forall uv \in E_G \setminus \{v_1 v_2, v_2 v_3, v_1 v_3\} \\ x_v^2 + y_v^2 + z_v^2 &= s_v, \quad \forall v \in V_G \setminus \{v_1, v_2, v_3\}, \end{aligned} \tag{5.2}$$

and we fix  $v_1$  in the origin and  $v_2$  on the  $y$ -axis with the coordinates  $(0, \lambda_{12}, 0)$ . The vertex  $v_3$  is fixed in the plane  $z = 0$ , with  $x_{v_3} \geq 0$ , so that the edge lengths  $\lambda_{13}$  and  $\lambda_{23}$  are fulfilled. We remark that there exist Geiringer graphs with no triangle, but they do not appear in this chapter. In this case the rotations and translations are removed just by setting  $z_{v_3}$  to be 0 and keeping all equations above that involve the vertex  $v_3$ .

We denote the zero set of the systems by  $S(G, \lambda, v_1, \dots, v_d) \subset \mathbb{C}^{d|V_G|}$ , where  $d = 2$  or  $3$  for Laman and Geiringer graphs respectively. The real solutions  $S(G, \lambda, v_1, \dots, v_d) \cap \mathbb{R}^{d|V_G|}$  are denoted by  $S_{\mathbb{R}}(G, \lambda, v_1, \dots, v_d)$  and we set  $r_d(G, \lambda) = |S_{\mathbb{R}}(G, \lambda, v_1, \dots, v_d)|$ .



The number of complex solutions is the same for generic edge lengths, we set  $c_d(G) = |S(G, \lambda, v_1, \dots, v_d)|$  for a generic  $\lambda$ . This is clearly not the case if we count only real solutions. In the real case, we are interested in the maximum finite number of non-congruent real realizations of a graph  $G$ :

$$r_d(G) = \max\{r_d(G, \lambda) : \lambda \text{ is a rigid labeling of } G\}.$$

Obviously,  $c_d(G) \geq r_d(G)$ . The inequality might be strict, as was shown by Jackson and Owen in [34]. They exploit the fact that  $r_2(G)$  is always divisible by 4 and provide an 8-vertex Laman graph  $\tilde{G}$  such that  $c_2(\tilde{G}) = 90$ . Nevertheless, there are many graphs for which these two numbers match, so we in general aim to find edge lengths  $\lambda$  such that  $r_d(G, \lambda) = c_d(G)$ .

For discussing how the number of realizations behaves w.r.t. the number of vertices, the maximum number  $r_d(G)$ , resp.  $c_d(G)$ , over all minimally rigid graphs  $G$  with  $n$  vertices is denoted by  $r_d(n)$ , resp.  $c_d(n)$ .

In order to obtain lower bounds on  $r_d(n)$ , small graphs with many real realizations can serve to build bigger ones by gluing many copies together. These so called caterpillar and fan constructions were proposed in [7] and generalized in [25], see Figure 5.1. The following theorem comes from the latter.

**Theorem 5.1.** *Let  $G$  be a generically rigid graph in  $\mathbb{R}^d$ , where  $d \in \{2, 3\}$ , with a generically rigid subgraph  $H$ . We construct a graph using  $k$  copies of  $G$ , where all the copies have the subgraph  $H$  in common. The new graph is generically rigid, has  $n = |V_H| + k(|V_G| - |V_H|)$  vertices, and the number of its real realizations is at least*

$$2^{(n-|V_H|) \bmod (|V_G|-|V_H|)} \cdot r_d(H) \cdot \left(\frac{r_d(G)}{r_d(H)}\right)^{\lfloor \frac{n-|V_H|}{|V_G|-|V_H|} \rfloor}.$$

Remember that for a triangle  $T$  we have that  $r_2(T) = 2$ , while  $r_3(T) = 1$ . The triangle is also the smallest graph that can be used if  $d = 3$ , whereas we can glue along an edge if  $d = 2$ . Notice also that the theorem is stated for generically rigid graphs, but every generically rigid graph is spanned by a minimally rigid graph whose number of realizations is clearly the same or greater.

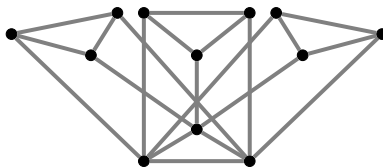


Figure 5.1.: Gluing three copies of 3-prism together using fan construction.

## 5.2. Laman Graphs

In this section we discuss the maximal number of real realizations of a Laman graph up to 10 vertices and we give a better lower bound on  $r_2(n)$ .

As we already mentioned, the number of real realizations  $r_2(G)$  is naturally bounded by the number of complex realizations  $c_2(G)$ . There is a recent algorithm [9] for determining  $c_2(G)$  for a given Laman graph  $G$ . The authors construct all Laman graphs up to 12 vertices using Henneberg steps and use their algorithm to find the graphs with the minimum and maximum  $c_2(G)$ . Their results are summarized in Table 5.1. They show that for  $6 \leq n \leq 12$ , there is always a unique graph  $G_{2,n}^{\max}$  with  $n$  vertices such that  $c_2(G_{2,n}^{\max}) = c_2(n)$ .

$n$	6	7	8	9	10	11	12
$\min c_2(G)$	16	32	64	128	256	512	1024
$c_2(n)$	24	56	136	344	880	2288	6180

Table 5.1.: The minimum and maximum numbers of complex realizations among Laman graphs with  $n$  vertices.

The graph  $G_{2,6}^{\max}$  is actually the 3-prism graph  $L_1$ . It is known that  $r_2(G_{2,6}^{\max}) = 24$  due to Borcea and Streinu [7]. The graph  $G_{2,7}^{\max}$  is the graph in Figure 3.1 and Emiris and Moroz [17] proved that  $r_2(G_{2,7}^{\max}) = 56$ . We focus on the graphs  $G_{2,8}^{\max}$ ,  $G_{2,9}^{\max}$  and  $G_{2,10}^{\max}$ , see Figure 5.2.

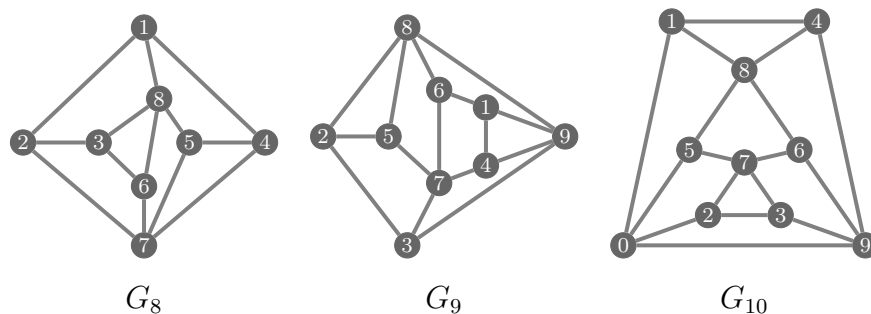


Figure 5.2.: The graphs with the maximum number of complex realizations among all Laman graphs with 8, 9 a 10 vertices.

We solve the system (5.1) for given edge lengths numerically using the Python package `phcpy` [59]. Since the starting system for PHC is constructed to have the number of solutions being the mixed volume of the target system, it is important to select a system with a low mixed volume to speed up the computation. Hence, we compute mixed volumes of (5.1) for  $G_{2,8}^{\max}$ ,  $G_{2,9}^{\max}$  and  $G_{2,10}^{\max}$  for all possible choices of the fixed edge

and pick the lowest one. For these graphs, the edges contained in a 3-cycle attain the minimum. We take advantage of this fact — the position of the third vertex in the triangle can be easily computed. This allows to eliminate some of the equations and reduce the computation time. The total number of realizations is then twice the number of realizations with the fixed triangle since we can reflect each of them with respect to the fixed edge.

Notice that the mixed volume does not match the number of complex solutions for the graphs we consider, see Table 5.2. Fortunately, this is not a problem for `phcpy` as the extra solutions of the starting system just diverge during tracking. It might happen that we get less solutions than expected, but due to randomization in the implementation, this can be avoided within few tries. Then, one can use the correct number of solutions together with the system as the starting system for computation with another edge lengths. This speeds up the computation multiple times.

Our strategy to find edge lengths with many real realizations is simple – we choose all edge lengths to be one plus a small random number, between  $10^{-5}$  and  $10^{-3}$ . For  $G_{2,8}^{\max}$  and  $G_{2,9}^{\max}$ , edge lengths with all solutions being real were found after few hundreds random tries. For  $G_{2,10}^{\max}$ , the size of the random perturbation was adjusted during the computation which led to edge lengths with 860 real solutions out of the total number 880.

$n$	8	9	10
mixed volume	192	512	1536
$c_2(G_{2,n}^{\max})$	136	344	880
$r_2(G_{2,n}^{\max}) \geq$	136	344	860

Table 5.2.: The mixed volumes and bounds on the number of real realizations.

We emphasize that the solutions are numeric — a solution is considered to be real if the imaginary part of every coordinate is at most  $10^{-14}$  in absolute value. We check the sanity of the result by substituting the real parts of the solutions back to the equations – the edge lengths induced by solutions differ at most by  $10^{-14}$  from the original ones. We also check using Cayley-Menger varieties, see [1] for details. Actually, this check gives the number 860 for  $G_{2,10}^{\max}$ , while PHC gives 868 real solutions. So we take the lower one to be on the safe side.

The edge lengths giving the number of real realizations mentioned above are:

$$G_{2,8}^{\max} : \\
\lambda_{12} = 1.000110, \quad \lambda_{14} = 1.000335, \quad \lambda_{18} = 1.000120, \quad \lambda_{23} = 1.000175, \\
\lambda_{27} = 1.000380, \quad \lambda_{36} = 1.000460, \quad \lambda_{38} = 1.000100, \quad \lambda_{45} = 1.000059,$$

$$\lambda_{47} = 1.000145, \quad \lambda_{57} = 1.000390, \quad \lambda_{58} = 1.000355, \quad \lambda_{67} = 1.000245, \\ \lambda_{68} = 1.000290,$$

$G_{2,9}^{\max}$  :

$$\lambda_{14} = 1.001000, \quad \lambda_{16} = 1.000460, \quad \lambda_{19} = 1.000570, \quad \lambda_{23} = 1.000580, \\ \lambda_{25} = 1.000750, \quad \lambda_{28} = 1.000840, \quad \lambda_{37} = 1.000730, \quad \lambda_{39} = 1.000420, \\ \lambda_{47} = 1.000960, \quad \lambda_{49} = 1.000150, \quad \lambda_{57} = 1.000830, \quad \lambda_{58} = 1.000030, \\ \lambda_{67} = 1.000860, \quad \lambda_{68} = 1.000080, \quad \lambda_{89} = 1.000390,$$

$G_{2,10}^{\max}$  :

$$\lambda_{14} = 1.0002169, \quad \lambda_{18} = 1.0001366, \quad \lambda_{01} = 1.0004509, \quad \lambda_{23} = 1.0007630, \\ \lambda_{27} = 1.0000575, \quad \lambda_{02} = 1.0006078, \quad \lambda_{37} = 1.0001763, \quad \lambda_{39} = 1.0007500, \\ \lambda_{48} = 1.0008574, \quad \lambda_{49} = 1.0005360, \quad \lambda_{57} = 1.0004910, \quad \lambda_{58} = 1.0002946, \\ \lambda_{05} = 1.0006778, \quad \lambda_{67} = 1.0004699, \quad \lambda_{68} = 1.0002724, \quad \lambda_{69} = 1.0005141, \\ \lambda_{09} = 1.0003913.$$

Notice that the corresponding realizations are rather degenerate, since all edge lengths are almost equal.

We get a lower asymptotic bound on  $r_2(n)$  by applying Theorem 5.1 on  $G_{2,10}^{\max}$ .

**Corollary 5.2.** *The maximum number of real realizations in the plane among Laman graphs with  $n$  vertices is bounded from below by*

$$2^{(n-3) \bmod 7} \cdot 2 \cdot 430^{\lfloor (n-3)/7 \rfloor}.$$

*The bound asymptotically behaves as  $2.378^n$ .*

The previous known lower bound was  $2.3003^n$  by [17].

### 5.3. Geiringer Graphs

In this section we focus on the number of real realizations of some Geiringer graphs and we give a lower bound on  $r_3(n)$ .

As in the planar case, we take the number of complex solutions as an upper bound on the number of real realizations. Contrary to the planar case, there is no combinatorial algorithm known. The authors in [25] determined  $c_3(G)$  for all Geiringer graphs up to 10 vertices by extensive Gröbner basis computation, see Table 5.3. They present unique graphs  $G_{3,n}^{\max}$  attaining the maximum number  $c_3(n)$  for  $6 \leq n \leq 10$ .

The graph  $G_{3,6}^{\max}$  is the skeleton of an octahedron and  $r_3(G_{3,6}^{\max}) = c_3(G_{3,6}^{\max}) = 16$  was shown in [19]. We focus on the graphs  $G_{3,7}^{\max}$  and  $G_{3,8}^{\max}$ , see Figure 5.3. For the former one, we present edge lengths proving  $c_3(G_{3,7}^{\max}) = r_3(G_{3,7}^{\max}) = 48$ . For the latter, we

$n$	6	7	8	9	10
$\min c_3(G)$	8	16	24	48	76
$c_3(n)$	16	48	160	640	2560

Table 5.3.: The minimum and maximum numbers of complex realizations among Geiringer graphs with  $n$  vertices.

provide edge lengths with 132 real realizations. In order to find such edge lengths, we introduce a method sampling the parameter space, which is inspired by coupler curves, similarly to [7] in the plane.

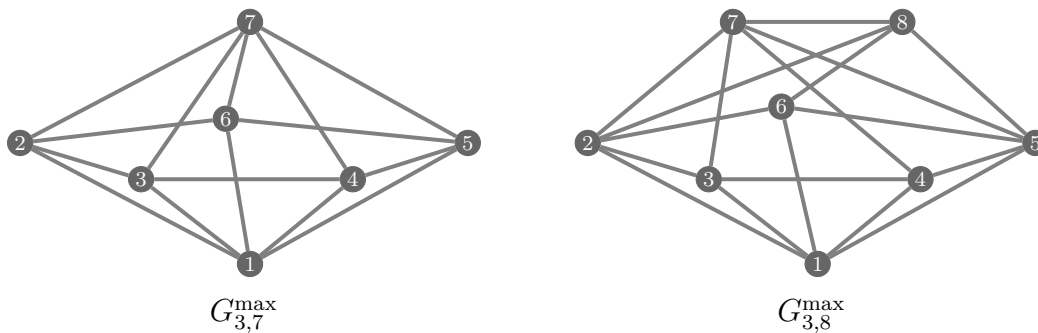


Figure 5.3.: The 7-vertex and 8-vertex graphs with the maximal number of complex realizations ( $G_{3,7}^{\max}$  and  $G_{3,8}^{\max}$ ).

Before we describe our method, let us mention that Vangelis Bartzos tried various approaches to maximize the number of real solutions during our investigations, but they failed to attain the maximum (see also [1, 2]):

- local search around edge lengths taken from random realizations or close to unit lengths,
- stochastic methods inspired by [17],
- parametric searching with Cylindrical Algebraic Decomposition via Maple's sub-package `RootFinding [Parametric]` in Maple18 [41],
- a variant of gradient descent optimization that was used by Dietmaier to show that Stewart-Gough Platform allows 40 real assembly modes [15].

### 5.3.1. Coupler curve method

The procedure we introduce now is motivated by the visualization of coupler curves of the graph  $G_{3,7}^{\max}$ , see our implementation [3]. The main idea is to sample only a subset of

edge lengths, try to maximize the number of real solutions and then choose a different edge for the next iteration.

Let  $G$  be a minimally rigid graph with a triangle and an edge  $uc$ , with  $u$  in the triangle. If  $H = (V_G, E_G \setminus \{uc\})$  is the graph obtained from  $G$  by removing the edge  $uc$ , then the set of realizations satisfying the constraints given by generic edge lengths and fixing the triangle is 1-dimensional. The projection of this curve to the coordinates of the vertex  $c$  is a so called *coupler curve*. Borcea and Streinu used this idea for proving that the 3-prism graph has 24 real realizations in  $\mathbb{R}^2$  [7]. Namely, they found edge lengths such that there are 24 intersections of the coupler curve with a circle representing the removed edge. This approach can be clearly extended into  $\mathbb{R}^3$  — the number of realizations of  $G$  is the same as the number of intersections of the coupler curve of  $c$  with the sphere centered at  $u$  with radius  $\lambda_{uc}$ . Now, we define specifically a coupler curve in  $\mathbb{R}^3$ .

**Definition 5.3.** *Let  $H$  be a graph with edge lengths  $\lambda$  and  $(v_1, v_2, v_3)$  be a 3-cycle in  $H$ . If the set  $S_{\mathbb{R}}(H, \lambda, v_1, v_2, v_3)$  is one dimensional and  $c \in V_H$ , then the set*

$$\mathcal{C}_{c,\lambda} = \{(x_c, y_c, z_c) : ((x_v, y_v, z_v))_{v \in V_H} \in S_{\mathbb{R}}(H, \lambda, v_1, v_2, v_3)\}$$

*is called a coupler curve of  $c$  w.r.t. the fixed triangle  $v_1v_2v_3$ .*

Assuming that a coupler curve is fixed, i.e., we have fixed edge lengths  $\lambda$  of the graph  $H$ , and  $u \in \{v_1, v_2, v_3\}$ , we can change the edge length  $\lambda_{uc}$  so that the number of intersections of the coupler curve  $\mathcal{C}_{c,\lambda}$  with the sphere with the center at  $u$  and radius  $\lambda_{uc}$ , i.e., the number of real realizations of  $G$ , is maximal.

The following lemma shows that we can change three more edge lengths within a 1-parameter family without changing the coupler curve. This 1-parameter family corresponds to shifting the center of the sphere along a line.

**Lemma 5.4.** *Let  $G$  be a Geiringer graph and  $u, v, w, p, c$  be vertices of  $G$  such that  $pv, vw \in E_G$  and the neighbours of  $u$  in  $G$  are  $v, w, p$  and  $c$ . Let  $H$  be the graph given by  $(V_H, E_H) = (V_G, E_G \setminus \{uc\})$  with generic edge lengths  $\lambda$ . Let  $\mathcal{C}_{c,\lambda}$  be the coupler curve of  $c$  w.r.t. the fixed triangle  $(v, u, w)$ . Then the set  $\{y_p : ((x_{v'}, y_{v'}, z_{v'}))_{v' \in V_H} \in S_{\mathbb{R}}(H, \lambda, v, u, w)\}$  has only one element  $y'_p$ . If the parametric edge lengths  $\lambda'(t)$  are given by*

$$\begin{aligned} \lambda'_{uw}(t) &= \|(x_w, y_w - t, 0)\|, & \lambda'_{up}(t) &= \|(0, y'_p - t, z_p)\|, \\ \lambda'_{uv}(t) &= t, & \text{and } \lambda'_e(t) &= \lambda_e \text{ for all } e \in E_H \setminus \{uv, uw, up\}, \end{aligned}$$

*where  $z_p$  is the altitude of  $p$  in the triangle  $(u, v, p)$  with lengths given by  $\lambda$ , then the coupler curve  $\mathcal{C}_{c,\lambda'(t)}$  of  $c$  w.r.t. the fixed triangle  $(v, u, w)$  is the same for all  $t \in \mathbb{R}_+$ , namely, it is  $\mathcal{C}_{c,\lambda}$ . Moreover, if  $cw \in E_G$ , then  $\mathcal{C}_{c,\lambda}$  is a spherical curve.*

*Proof.* All coupler curves in the proof are w.r.t. the triangle  $(v, u, w)$ . Figure 5.4 illustrates the statement. Since  $G$  is minimally rigid, the set  $S_{\mathbb{R}}(H, \lambda, v, u, w)$  is 1-dimensional. The coupler curve  $\mathcal{C}_{p,\lambda}$  of  $p$  is a circle whose axis of symmetry is the  $y$ -axis. Hence, the set  $\{y_p: ((x_{v'}, y_{v'}, z_{v'}))_{v' \in V_H} \in S_{\mathbb{R}}(H, \lambda, v, u, w)\}$  has indeed only one element. The parametrized edge lengths  $\lambda'(t)$  are such that the position of  $v$  and  $w$  is the same for all  $t$ . Moreover, the coupler curve  $\mathcal{C}_{p,\lambda'(t)}$  of  $p$  is independent of  $t$ . Hence, the coupler curve  $\mathcal{C}_{c,\lambda'(t)}$  is independent of  $t$ , because the only vertices adjacent to  $u$  in  $H$  are  $p, v$  and  $w$ . Thus, the positions of the other vertices are not affected by the position of  $u$ .  $\square$

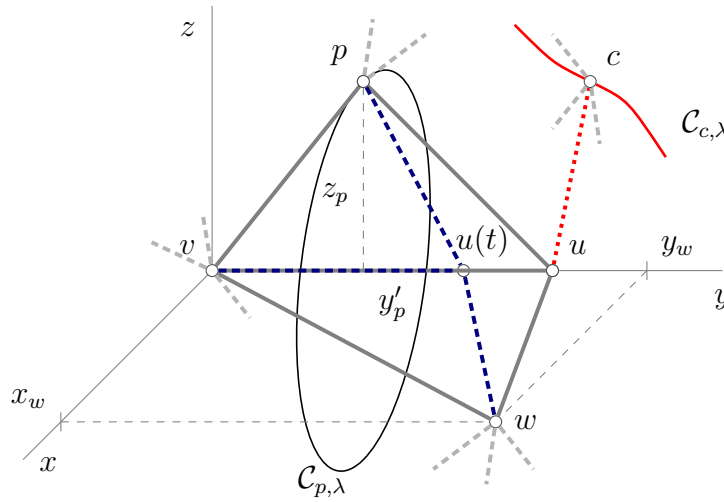


Figure 5.4.: Since the lengths of  $up$  and  $uw$  are changed accordingly to the length of  $uv$  (blue dashed edges), the coupler curves  $\mathcal{C}_{p,\lambda'(t)}$  and  $\mathcal{C}_{c,\lambda'(t)}$  are independent of  $t$ . The red dashed edge  $uc$  is removed from  $G$ .

Therefore, for every subgraph of  $G$  induced by vertices  $u, v, w, p, c$  such that  $\deg u = 4$  and  $pv, vw, uv, uw, up, uc \in E_G$ , we have a 2-parametric family of lengths  $\lambda(t, r)$  such that the coupler curve  $\mathcal{C}_{c,\lambda(t,r)}$  w.r.t. the fixed triangle  $(v, u, w)$  is independent of  $t$  and  $r$ . The parameter  $r$  represents the length of  $uc$ , which corresponds to the radius of the sphere, and the parameter  $t$  determines the lengths of  $uv, uw$  and  $up$ . Now, we aim to find  $r$  and  $t$  such that  $r_3(G, \lambda(t, r))$  is maximized.

Let us clarify that whereas Borcea and Streinu [7] were changing the coupler curve and moving the center of the circle, our approach is different in the sense that the coupler curve is preserved within one iteration of our method, only the position and radius of the sphere corresponding to the removed edge are changed in order to have as many intersections as possible. In the next iteration, we pick a different edge to be removed. We discuss later how these steps are combined for various subgraphs.

5. Number of Real Realizations compatible with a Rigid Labeling

---

We illustrate the method on the graph  $G_{3,7}^{\max}$ . Let  $\lambda$  be edge lengths of  $G_{3,7}^{\max}$  given by

$$\begin{aligned} \lambda_{12} &= 1.99993774567597, & \lambda_{27} &= 10.5360917228793, & \lambda_{23} &= 0.99961432208948, \\ \lambda_{13} &= 1.99476987780024, & \lambda_{37} &= 10.5363171636461, & \lambda_{34} &= 1.00368644488060, \\ \lambda_{14} &= 2.00343646098439, & \lambda_{47} &= 10.5357233031495, & \lambda_{45} &= 1.00153014850485, \\ \lambda_{15} &= 2.00289249524296, & \lambda_{57} &= 10.5362736599978, & \lambda_{56} &= 0.99572361653574, \\ \lambda_{16} &= 2.00013424746814, & \lambda_{67} &= 10.5364788463527, & \lambda_{26} &= 1.00198771097407. \end{aligned}$$

Using `Matplotlib` [33], our program [3] can plot the coupler curve of the vertex 6 of the graph  $G_{3,7}^{\max}$  with the edge  $\{2, 6\}$  removed w.r.t. the fixed triangle  $(1, 2, 3)$ , see Figure 5.5. There are 28 realizations. Following Lemma 5.4 for the subgraph given by  $(u, v, w, p, c) = (2, 3, 1, 7, 6)$ , one can find a position and radius of the sphere corresponding to the removed edge  $\{2, 6\}$  such that there are 32 intersections. Such edge lengths are obtained by taking  $\lambda_{12} = 4.0534$ ,  $\lambda_{27} = 11.1069$ ,  $\lambda_{26} = 3.8545$ ,  $\lambda_{23} = 4.0519$ . Let us mention that the edge lengths above were chosen so that the edges incident to the “top” vertex 7 have similar lengths, edges incident to the “bottom” vertex 1 have similar lengths and also the edges on the “ring” have similar lengths. Such a choice seems to be a good starting point for our method.

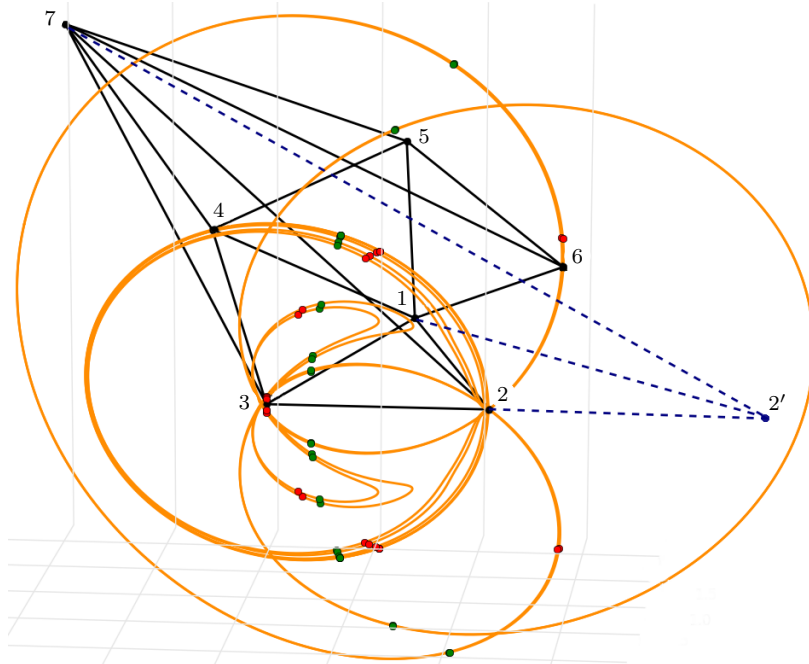


Figure 5.5.: The coupler curve  $\mathcal{C}_{6,\lambda}$  of  $G_{3,7}^{\max}$  with the edge  $\{2, 6\}$  removed. The 28 red points are intersections of  $\mathcal{C}_{6,\lambda}$  with the sphere centered at 2 with the edge lengths  $\lambda$ , whereas the 32 green ones are for the adjusted edge lengths (illustrated by blue dashed lines).



### Sampling procedure

Instead of finding suitable parameters for the position and radius of the sphere by looking at visualizations, we implemented a sampling procedure that tries to maximize the number of intersections [3]. The inputs of the function `sampleToGetMoreEmb()` are starting edge lengths  $\lambda$  and vertices  $u, v, w, p, c$  satisfying the assumptions of Lemma 5.4, including the extra requirement that  $cw$  is an edge. For simplicity, we identify vertices with their positions in  $\mathbb{R}^3$  and edges with the corresponding lines in the explanation of the procedure.

Let  $S_u$  be the sphere centered at  $u$  representing the removed edge  $uc$ . The extra assumption that  $cw$  is an edge is useful since then the coupler curve lies in a sphere  $S_w$  centered at  $w$ . Hence, the intersections of the coupler curve of  $c$  with  $S_u$  are on the intersection  $S_u \cap S_w$ , which is a circle. Thus, we can sample circles on the sphere  $S_w$  instead of sampling the parameters  $t$  and  $r$ .

The center of the intersection circle  $S_u \cap S_w$  is on the line  $uw$ , which is perpendicular to the plane of the circle. Hence, the circle is determined by the angle  $\varphi \in (-\pi/2, \pi/2)$  between the altitude of  $w$  in the triangle  $(u, v, w)$  and the line  $uw$ , and by the angle  $\theta \in (0, \pi)$  between  $uw$  and  $cw$ , see Figure 5.6. Clearly, the lengths of  $uv, uw, up$  and  $uc$  are defined uniquely by the pair  $(\varphi, \theta)$  and the other edge lengths. Thus, we sample  $\varphi$  and  $\theta$  in their intervals instead of sampling the parameters  $r$  and  $t$ . An advantage of this approach is that  $\varphi$  and  $\theta$  are in bounded intervals, whereas  $t$  and  $r$  are unbounded. Moreover, sampling the angles uniformly gives a more reasonable distribution of the intersection circles on the sphere  $S_w$  than the uniform sampling of  $t$  and  $r$ .

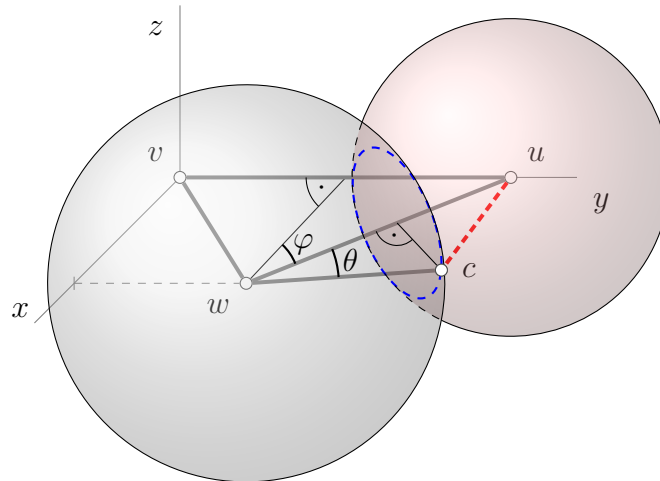


Figure 5.6.: For fixed position of  $v$  and  $w$ , the angle  $\varphi$  determines the position of  $u$ , since  $u$  lies on the  $y$ -axis. If also the length of  $cw$  is given, then  $\theta$  determines the length of  $uc$ . The intersection circle is blue.

Since for every sample we have to solve a system of equations in order to count the number of real realizations, we exploit the following strategy to decrease the number of computations: In the first phase, we sample both angles at approximately 20–24 points each and we take the pairs  $(\varphi, \theta)$  attaining the maximum number. In the second phase, we sample few more points around each of these pairs to have a finer sampling in relevant areas. Of course, edge lengths with the maximum number of real realizations are returned.

A significant speedup of the computation with `phcpy` is achieved by tracking the solutions from a previous system, instead of solving the system every time from scratch. Besides the fact that `phcpy` is parallelized, our implementation splits the samples into two parts and computes the numbers of realizations for them in parallel.

### More subgraphs suitable for sampling

It is likely that the sampling procedure for one choice of  $(u, v, w, p, c)$  does not yield the number of real realizations that matches the complex bound. Hence, we repeat the procedure for various choices of  $(u, v, w, p, c)$ , assuming that there are more subgraphs satisfying the conditions of Lemma 5.4.

If the sampling procedure produces more edge lengths with the same number of real realizations, then we need to select starting edge lengths for sampling with a different subgraph, since it is not computationally feasible to test all of them.

We use a heuristic based on clustering of pairs  $(\varphi, \theta)$  corresponding to the edge lengths by the function `DBSCAN` from `sklearn` package [46]. We take either the edge lengths belonging to the center of gravity of each cluster, or the pair  $(\varphi, \theta)$  closest to this center if the edge lengths corresponding to the center have a lower number of real realizations.

We propose two different approaches for iterating the sampling procedure for various subgraphs. The first one, called *tree search*, applies the sampling procedure using all suitable subgraphs for a given  $\lambda$ . Then, the same is done recursively for all output edge lengths whose number of real realizations increased. The state tree is traversed depth-first, until the required number of real realizations is reached (or there are no increments). This algorithm is implemented in the function `findMoreEmbeddings_tree()` in our code.

The function `findMoreEmbeddings()` uses the second approach, called *linear search*. Assume an order of the suitable subgraphs. The output from the sampling procedure applied to starting edge lengths with the first subgraph is the input for the procedure with the second subgraph, etc. The output from the last subgraph is used again as the input for the first one. There is also a branching because of multiple clusters — all of them are tested in depth-first way. Again, we stop either if the required number of real realizations is reached, or all the subgraphs are used without increment of the number of real realizations.

For both, the subgraphs to be used can be specified, or the program computes all suitable subgraphs by itself. Tree search is useful when one wants to find subgraphs whose application leads to the desired number of realizations in the least number of iterations. On the other hand, linear search seems more efficient. We remark that there is also an option to relax the condition that  $\deg u = 4$ . Then, such a subgraph can also be used for sampling, but the coupler curve changes during the process.

### 5.3.2. Results

We used the coupler curve method for various Geiringer graphs. For instance for  $G_{3,6}^{\max}$ , the known result that  $r_3(G_{16}) = 16$  can be verified within a few tries with random starting lengths.

Maximization of the number of real realizations of the graph  $G_{3,7}^{\max}$  was the main goal of our research. There are 20 subgraphs satisfying the assumption in Lemma 5.4. Applying the tree search approach, we obtained edge lengths  $\lambda$  such that  $r_3(G_{3,7}^{\max}, \lambda) = 48$ :

$$\begin{aligned} \lambda_{1,2} &= 1.9999, & \lambda_{1,6} &= 2.0001, & \lambda_{4,5} &= 7.0744, & \lambda_{4,7} &= 11.8471, & \lambda_{1,3} &= 1.9342, \\ \lambda_{2,6} &= 1.0020, & \lambda_{5,6} &= 4.4449, & \lambda_{5,7} &= 11.2396, & \lambda_{1,4} &= 5.7963, & \lambda_{2,3} &= 0.5500, \\ \lambda_{2,7} &= 10.5361, & \lambda_{6,7} &= 10.5365, & \lambda_{1,5} &= 4.4024, & \lambda_{3,4} &= 5.4247, & \lambda_{3,7} &= 10.5245. \end{aligned}$$

They can be found from the starting edge lengths given in Section 5.3.1 with 28 real realizations in only 3 iterations, using the subgraphs induced by  $(u, v, w, p, c) = (5, 6, 1, 7, 4)$ ,  $(4, 3, 1, 7, 5)$  and  $(3, 2, 1, 7, 4)$ .

Next, we were able to find parameters  $\lambda$  such that  $r_3(G_{3,8}^{\max}, \lambda) = 132$ :

$$\begin{aligned} \lambda_{1,2} &= 1.999, & \lambda_{2,3} &= 1.426, & \lambda_{3,7} &= 10.447, & \lambda_{5,8} &= 4.279, & \lambda_{1,3} &= 1.568, \\ \lambda_{2,6} &= 0.879, & \lambda_{4,5} &= 7.278, & \lambda_{6,8} &= 0.398, & \lambda_{1,4} &= 6.611, & \lambda_{2,7} &= 10.536, \\ \lambda_{4,7} &= 11.993, & \lambda_{7,8} &= 10.474, & \lambda_{1,5} &= 4.402, & \lambda_{2,8} &= 0.847, & \lambda_{5,6} &= 4.321, \\ \lambda_{1,6} &= 1.994, & \lambda_{3,4} &= 6.494, & \lambda_{5,7} &= 11.239. \end{aligned}$$

Unfortunately, there is still a big gap between  $r_3(G_{3,8}^{\max}, \lambda) = 132$  and  $c_3(G_{3,8}^{\max}) = 160$ , but we could not find starting lengths giving better bound.

We remark that the method was applied also to other Geiringer graphs with 7 and 8 vertices, see [1, 2]. The full list of graphs can be found in [3].

Gluing many copies of  $G_{3,8}^{\max}$  along a triangle according to Theorem 5.1 gives the following lower bound on  $r_3(n)$ .

**Corollary 5.5.** *The maximum number of real realizations in the space among Geiringer graphs with  $n$  vertices is bounded from below by*

$$2^{(n-3) \bmod 5} 132^{\lfloor (n-3)/5 \rfloor},$$

*The bound behaves asymptotically as  $2.6553^n$ .*

The previously known lower bound for Geiringer graphs was  $2.51984^n$  [19]. Using the graph  $G_{3,7}^{\max}$  yields  $2.6321^n$ .

## Implementation

The package `FlexRiLoG` considers only realizations in the plane, i.e., the following is relevant only for Section 5.2. The functions strongly depend on the package `phcpy`.

### FlexRiGraph

`system_of_equations(edge_lengths, fixed_edge)` returns the system (5.1) for given *edge\_lengths* and *fixed\_edge*.

`mixed_volume()` computes the mixed volume of `system_of_equations()` with random edge lengths for all choices of the fixed edge and returns the minimum.

`random_realization()` returns a random realization of the graph.

`realization2edge_lengths(realization)` measures the edge lengths for a given *realization*.

`realizations(edge_lengths)` returns the list of real and complex realizations compatible with given *edge\_lengths*.

### GraphGenerator

`MaxEmbeddingsLamanGraph()` returns the graph  $G_{2,n}^{\max}$  for a given  $n$ .

For Geiringer graphs, we provide a separate source code [3]. It contains a GUI for the visualization of coupler curves of  $G_{3,7}^{\max}$  and the implementation of our method. The important functions were already mentioned in the method description, more can be found in the documentation.

## 6. Conclusion

In this thesis, we have studied flexible and rigid labelings of graphs. For the former, the main focus was on graphs spanned by a Laman graph, whereas for the latter, we have investigated the number of realizations for both Laman and Geiringer graphs. The NAC-colorings of a graph were introduced as a combinatorial object providing rich information about flexibility like:

- a flexible labeling exists if and only if a NAC-coloring exists (Theorem 2.7),
- the constant distance closure of a graph giving a necessary condition on the existence of proper flexible labelings is defined via NA-colorings (Corollary 3.8),
- an active singleton NAC-coloring imposes algebraic constraints on edge lengths (Section 4.1), or
- possible active NAC-colorings of a motion can be determined for graphs with enough 4-cycles (Section 4.3).

So far we did not deeply investigate NAC-colorings from the combinatorial point of view. For instance to provide a better algorithm for listing all NAC-colorings of a graph or to give some bounds on the number of NAC-colorings is subject to future research. Of course, Conjecture 2.20 remains open.

We work on the classification of proper flexible labelings of some other movable graphs from Theorem 3.12, using the tools described in Chapter 4.

Regarding rigid labelings, there is always the challenge to determine the numbers of realizations for graphs with more vertices than in Chapter 5. A big open problem is a combinatorial algorithm for determining the number of realizations of Geiringer graphs. Realizations on the sphere can be seen as a border case between the plane and space — a combinatorial algorithm computing the number of realizations of minimally rigid graphs on the sphere, which correspond to Laman graphs, was proposed recently by Georg Grasegger, Matteo Gallet and Josef Schicho [23]. There is an ongoing work on the existence of flexible labelings on the sphere and classification of proper flexible labelings of  $K_{3,3}$  by the author of the thesis with the authors of [23].



# A. Appendix

This appendix serves as a brief introduction into the notions used in the thesis.

## A.1. Graph Theory

In this section we summarize some basic definitions from Graph Theory. A nice introductory text on Graph Theory are the lecture notes by Tero Harju [31].

A graph  $G$  is a pair  $(V_G, E_G)$  where  $V_G$  is a finite nonempty set and  $E_G$  is a set of subsets of  $V_G$  of size two. The elements of  $V_G$  are called *vertices*, the elements of  $E_G$  are *edges*. To simplify the notation, we use  $uv$  for an edge  $\{u, v\} \in E_G$ . All graphs we consider are undirected, hence,  $uv = vu$ . Two vertices  $u$  and  $v$  are called adjacent if there is an edge  $uv \in E_G$ . We remark that for any graph  $G$ , the set of vertices, resp. edges, is always denoted by  $V_G$ , resp.  $E_G$ .

The vertices adjacent to a vertex  $v$  are called *neighbors* of  $v$ . The number of neighbors of  $v$  is the *degree* of  $v$ , denoted by  $\deg_G v$ .

A *subgraph*  $H$  of a graph  $G$  is a graph such that  $V_H \subset V_G$  and  $E_H \subset E_G$ . There are some special subgraphs:

- $H$  is a *spanning* subgraph of  $G$  if  $V_H = V_G$ . We also say that  $H$  *spans*  $G$ .
- $H$  is an *induced* subgraph of  $G$  if  $uv \in E_G$  implies  $uv \in E_H$  for every  $u, v \in V_H$ .

A *path* from  $u$  to  $v$  is a tuple  $(u = u_1, u_2, \dots, u_n = v)$  of pairwise distinct vertices such that  $u_i u_{i+1} \in E_G$  for every  $i \in \{1, \dots, n-1\}$ . An  *$n$ -cycle* is a path  $(u_1, \dots, u_n)$  such that  $u_1 u_n \in E_G$ . We sometimes call a 3-cycle a *triangle*. It is always clear from context whether  $(u_1, \dots, u_n)$  denotes a path or cycle. A connected component is a maximal induced subgraph such that any two vertices are connected by a path.

A graph  $G$  is called *bipartite* if there exist nonempty sets  $V_1$  and  $V_2$  such that  $V_G = V_1 \cup V_2$ ,  $V_1 \cap V_2 = \emptyset$  and there is no edge between vertices in  $V_1$ , resp.  $V_2$ .

We follow commonly used notation for some special graphs:

- $K_n$  is the *complete* graph on  $n$  vertices, i.e., every two vertices are adjacent.
- $C_n$  is the  $n$ -cycle.
- $K_{m,n}$  is the *complete bipartite* graph on  $m+n$  vertices, i.e.,  $V_{K_{m,n}} = \{x_1, \dots, x_m\} \cup \{y_1, \dots, y_n\}$  and  $E_{K_{m,n}} = \{x_i y_j : i \in \{1, \dots, m\}, j \in \{1, \dots, n\}\}$ .

We use two different names for maps assigning values to edges according to the codomain: while a *labeling* maps each edge to a positive real number, an *edge coloring* has a finite set of colors as its codomain.

A set of vertices such that no two of them are adjacent is called *independent*. We say that a set of vertices, resp. edges, *separates* a graph, if removing these vertices (together with incident edges), resp. edges, from the graph increases the number of connected components.

## A.2. Algebraic Geometry

We recall a few notions from algebraic geometry, see for instance [50, 51].

Let  $\mathbb{K}$  be  $\mathbb{R}$  or  $\mathbb{C}$ . The *affine space*  $\mathbb{A}_{\mathbb{K}}^n$  is the set  $\{(a_1, \dots, a_n) : a_i \in \mathbb{K}\}$ . The elements of  $\mathbb{A}_{\mathbb{K}}^n$  are *points*. Let  $S \subset \mathbb{K}[x_1, \dots, x_n]$  be a set of polynomials. The *zero set* of  $S$  is the set

$$\{(a_1, \dots, a_n) \in \mathbb{A}_{\mathbb{K}}^n : f(a_1, \dots, a_n) = 0 \forall f \in S\}.$$

The zero sets of  $S$ , the ideal generated by  $S$  and its radical are the same. By Hilbert's basis theorem, any ideal has a finite set of generators. Computations with ideals can be done using Gröbner basis, see [12]. A set  $X \subset \mathbb{A}_{\mathbb{K}}$  is called an *algebraic set* or *variety* if it is a zero set for some set of polynomials.

An algebraic set  $X$  is called *irreducible* if it cannot be written as a union of two proper algebraic subsets. The maximal algebraic subsets of an algebraic set are called *irreducible components*. An irreducible algebraic set is called a *curve* if the only proper algebraic subsets are points.

For an algebraic set  $X$ , the set of polynomials that vanish on all points of  $X$ , namely

$$I(X) = \{f \in \mathbb{K}[x_1, \dots, x_n] : f(\bar{a}) = 0 \forall \bar{a} \in X\},$$

forms an ideal in  $\mathbb{K}[x_1, \dots, x_n]$ . It is called the *ideal* of  $X$ . The ideal  $I(X)$  is a prime ideal if and only if  $X$  is irreducible.

A property  $P$  holds *generically* on a variety  $X$  if there is a proper algebraic subset  $Y$  of  $X$  such that  $P$  holds at every point in  $X \setminus Y$ . A sentence that a *generic point* has a property  $P$  must be read as  $P$  holds generically on  $X$ .

The *coordinate ring* of an irreducible algebraic set  $X$  is defined as the quotient ring  $\mathbb{K}[x_1, \dots, x_n]/I(X)$ . The coordinate ring is an integral domain. The *function field* of  $X$  is the field of fractions of the coordinate ring of  $X$ , denoted by  $F(X)$ . The elements of  $F(X)$  are *rational functions*. A rational function can be locally defined as a quotient of polynomials. By the *complex function field* of an irreducible algebraic set  $X \subset \mathbb{A}_{\mathbb{R}}^n$  we mean the function field of the zero set  $Y \subset \mathbb{A}_{\mathbb{C}}^n$  of the polynomials in  $I(X)$  considered as polynomials over  $\mathbb{C}$ .



Let  $\mathcal{C}$  be an algebraic irreducible curve and  $f: \mathcal{C} \rightarrow \mathbb{A}_{\mathbb{K}}^r$  be the projection of the curve  $\mathcal{C}$  to the first  $r$  coordinates. If  $f(\mathcal{C})$  is also a curve, then the function field  $F(\mathcal{C})$  is an algebraic extension of the function field  $F(\mathcal{C}')$ . The *degree* of the map  $f$  is defined as  $\deg(f) = [F(\mathcal{C}) : F(\mathcal{C}')]$ , which is the cardinality of a generic fibre  $f^{-1}(y)$ .

### A.3. Valuations

Some basic definitions and facts about valuations are summarized in this section. See the books [14, 20, 24] for further details.

An *algebraic function field* is a field which has the transcendence degree one over  $\mathbb{C}$  and it is finitely generated over  $\mathbb{C}$ . If  $\mathcal{C}$  is an algebraic curve, then the complex function field  $F(\mathcal{C})$  is an algebraic function field.

A *valuation* of  $F(\mathcal{C})$  is a map  $\nu: F(\mathcal{C})^* \rightarrow \mathbb{Q}$  such that for all  $a, b \in \nu: F(\mathcal{C})^*$ :

- (i)  $\nu(ab) = \nu(a) + \nu(b)$ , and
- (ii) if  $a + b \neq 0$ , then  $\nu(a + b) \geq \min(\nu(a), \nu(b))$ .

The definition is sometimes extended to the whole  $F(\mathcal{C})$  by setting  $\nu(0) = \infty$ . We assume all valuations  $\nu$  to be *trivial* on the base field  $\mathbb{C}$ , i.e.,  $\nu(\mathbb{C}^*) = \{0\}$ .

An important fact for this thesis is that if a sum of functions in  $F(\mathcal{C})$  is zero, then there are at least two summands with the same valuation, namely the minimal one.

By Chevalley's Extension Theorem we have that if  $x$  is a transcendental element of  $F(\mathcal{C})$ , then there is at least one valuation  $\nu$  trivial on  $\mathbb{C}$  such that  $\nu(x) > 0$ .

Given a valuation  $\nu$ ,  $\mathcal{O}_\nu = \{x \in F(\mathcal{C}) : \nu(x) \geq 0\}$  is a *valuation ring*, namely,  $x$  or  $x^{-1}$  lies in  $\mathcal{O}_\nu$  for every  $x \in F(\mathcal{C})$ . The set  $m_\nu = \{x \in F(\mathcal{C}) : \nu(x) > 0\}$  is the maximal ideal of  $\mathcal{O}_\nu$ . The *residue field*  $\mathcal{O}_\nu/m_\nu$  is isomorphic to  $\mathbb{C}$ .

Two valuations  $\nu_1$  and  $\nu_2$  are *equivalent* if there exists  $\alpha \in \mathbb{Q}$  such that  $\nu_1(a) = \alpha\nu_2(a)$  for all  $a \in F(\mathcal{C})^*$ . The valuations of the complex function field  $F(\mathcal{C})$  are *discrete* — the codomain can be chosen to be  $\mathbb{Z}$  by taking an equivalent valuation. We denote the set of valuations of  $F(\mathcal{C})$  that are surjective on  $\mathbb{Z}$  by  $\text{Val}(\mathcal{C})$ .

Let  $\mathcal{C}'$  be a curve that is a projection of an algebraic irreducible curve  $\mathcal{C}$ . If  $\nu \in \text{Val}(\mathcal{C})$ , then  $\nu(F(\mathcal{C}')^*) = r\mathbb{Z}$  for some positive integer  $r$  and there is a valuation  $\nu' \in \text{Val}(\mathcal{C}')$  surjective on  $\mathbb{Z}$  such that  $\nu(x) = r\nu'(x)$  for all  $x \in F(\mathcal{C}')$ . We say that  $\nu$  *extends*  $\nu'$ . The number  $r$  is called the *ramification index* of  $\nu$  over  $F(\mathcal{C}')$ , denoted by  $\text{ram}_{F(\mathcal{C})/F(\mathcal{C}')}(\nu)$ . Since the residue field of a function field of a curve over complex numbers is always  $\mathbb{C}$ , we have the following for a valuation  $\nu'$  of  $F(\mathcal{C}')$ :

$$\sum_{\substack{\nu \in \text{Val}(\mathcal{C}) \\ \nu \text{ ext. } \nu'}} \text{ram}_{F(\mathcal{C})/F(\mathcal{C}')}(\nu) = \deg(f).$$



# Bibliography

- [1] E. Bartzos, I. Z. Emiris, J. Legerský, and E. Tsigaridas. On the maximal number of real embeddings of minimally rigid graphs in  $\mathbb{R}^2$ ,  $\mathbb{R}^3$  and  $S^2$ , 2018. arXiv:1811.12800.
- [2] E. Bartzos, I. Z. Emiris, J. Legerský, and E. Tsigaridas. On the Maximal Number of Real Embeddings of Spatial Minimally Rigid Graphs. In *Proceedings of the 2018 ACM International Symposium on Symbolic and Algebraic Computation*, ISSAC '18, pages 55–62, New York, NY, USA, 2018. ACM. doi:10.1145/3208976.3208994.
- [3] E. Bartzos and J. Legerský. Graph embeddings in the plane, space and sphere — source code and results. Zenodo, 2018. doi:10.5281/zenodo.1495153.
- [4] A. R. Berg and T. Jordán. Algorithms for graph rigidity and scene analysis. In *Algorithms – ESA 2003*, pages 78–89. Springer Berlin Heidelberg, 2003. doi:10.1007/978-3-540-39658-1\_10.
- [5] D. N. Bernshtein. The number of roots of a system of equations. *Functional Analysis and Its Applications*, 9(3):183–185, Jul 1975. doi:10.1007/BF01075595.
- [6] E. Bolker and B. Roth. When is a bipartite graph a rigid framework? *Pacific Journal of Mathematics*, 90(1):27–44, 1980. doi:10.2140/pjm.1980.90.27.
- [7] C. S. Borcea and I. Streinu. The Number of Embeddings of Minimally Rigid Graphs. *Discrete and Computational Geometry*, 31:287–303, 2004. doi:10.1007/s00454-003-2902-0.
- [8] L. Burmester. Die Brennpunktmechanismen. *Zeitschrift für Mathematik und Physik*, 38:193–223, 1893.
- [9] J. Capco, M. Gallet, G. Grasegger, C. Koutschan, N. Lubbes, and J. Schicho. The Number of Realizations of a Laman Graph. *SIAM Journal on Applied Algebra and Geometry*, 2(1):94–125, 2018. doi:10.1137/17M1118312.
- [10] J. Capco, M. Gallet, G. Grasegger, C. Koutschan, N. Lubbes, and J. Schicho. The number of realizations of all Laman graphs with at most 12 vertices. Zenodo, May 2018. doi:10.5281/zenodo.1245517.
- [11] D. A. Cox, J. B. Little, and D. O’Shea. *Using Algebraic Geometry*, volume 185 of *Graduate Texts in Mathematics*. Springer, first edition, 1998. doi:10.1007/978-1-4757-6911-1.

- [12] David A. Cox, John Little, and Donal O’Shea. *Ideals, Varieties, and Algorithms: An Introduction to Computational Algebraic Geometry and Commutative Algebra*. Springer Publishing Company, Incorporated, 4th edition, 2015. doi:10.1007/978-3-319-16721-3.
- [13] H. Crapo. On the generic rigidity of plane frameworks. *Institut de recherche d’informatique et d’automatique*, (1278), 1990.
- [14] M. Deuring. *Lectures on the theory of algebraic functions of one variable*, volume 314 of *Lecture notes in mathematics*. Springer, 1973. doi:10.1007/BFb0060944.
- [15] P. Dietmaier. The Stewart-Gough platform of general geometry can have 40 real postures. *Advances in Robot Kinematics: Analysis and Control*, pages 1–10, 1998. doi:10.1007/978-94-015-9064-8\_1.
- [16] A. C. Dixon. On certain deformable frameworks. *Messenger*, 29(2):1–21, 1899.
- [17] I. Z. Emiris and G. Moroz. The assembly modes of rigid 11-bar linkages. *IFTOMM 2011 World Congress, Jun 2011, Guanajuato, Mexico*, 2011.
- [18] I. Z. Emiris and B. Mourrain. Computer algebra methods for studying and computing molecular conformations. *Algorithmica*, 25(2):372–402, Jun 1999. doi:10.1007/PL00008283.
- [19] I. Z. Emiris, E. Tsigaridas, and A. Varvitsiotis. Mixed volume and distance geometry techniques for counting Euclidean embeddings of rigid graphs. *Distance Geometry: Theory, Methods and Applications*, pages 23–45, 2013. doi:10.1007/978-1-4614-5128-0\_2.
- [20] A. J. Engler and A. Prestel. *Valued Fields*. Springer Monographs in Mathematics. Springer Berlin Heidelberg, 2005. doi:10.1007/3-540-30035-X.
- [21] Z. Fekete, T. Jordán, and V. E. Kaszanitzky. Rigid Two-Dimensional Frameworks with Two Coincident Points. *Graphs and Combinatorics*, 31(3):585–599, 2015. doi:10.1007/s00373-013-1390-0.
- [22] H. N. Gabow and H. H. Westermann. Forests, frames, and games: Algorithms for matroid sums and applications. *Algorithmica*, 7(1):465–497, 1992. doi:10.1007/BF01758774.
- [23] M. Gallet, G. Grasegger, and J. Schicho. Counting realizations of Laman graphs on the sphere, 2019. arXiv:1903.01145.
- [24] D. Goldschmidt. *Algebraic Functions and Projective Curves*. Graduate Texts in Mathematics. Springer, 2003. doi:10.1007/b97844.

- [25] G. Grasegger, C. Koutschan, and E. Tsigaridas. Lower Bounds on the Number of Realizations of Rigid Graphs. *Experimental Mathematics*, pages 1–12, 2018. doi:10.1080/10586458.2018.1437851.
- [26] G. Grasegger and J. Legerský. FlexRiLoG — SageMath package for Flexible and Rigid Labelings of Graphs. Zenodo, May 2019. doi:10.5281/zenodo.3078758.
- [27] G. Grasegger, J. Legerský, and J. Schicho. Graphs with Flexible Labelings. *Discrete & Computational Geometry*, 2018. doi:10.1007/s00454-018-0026-9.
- [28] G. Grasegger, J. Legerský, and J. Schicho. Rigid graphs that are movable. In *EuroCG 2019*, 2019. <http://www.eurocg2019.uu.nl/papers/54.pdf>.
- [29] G. Grasegger, J. Legerský, and J. Schicho. Graphs with Flexible Labelings allowing Injective Realizations, 2018. arXiv:1811.06709.
- [30] Jack Graver, Brigitte Servatius, and Herman Servatius. *Combinatorial rigidity*. Graduate Studies in Mathematics. American Mathematical Society, 1993. doi:10.1090/gsm/002.
- [31] T. Harju. Lecture notes on Graph Theory, 2012. <http://users.utu.fi/harju/graphtheory/graphtheory.pdf>.
- [32] L. Henneberg. Die graphische Statik der starren Körper. In *Encyklopädie der mathematischen Wissenschaften mit Einschluss ihrer Anwendungen*, volume IV, pages 345–434. B.G. Teubner Verlag, 1903. doi:10.1007/978-3-663-16021-2\_5.
- [33] J. D. Hunter. Matplotlib: A 2D graphics environment. *Computing In Science & Engineering*, 9(3):90–95, 2007. doi:10.1109/MCSE.2007.55.
- [34] B. Jackson and J.C. Owen. Equivalent realisations of a rigid graph. *Discrete Applied Mathematics*, 256:42–58, 2019. doi:10.1016/j.dam.2017.12.009.
- [35] Bill Jackson and Tibor Jordán. Rigid Two-Dimensional Frameworks with Three Collinear Points. *Graphs and Combinatorics*, 21(4):427–444, 2005. doi:10.1007/s00373-005-0629-9.
- [36] Donald J. Jacobs and Bruce Hendrickson. An Algorithm for Two-Dimensional Rigidity Percolation: The Pebble Game. *Journal of Computational Physics*, 137(2):346–365, 1997. doi:10.1006/jcph.1997.5809.
- [37] G. Laman. On graphs and rigidity of plane skeletal structures. *Journal of Engineering Mathematics*, 4:331–340, 1970. doi:10.1007/BF01534980.

- [38] A. Lee and I. Streinu. Pebble game algorithms and sparse graphs. *Discrete Mathematics*, 308(8):1425–1437, 2008. doi:10.1016/J.DISC.2007.07.104.
- [39] J. Legerský. Movable graphs, 2018. <http://jan.legersky.cz/project/movablegraphs/>.
- [40] J. Legerský. Flexible and Rigid Labelings of Graphs — supporting material. Zenodo, May 2019. doi:10.5281/zenodo.3079628.
- [41] S. Liang, J. Gerhard, D. J. Jeffrey, and G. Moroz. A Package for Solving Parametric Polynomial Systems. *ACM Communications in Computer Algebra*, 43(3):61–72, 2009. doi:10.1145/1823931.1823933.
- [42] L. Liberti, B. Masson, J. Lee, C. Lavor, and A. Mucherino. On the number of realizations of certain Henneberg graphs arising in protein conformation. *Discrete Applied Mathematics*, 165:213–232, 2014. doi:10.1016/J.DAM.2013.01.020.
- [43] H. Maehara. Geometry of frameworks. *Yokohama Mathematical Journal*, 47:41–65, 1999.
- [44] H. Maehara and N. Tokushige. When does a planar bipartite framework admit a continuous deformation? *Theoretical Computer Science*, 263(1–2):345–354, 2001. doi:10.1016/S0304-3975(00)00254-1.
- [45] J. C. Maxwell. On the calculation of the equilibrium and stiffness of frames. *The London, Edinburgh, and Dublin Philosophical Magazine and Journal of Science*, 27(182):294–299, 1864. doi:10.1080/14786446408643668.
- [46] F. Pedregosa, G. Varoquaux, A. Gramfort, V. Michel, B. Thirion, O. Grisel, M. Blondel, P. Prettenhofer, R. Weiss, V. Dubourg, J. Vanderplas, A. Passos, D. Cournapeau, M. Brucher, M. Perrot, and E. Duchesnay. Scikit-learn: Machine Learning in Python. *Journal of Machine Learning Research*, 12:2825–2830, 2011.
- [47] H. Pollaczek-Geiringer. Über die Gliederung ebener Fachwerke. *Zeitschrift für Angewandte Mathematik und Mechanik (ZAMM)*, 7:58–72, 1927. doi:10.1002/zamm.19270070107.
- [48] H. Pollaczek-Geiringer. Zur Gliederungstheorie räumlicher Fachwerke. *Zeitschrift für Angewandte Mathematik und Mechanik (ZAMM)*, 12(6):369–376, 1932. doi:10.1002/zamm.19320120606.
- [49] J. Qi. How to avoid collision of 3D-realization for moving graphs, 2019. arXiv:1904.13260.

- [50] M. Reid. *Undergraduate Algebraic Geometry*. London Mathematical Society Student Texts. Cambridge University Press, 1988. doi:10.1017/CBO9781139163699.
- [51] I.R. Shafarevich. *Basic algebraic geometry 1*. Springer, Berlin, 3rd edition, 2013. doi:10.1007/978-3-642-37956-7.
- [52] M. Sitharam, A. St. John, and J. Sidman. *Handbook of Geometric Constraint Systems Principles*. Chapman and Hall/CRC, 2018. doi:10.1201/9781315121116.
- [53] H. Stachel. On the flexibility and symmetry of overconstrained mechanisms. *Philosophical Transactions of the Royal Society of London A: Mathematical, Physical and Engineering Sciences*, 372, 2013. doi:10.1098/rsta.2012.0040.
- [54] R. Steffens and T. Theobald. Mixed volume techniques for embeddings of Laman graphs. *Computational Geometry*, 43(2):84–93, 2010. doi:10.1016/j.comgeo.2009.04.004.
- [55] I. Streinu and L. Theran. Combinatorial genericity and minimal rigidity. In *Proceedings of the twenty-fourth annual symposium on Computational geometry – SCG ’08*, pages 365–374. ACM Press, 2008. doi:10.1145/1377676.1377738.
- [56] T. S. Tay and W. Whiteley. Generating isostatic frameworks. *Topologie Structurale*, 11:21–69, 1985.
- [57] The Sage Developers. *SageMath, the Sage Mathematics Software System (Version 7.5.1)*, 2017. <https://www.sagemath.org>.
- [58] C.D. Tóth, J. O’Rourke, and J.E. Goodman. *Handbook of Discrete and Computational Geometry*. Discrete Mathematics and Its Applications. CRC Press, 2017. doi:10.1201/9781420035315.
- [59] J. Verschelde. Modernizing PHCpack through phcpy. In *Proceedings of the 6th European Conference on Python in Science (EuroSciPy 2013)*, pages 71–76, 2014.
- [60] D. Walter and M.L. Husty. On a nine-bar linkage, its possible configurations and conditions for paradoxical mobility. In *12th World Congress on Mechanism and Machine Science, IFToMM 2007*, 2007.
- [61] W. Whiteley. Infinitesimal motions of a bipartite framework. *Pacific Journal of Mathematics*, 110(1):233–255, 1984. doi:10.2140/pjm.1984.110.233.
- [62] W. Wunderlich. Ein merkwürdiges Zwölfstabgetriebe. *Österreichisches Ingenieur-Archiv*, 8:224–228, 1954.

- [63] W. Wunderlich. On deformable nine-bar linkages with six triple joints. *Indagationes Mathematicae (Proceedings)*, 79(3):257–262, 1976. doi:10.1016/1385-7258(76)90052-4.
- [64] W. Wunderlich. Mechanisms related to Poncelet’s closure theorem. *Mechanisms and Machine Theory*, 16:611–620, 1981. doi:10.1016/0094-114X(81)90067-7.
- [65] D. Zelazo, A. Franchi, F. Allgöwer, H. H. Büthoff, and P.R. Giordano. Rigidity Maintenance Control for Multi-Robot Systems. *Robotics: Science and Systems, Sydney, Australia*, 2012.